AN ABSTRACT OF THE THESIS OF

Larry R. Higinbotham for the degree of Master of Science in Geology presented on April 28, 1986

Title: Stratigraphy, Depositional History, and Petrology of the Upper Cretaceous(?) to Middle Eocene Montgomery Creek Formation, Northern California

Signature redacted for privacy.

Abstract approved: Edward M. Taylor

The Upper Cretaceous to Eocene Montgomery Creek Formation is exposed between the Klamath and Cascade Mountains in the vicinity of Big Bend and Montgomery Creek, northern California.

The formation is divided into a northern and a southern section. The rocks consist of a basal conglomerate succeeded by feldspathic to lithic graywackes, conglomerates, shales, carbonaceous shales, and minor lignites. The northern section is 3,188 feet thick. Fining upward point bar deposits, abundant foreset- and cross-bedding, and thick flood-basin deposits indicate the northen section strata were deposited by meandering rivers. Carbonaceous shales, lignites and fossil leaves define the swamps that were present in the basins. The southern section is 4,596 feet thick. Thick and

laterally extensive sandstone bodies, numerous conglomerate interbeds, and abundant planar cross-bedding suggest that these strata were deposited by braided rivers. A few outcrops low in the section resemble the northern section strata, and are interpreted to be meandering river deposits.

A progressive change in composition of the sandstones from the base to the top of the formation occurs in both the northern and southern sections. This reflects the change from metamorphic and plutonic source rocks of the Klamath Mountains to volcanic source rocks of the early Cascade Range. The southern section maintains a more lithic-rich composition, reflecting higher discharge rates and steeper gradients responsible for braided-river deposition.

Paleocurrent readings from foreset bedding and imbricated pebbles indicate a north-to-south transport direction in most of both sections. Some westerly transport occurred high in the southern section.

Eocene strata four miles north of the northern section reflect a meandering river depositional environment. These strata have a higher shale-to-sandstone ratio, larger proportions of carbonaceous shales and coal, and a different sandstone mineralogy than Eocene rocks to the south.

Analysis revealed that the Montgomery Creek Formation carbonaceous shales and coal are sufficiently rich in organic carbon to be hydrocarbon source rocks. Most of the samples are thermally immature, but could produce gas through bacterial-fungal breakdown of organic matter. The Eocene sandstones have adequate porosity and permeability to be petroleum reservoir rocks.

The Klamath Mountains acted as a source area for Cretaceous marine deposits in basins north and south of the study area. Either the Cretaceous seas did not transgress into the study area, or such deposits were subsequently removed by erosion.

Stratigraphy, Depositional History, and Petrology of the Upper Cretaceous(?) to Middle Eocene Montgomery Creek Formation, Northern California

by

Larry R. Higinbotham

A THESIS

submitted to

Oregon State University

in partial fulfillment of
the requirements for the
degree of

Master of Science

Completed April 28, 1986

Commencement June 1986

ACKNOWLEDGEMENTS

I would like to thank Dr. Edward M. Taylor for his guidance during this graduate project. Dr. Taylor has devoted many hours to reading this thesis and has given me much encouragement and valuable advice. Special thanks also go to Drs. Keith F. Oles, Robert D. Lawrence, and Laverne D. Kulm for the critical reading of the thesis.

I would also like to thank Jere B. Jay of Tenneco Oil Company. Jere's correspondence and helpful suggestions in the field have been appreciated. A generous grant from Tenneco provided funds for six weeks' study in the field (Shasta County, California) and for the expenses that followed in preparing this paper. I am grateful for the friendship and hospitality of residents in the communities of Big Bend and Montgomery Creek, California, during my stay in the area, especially Joe Mazzini, Ed Dyer, Ray Hamby, the Fesslers, the Rideouts, and Wild Bill.

I would like to thank Paula Pitts for the quality drafting in this paper, and my typist, Sadie Airth. Finally, my deepest appreciation goes to my family and friends in the Corvallis area, and to Vickie and her family in Eugene, for their collective support and encouragement.

TABLE OF CONTENTS

LIST OF FIGURES

LIST OF TABLES

STRATIGRAPHY, DEPOSITIONAL HISTORY, AND PETROLOGY OF THE UPPER CRETACEOUS(?) TO MIDDLE EOCENE MONTGOMERY CREEK FORMATION, NORTHERN CALIFORNIA

INTRODUCTION

The purpose of this report is to present results of a detailed study of the Montgomery Creek Formation, Shasta County, northern California. Most of the study area is located between the towns of Montgomery Creek and Big Bend (Figs. 1 and 2). To date, only reconnaissance studies have been made on the Upper Cretaceous(?) to Eocene strata of this area. Detailed field and laboratory investigations reveal: (1) stratigraphic sequence, thicknesses, contact relationships, depositional environments, and ages of the strata; (2) mineralogical trends, heavy mineral distribution, and post-depositional alteration of the sandstone; (3) transport directions of the sediments; (4) location and lithology of the source areas; (5) relation of the strata to Klamath Mountain and Cascade Range geologic history; and (6) potential of the strata for hydrocarbon production.

Sediments of the Montgomery Creek Formation record the early Tertiary tectonic history of the Klamath Mountains and the birth of the Cascade Range. It is hoped this study will clarify some of the history of these two large geologic provinces.

Location of Investigation

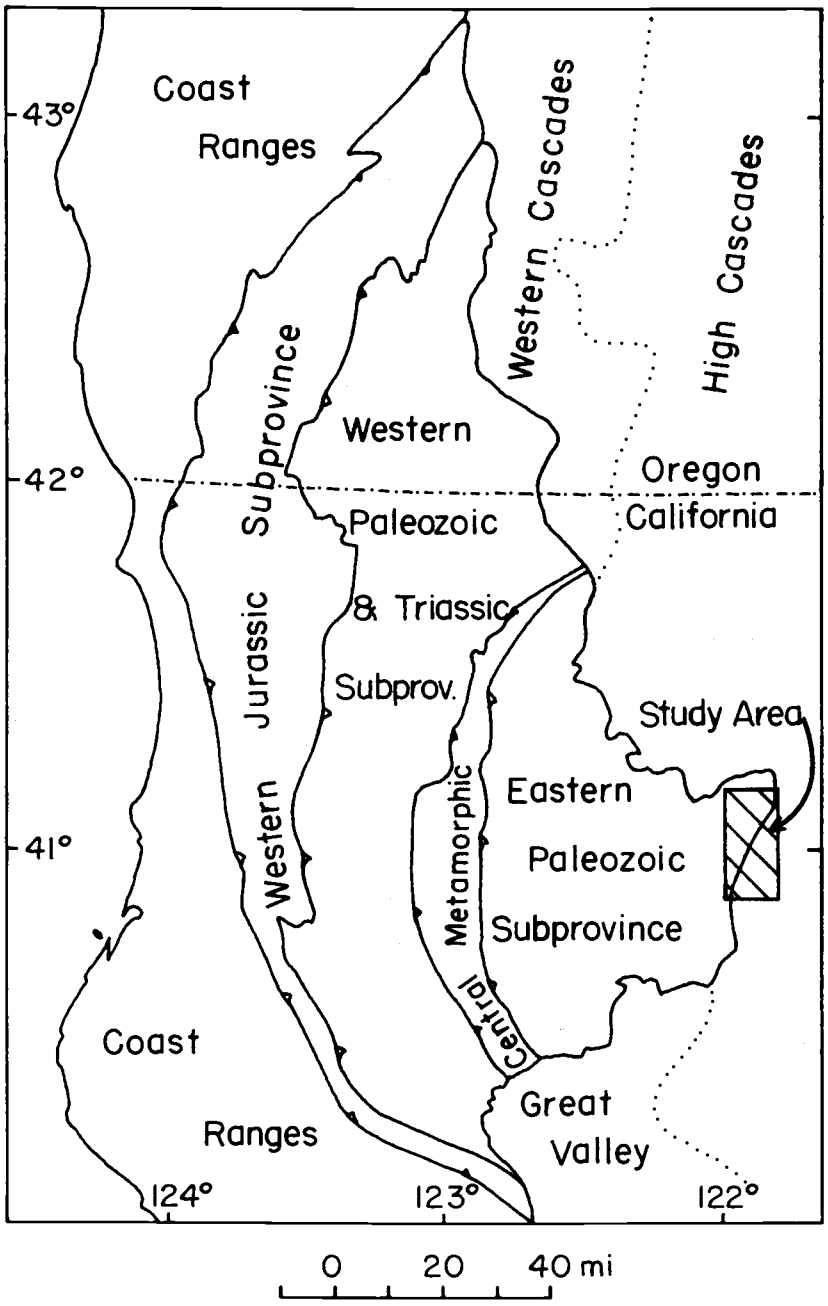

Figure 1. Index map showing study area, subprovinces of the Klamath Mountains, the Cascade Range, and other major physiographic provinces (From Irwin, 1966).

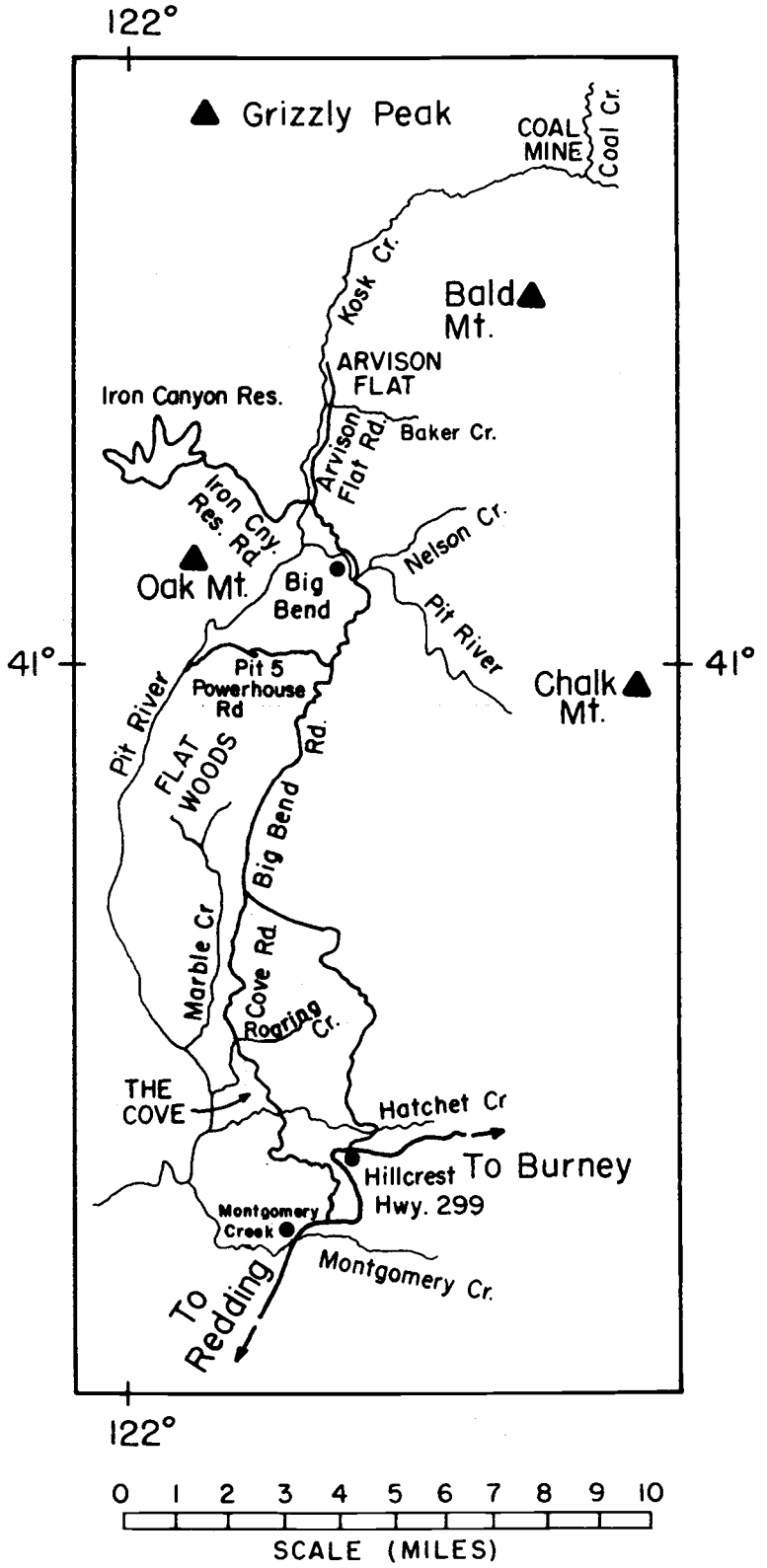

Figure 2. Map showing important geographic features in and adjacent to the study area.

PREVIOUS WORK

Several geologists have contributed to the present body of knowledge about the Montgomery Creek Formation. The following is a chronological account of their findings:

1889: J.S. Diller (1889) described rocks of the Ione Formation just south of the study area. These strata are now recognized as the Montgomery Creek Formation.

1893: H.W. Fairbanks (1893) considered the coal-bearing shales and conglomerates in the Big Bend area to be Cretaceous in age.

1906: J.S. Diller (1906) revised the stratigraphy of the present study area in the Redding Folio. He assigned lacustrine deposits near Big Bend and along Kosk Creek to the Ione Formation. Diller considered these deposits to be Miocene on the basis of their flora.

1932: H. Williams (1932) was the first to acknowledge the Montgomery Creek Formation in the literature. Both he and N.E.A. Hinds (1933) credited the name to an unpublished manuscript by R. Dana Russell. R. W. Chaney determined that a Montgomery Creek Formation flora discovered by Russell was of late middle Eocene age.

1939: C.A. Anderson and R.D. Russell (1939) designated the type locality of the Eocene strata to be along Montgomery Creek, 2.5 miles northeast of the town of Montgomery Creek.

1960: A.F. Sanborn (1960) examined the Mesozoic and Cenozoic strata in the vicinity of Big Bend. In this condensation of his Ph.D. thesis, he briefly described the lithology and stratigraphy of the Eocene strata. He estimated a maximum thickness of 2,600 feet for the Montgomery Creek Formation.

1975: R.P. Hilton (1975) described outcrops of the formation south of the study area, near the towns of Ingot and Round Mountain. He interpreted an up-section change from a fluvial to a swampy deltaic depositional environment.

REGIONAL GEOLOGY

The Upper Cretaceous to Eocene rocks of this study are exposed as a series of isolated outcrops along the eastern margin of the Klamath Mountains geologic province in northern California (Fig. 1). The outcrops occur for 17 miles in a north-south-trending zone from the town of Montgomery Creek, northward to the Big Bend area (Fig. 2).

The Montgomery Creek Formation is located between two large geologic provinces. The base of this formation is an Upper Cretaceous to lower Eocene(?) basal conglomerate. This conglomerate is overlain by an Eocene sequence of sandstone, conglomerate, siltstone, shale, carbonaceous shale, and minor lignite. These rocks lie unconformably upon the rocks of the Klamath Mountains province to the west, and are overlain to the east with slight angular unconformity by rocks of the High Cascade series (Fig. 3).

Klamath Mountains Province

The Klamath Mountains are distinct from the younger Cascade volcanics to the east, having a more rugged topography and supporting sparser vegetation. The Klamath rocks were deformed and tilted steeply during the Late Jurassic Nevadan orogeny; in some cases, tight folds were produced.

Figure 3. The northern section of the study area near the town of Big Bend. Foreground: Klamath province strata; left, background: Volcanic rocks of the Tertiary High Cascade series; middleground: the Eocene Montgomery Creek Formation, occupying the lowest areas of this basin. The white strata on the mountain to the upper right is a Pliocene diatomite deposit.

The principal rocks of the Klamath Mountains are eugeosynclinal metasediments and metavolcanics, ranging in age from Ordovician to Late Jurassic (Irwin, 1966). Late Jurassic ultramafic, gabbroic and granitic rocks intrude the Klamath strata.

The Klamaths consist of four concentric, arcuate belts that are concave eastward (Fig. 1). Irwin (1966, 1977) named the belts (from east to west): the Eastern Klamath, the Central Metamorphic, the Western Paleozoic and Triassic, and the Western Jurassic. The arcuate pattern of the lithic belts is emphasized by linear bodies of ultramafic rock that tend to be concentrated along the boundaries between the belts. The belts are considered by Irwin (1966, 1977) to be thrust plates that successively overlap adjacent plates to the west. Only the Eastern Klamath belt extends into the study area.

The Eastern Klamath belt is generally an east-dipping, homoclinal sequence that to the west is deformed and terminated against ultramafic rocks (Irwin, 1966). The strata of the belt constitute, in the aggregate, a stratigraphic column 40,000 to 50,000 feet thick. This sequence was deposited during Ordovician to Late Jurassic time. Only the Late Triassic and Jurassic rocks occur immediately adjacent to and within the study area. These rocks have been studied in detail by Sanborn (1960) and Diller (1906).

In the extreme southern part of the map area, the Middle Jurassic Bagley Andesite crops out at Montgomery Falls, 0.25 miles southwest of the town of Montgomery Creek. Here the metavolcanics are deeply incised by the Montgomery Creek drainage, resulting in cliffy exposures. The andesite is dark gray to black, with large phenocrysts of plagioclase feldspar. The Bagley Andesite was mapped north of this location, cropping out sporadically for 12 miles along a narrow, north-trending belt which roughly parallels the Pit River drainage (Fig. 4). The Bagley Andesite is best exposed along the Pit River Canyon and in smaller canyons cut by west-flowing tributaries to the river.

Near Little Joe Flat (T36N, R1W, Sec. 3) the Bagley Andesite outcrop belt trends more northeasterly, paralleling the Pit River for two miles to Kosk Creek. At the confluence of Kosk Creek and the Pit River, and for 0.5 miles upstream on Kosk Creek, a hypabyssal gabbroic intrusion is found (Fig. 5). This poorly exposed intrusive body covers 0.25 $mi.^2$ and is somewhat circular in shape, suggesting that it is a volcanic neck. The age of the intrusion is unknown, but the stratigraphic and geographic position suggests that it is similar in age to the Jurassic Bagley Andesite.

Upstream from the intrusive on Kosk Creek, the Lower Jurassic Arvison Formation (Fig. 6) is exposed

Figure 4. The Jurassic Bagley Andesite is exposed in canyons cut by Pit River tributaries, on the west side of a basin called The Cove. In the background (north) is a Tertiary volcanic plateau called the Flat Woods.

Figure 5. Jurassic gabbroic intrusion near the confluence of Kosk Creek and the Pit River.

Figure 6. The Lower Jurassic Arvision Formation andesite is exposed along Kosk Creek.

sporadically for 2.5 miles. The Arvison Formation underlies both the Bagley Andesite and Jurassic Potem Formation (Sanborn, 1960). The Arvison Formation rocks observed in the map area consist of dark gray to black andesite and andesitic breccia. The andesite is both aphyric and porphyritic, with large phenocrysts of plagioclase feldspar.

The Arvison Formation was observed almost entirely on the west side of Kosk Creek, whereas the younger Eocene Montgomery Creek Formation is restricted to the east side of the creek. In addition, the outcrop belts of both the Arvison Formation and the Montgomery Creek Formation trend due north. This northerly trend is parallel to the unusual linear drainage of Kosk Creek. This evidence suggests that there is a fault separating the older Klamath rocks from the Montgomery Creek Formation.

Just within and west of the mapped area, the Bagley Andesite overlies and is intercalated with the lower beds of the Middle Jurassic Potem Formation (Sanborn, 1960), although most of the Potem is younger than the Bagley Andesite. The observed Potem rocks are tan to gray argillites and tuffaceous metasediments. Sanborn (1960) estimated the maximum thickness of the Potem Formation to be 1,000 feet. The strata are one to six inches thick. The strata were deformed by the Late Jurassic Nevadan Orogeny; some beds are steeply dipping and others are contorted into tight folds (Fig. 7). Some good Potem Formation

outcrops are exposed along the road to Iron Canyon reservoir, west of the study area.

A mile north of the map area, Klamath province Upper Triassic argillites crop out along Kosk Creek near Arvison Flat (Fig. 8). These dark gray to black sediments are part of the Kosk member of the Modin Formation (Sanborn, 1960). The strata are mostly 0.5 inches to 3 inches in thickness. The argillites are considerably more indurated than the Middle Jurassic Potem Formation. The beds dip rather steeply, but are not buckled into folds as in the Potem strata. Intercalated with the Kosk member argillites are andesitic breccias and flows, some reaching thicknesses of 300 feet (Sanborn, 1960). The total thickness of the Kosk member is approximately 3,600 feet (Sanborn, 1960).

Cascade Range

The Tertiary Cascade Range in Oregon is divided into the Western Cascade Range and the High Cascade Range (Callaghan, 1933; Peck et al., 1964, Fig. 1). The northern part of the Cascade Range in California contains both Western and High Cascade rocks (MacDonald, 1966). The High Cascade rocks overlie the Eocene Montgomery Creek Formation. The volcanics extend no farther west than Kosk Creek and the Pit River, with the exception of a small

Figure 7. Strata of the Middle Jurassic Potem Formation are exposed in a roadcut on Iron Canyon Reservoir Road. These beds were contorted into tight folds by the Late Jurassic Nevadan orogeny.

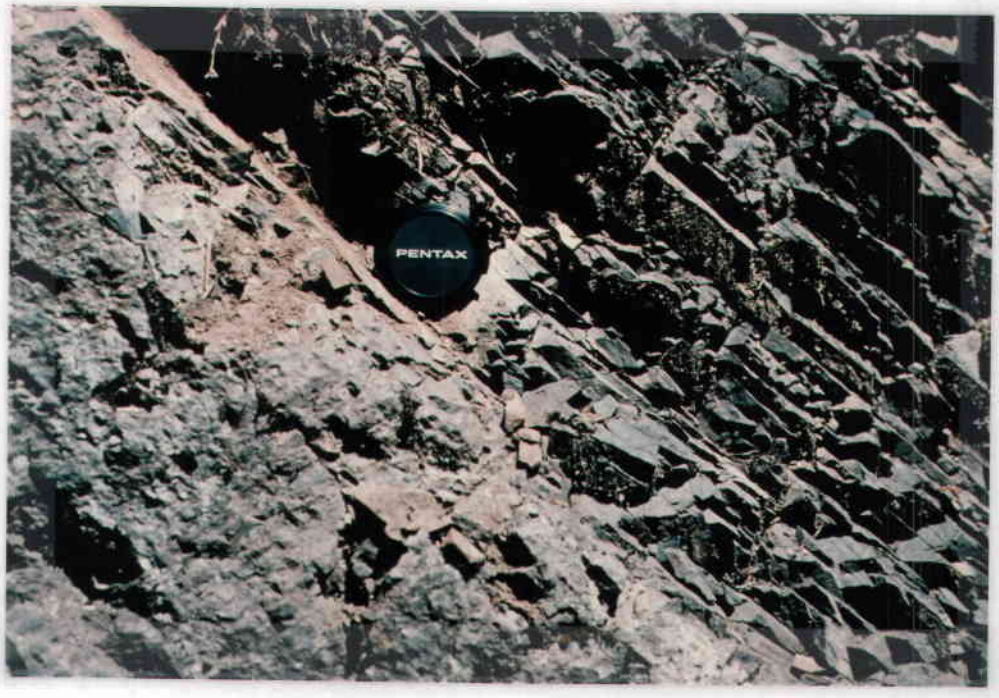

Figure 8. The Upper Triassic Kosk Member of the Modin Formation crops out near Arvison Flat a mile north of the map area. Steeply dipping argillites sharply overlie a volcanic breccia at this location.

flow near Iron Canyon (Sanborn, 1960).

In the northern five miles of the study area, light to dark gray porphyritic pyroxene andesites and olivine basalts overlie the Montgomery Creek Formation with slight unconformity. These volcanics dip at a lesser eastward angle than the underlying strata. These volcanic flows thicken to about 3,500 feet at Hagan Flat, 2.5 miles east of the study area. The contact with the underlying Eocene rocks is very poorly exposed and is hidden beneath well-developed soils and thick vegetation. The only contact observed lies about 200 yards southwest of Reynolds Creek (T37N, R1E, Sec. 29) in a roadcut. Underlying tan arkosic wackes grade to a reddish orange tuffaceous sandstone near the contact. In most cases, contacts were determined from topographic and botanic criteria. The capping volcanics form gently sloping plateaus and support a more conifer-rich flora than the underlying Eocene sediments. Outcrops of the andesite are confined mainly to roadcuts and incised stream valleys. Locally, well-developed platy jointing was observed (Fig. 9).

Although Western Cascade rocks are not recognized south of the Mount Shasta region (some 30 miles north of the study area), these volcanic rocks may be equivalent in age to some of them (MacDonald, 1966). Aune (1964) inferred a Miocene age for these volcanics because they are

Figure 9. Tertiary basalt flow exposed in a roadcut near Reynolds Creek. This basalt has well-developed platy jointing.

overlain by middle Pliocene diatomite beds east of the study area.

Southward from the town of Big Bend, the Eocene strata are overlain by dark gray to black basalts designated "Pliocene" on the Westwood Sheet (Lydon et al., 1960). These basalts are vesicular at some locations. As with the basalts and andesites to the north, these basalts are sporadically exposed, but contact relations with the underlying Eocene rocks are more frequently observed. The basalts dip at a lesser eastward angle than the volcanics to the north, and are nearly flat lying in places. Two miles south of Big Bend, the basalts form a highland called the Flat Woods, a relatively undissected plateau. The Flat Woods plateau extends for five miles to the south, capping the Montgomery Creek Formation (Fig. 4). The basalt flows are about 200 feet thick, and are much thinner than the volcanics to the north.

On the northern flanks of the Flat Woods, a basalt dike trending N65W cuts an Upper Cretaceous to lower Eocene conglomerate of the Montgomery Creek Formation (Fig. 10). This dike is probably related to the northern section basalts, based on petrographic similarity.
On the south flanks of the Flat Woods on Cove Road (T35N, R1W, Sec. 11), a contact between the Pliocene basalts and the underlying Eocene sediments is well exposed. The light gray Eocene arkosic wackes grade upward into a

Figure 10. Tertiary basalt dike cutting an Upper Cretaceous-lower Eocene(?) basal conglomerate of the Montgomery Creek Formation, near Pit 5 Powerhouse Road.

reddish orange tuff. Gray, white, and light orange altered volcanics and pumice are suspended in a tuffaceous matrix (Fig. 11). These volcanic clasts range from 0.5 to 8 inches in diameter. This tuffaceous zone is 20 feet thick, and is capped by Pliocene basalts.

The basalts crop out sporadically south of this contact for three miles along the east edge of a basin called The Cove. North of Hatchet Creek, these basalts crop out as low as 2,200 feet in elevation. South of the creek, the basalts overlie a thick succession of Eocene sandstones near the 2,600 foot contour (Fig. 12). This elevation discrepancy cannot be accounted for by regional dips and the basalts on both sides of the creek are petrographically similar. Therefore, faulting has possibly uplifted the volcanics on the south side of Hatchet Creek, or downdropped the volcanics on the north side. The fault trace is occupied by Hatchet Creek. An alternative to faulting could be that north of Hatchet Creek the basalt flows occupied a paleotopographic low.

South of Hatchet Creek on Cove Road (T35N, R1W, Sec. 25) the contact between the Eocene sandstones and the overlying basalts is well exposed. The buff arkosic wackes pass upward into reddish brown volcanic breccia, which in turn grades upward into the basalt. One-half mile to the west (Sec. 26) the gray Eocene sandstones

Figure 11. This tuff crops out along Cove Road on the south flanks of the Flat Woods. Altered volcanic rocks and pumice are suspended in a tuffaceous matrix. The tuff is overlain by Pliocene basalt flows.

Figure 12. Dark gray Pliocene basalt flows overlie tan-colored Eocene Montgomery Creek Formation sandstones on the south side of Hatchet Creek.

underlie a pale orange tuff. The tuff is overlain by dark gray Pliocene basalts (Fig. 13).

The Pliocene basalts crop out from Hillcrest (on Highway 299) southward for three miles to the southern limit of the study area. The basalts are poorly exposed; consequently contacts were estimated from topographic and floral changes. The basalts form more gradual terrain and support a more conifer-rich growth than the underlying sandstones.

Figure 13. Light gray strata of the Montgomery Creek Formation are overlain by dark gray Pliocene basalt flows on the south side of Hatchet Creek.

FIELD DESCRIPTION OF THE MONTGOMERY CREEK FORMATION

The Montgomery Creek Formation is composed of two distinct units differing widely in lithology. The lower unit, an Upper Cretaceous to lower Eocene(?) (Tenneco, 1984) basal conglomerate is overlain by an Eocene sequence of sandstones, siltstones, shales, conglomerates, and local lignite seams.

The Montgomery Creek Formation stratigraphic section was measured in two separate areas. One section is north of the Flat Woods basaltic plateau. The other section is located south of the plateau, a separation of about 5.5 miles. The Upper Cretaceous-lower Eocene conglomerate is recognized as the base of the Montgomery Creek Formation in both sections. The contact between the conglomerate and the underlying Middle Jurassic Bagley Andesite is well exposed in the northern section.

The rocks in both sections are very poorly exposed. They occur as several isolated outcrops. For this reason, the generalized columnar sections of the Montgomery Creek Formation were divided as shown in Fig. 14 (a-e). More detailed stratigraphic sections (designated as outcrops X_1, X_2, etc.) and descriptions of the Upper Cretaceous and Eocene strata are given in Appendix 1. Locations of the detailed sections are indicated on the geologic map of the area (Plate 1). Section measurement was by tape; offsets

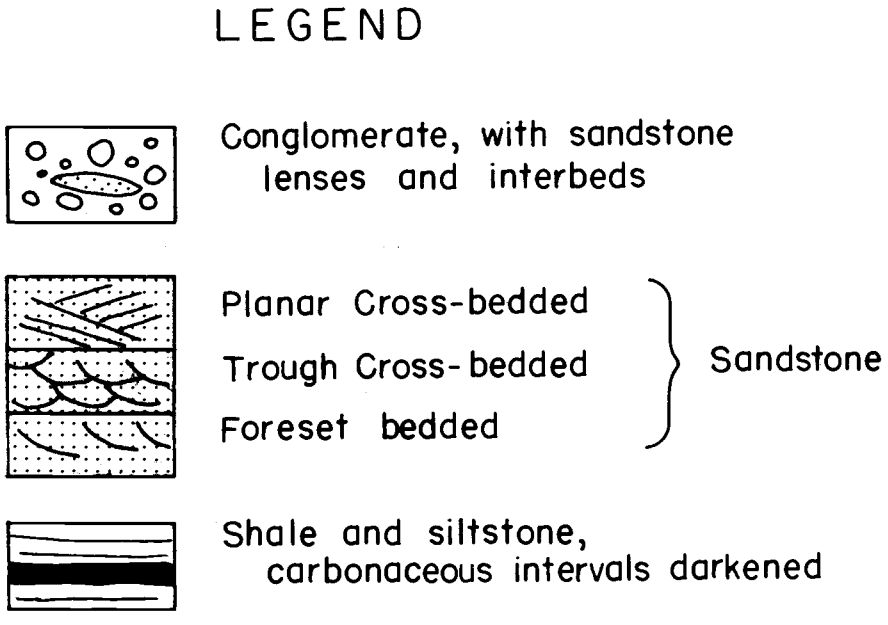

Figure 14(a). Legend for the Eocene Montgomery Creek Formation generalized stratigraphic columns.

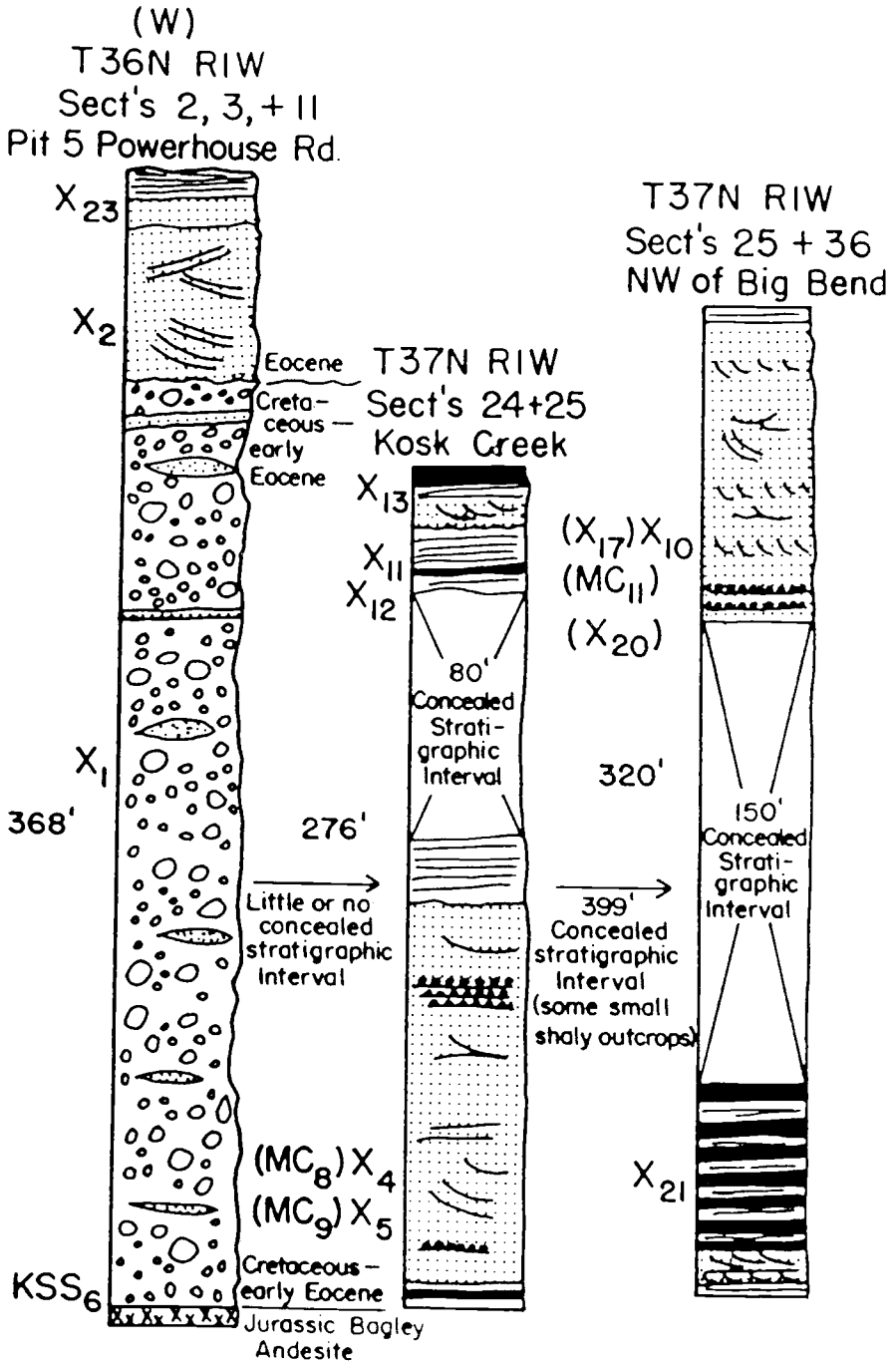

Figure 14(b): The northern section stratigraphic columns. Outcrop numbers indicated on left (X_1, X_2, etc.). Other outcrops or samples in a similar stratigraphic position shown in parentheses. The section is estimated to be 3,188 feet thick.

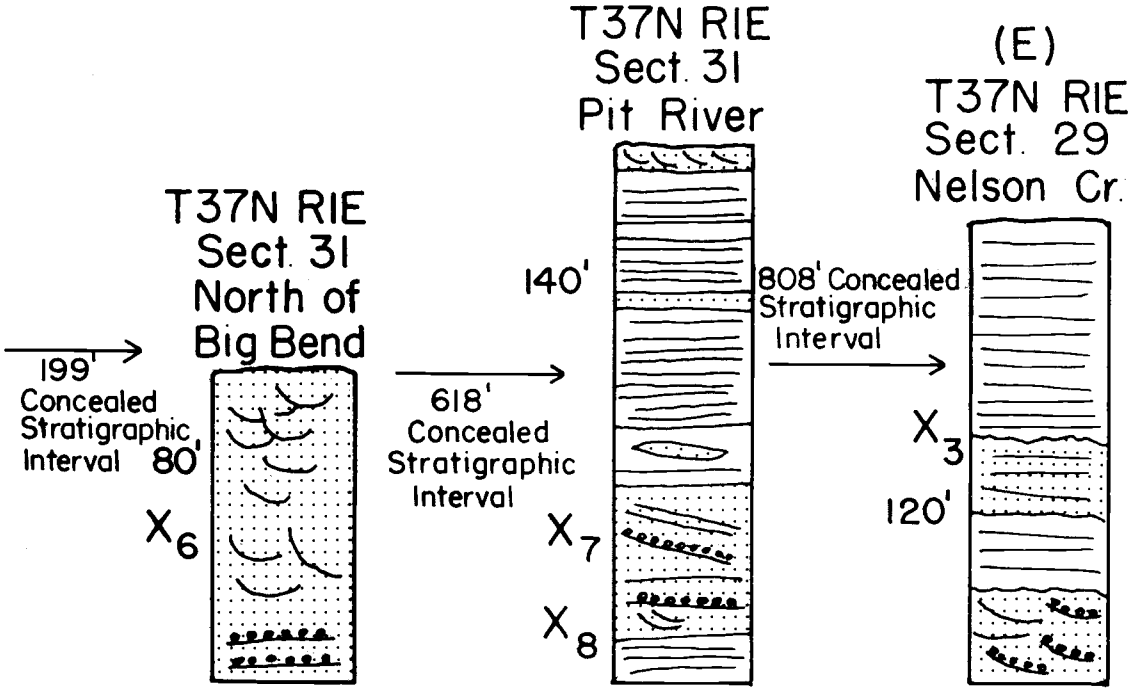

Figure 14(c). The northern section columns (continued)

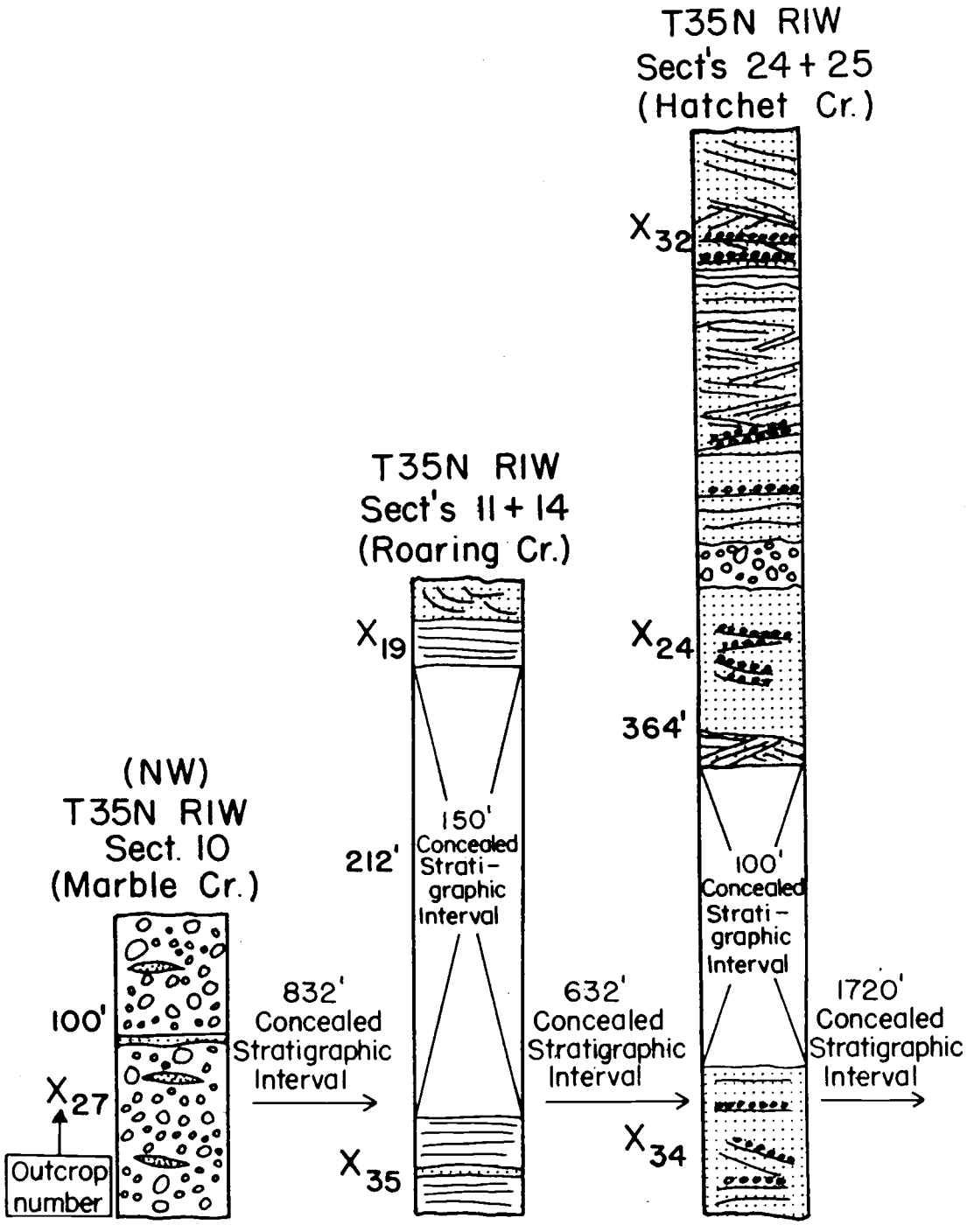

Figure 14(d). The southern section stratigraphic columns. The section is estimated to be 4,596 ft. thick.

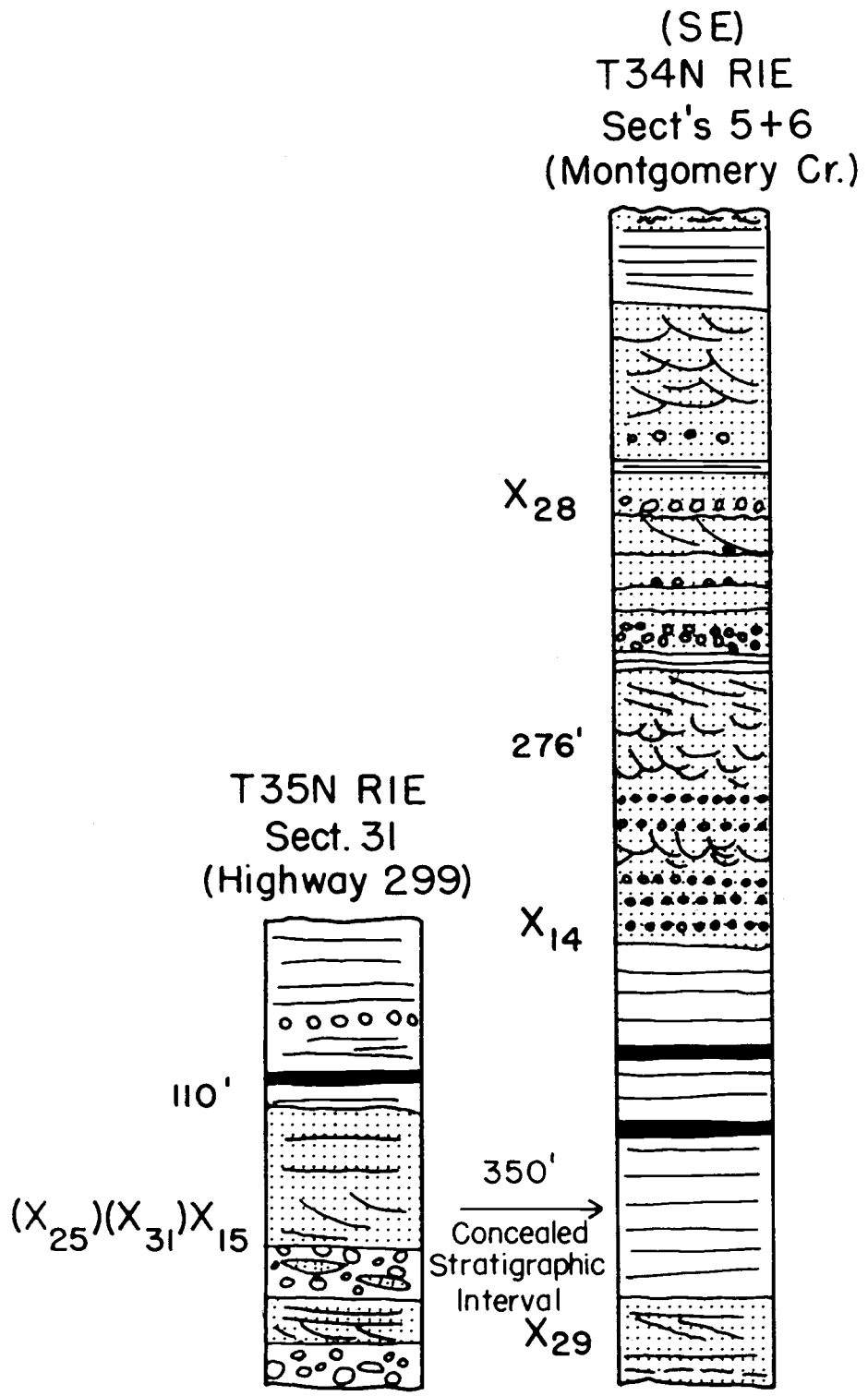

Figure 14(e). The southern section columns (continued)

were taken where appropriate. Lithologic samples were collected at various levels in both sections.

Northern Section

The Montgomery Creek Formation northern section is 3,188 feet thick. The calculation of this thickness was accomplished in the following ways: (1) The average regional strike and dip (N5E, 14SE) of the strata were calculated from several outcrop readings; (2) actual outcrop thickness was measured; (3) elevation difference and horizontal distance between outcrops were estimated from the map; (4) on the basis of the regional dip, horizontal distance and elevation difference, the thicknesses of obscured strata between outcrops were calculated (Fig. 15). The calculated and outcrop thicknesses were then added together to obtain the total thickness of the stratigraphic section.

The formation is composed of a 300 foot basal conglomerate, overlain by shales, siltstones, sandstones, pebbly conglomerates and local lignite seams.

The basal contact is marked by an angular unconformity between the Upper Cretaceous-lower Eocene conglomerate and the underlying Middle Jurassic Bagley Andesite (Fig. 16). This contact is exposed on Pit 5 Powerhouse Road, 1.75 miles west of the Big Bend Road (T36N, R1W, Sec. 11).

T_1 = (100') Cos 14° = 97.02'

T_2 = (1000') Sin 14° = 241.92'

$T_1 + T_2$ = 97.02' + 241.92'
= 338.94'

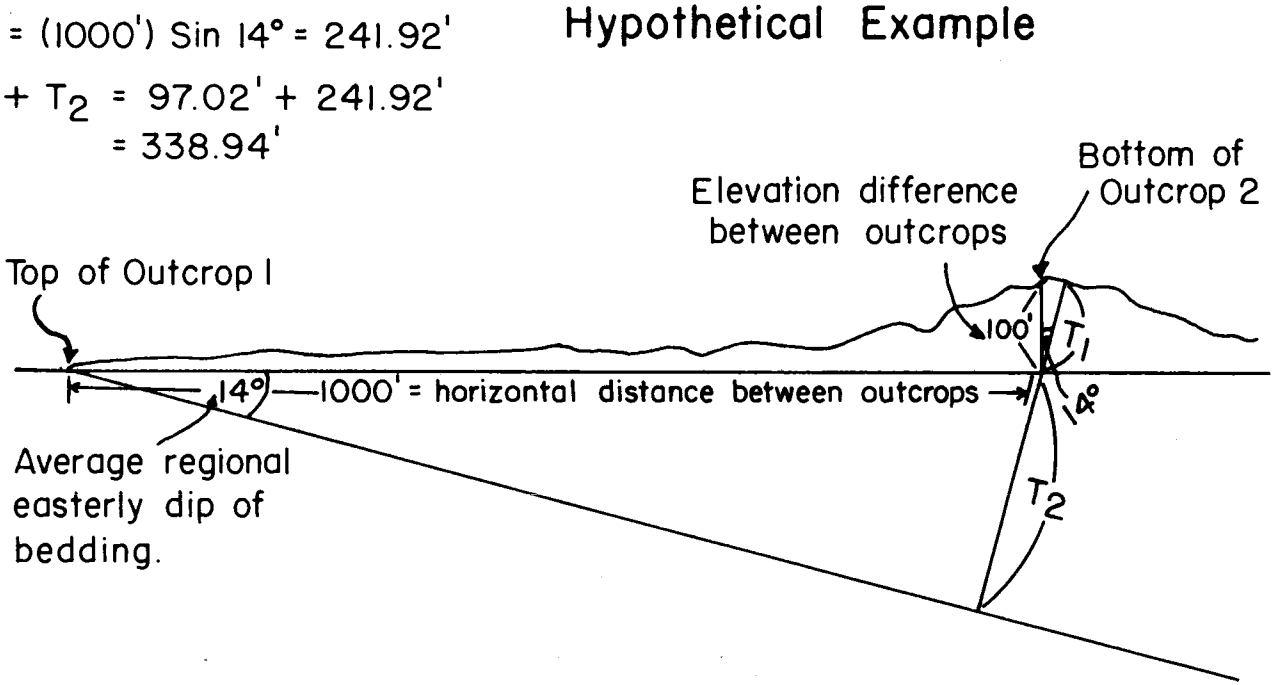

Figure 15. Method used in calculating unknown stratigraphic thickness between two isolated outcrops. In this hypothetical example, T_1 = stratigraphic thickness due to elevation difference between outcrops; T_2 = stratigraphic thickness concealed between the two outcrops; T_1 and T_2 = total stratigraphic thickness concealed between the two outcrops.

Figure 16. Contact between the Jurassic Bagley Andesite (below) and the Upper Cretaceous-lower Eocene basal conglomerate of the Montgomery Creek Formation. This contact is exposed on Pit 5 Powerhouse Road.

The attitude of the andesite is uncertain. The upper contact is unconformably overlain by Tertiary pyroxene andesites and basalts of the High Cascade Range.

Basal Conglomerate

The Upper Cretaceous-lower Eocene conglomerate (outcrop X_1 in appendix 1 and Fig. 17) crops out for nearly a mile along Pit 5 Powerhouse Road, and is 300 feet thick. The conglomerate is regarded as nonmarine because: (1) marine fossils are lacking and (2) carbonaceous mudstone beds and carbonized wood fragments are present within the conglomerate.

The conglomerate is very poorly sorted. Clasts range from 0.25 to 12 inches in diameter. The conglomerate is matrix-supported near the base; the clasts are enclosed in a medium- to fine-grained sandstone. The conglomerate is mostly clast-supported near the top. The clasts are well rounded to rounded (Powers, 1953), with tabular clasts imbricated in subparallel fashion. Imbricated pebbles and cobbles dip in an upstream direction in fluvial environments, as reported by Reineck and Singh (1973). The conglomerate framework clasts are composed mainly of porphyritic and aphyric mafic volcanics, and dark gray to black argillite. Smaller amounts of rhyolite, chert, and quartzite were also found as framework clasts. Interbedded with the conglomerate are discontinuous lens-shaped

Figure 17. The Upper Cretaceous-lower Eocene basal conglomerate is exposed along Pit 5 Powerhouse Road. Lighter colored sandstones form thin interbeds in the conglomerate.

beds of medium- to fine-grained arkosic wackes, from one to three feet in thickness. Foreset bedding was observed in some of these sandstone lenses. Discontinuous lenses of dark gray mudstone also were found in the conglomerate, ranging up to a foot in thickness. One mudstone lens yielded pollen used to obtain a Late Cretaceous to early Eocene age for the enclosing conglomerates (Tenneco, 1984).

This basal conglomerate was deposited very close to its source during extremely high-energy flow conditions, as judged by the size and poor sorting of its framework clasts. Also, some of the volcanic clasts are similar petrographically to the underlying Jurassic Bagley Andesite. The stratigraphic column of the basal conglomerate (Fig. 18) is similar to profiles drawn by Miall (1977). In his "Scott-type" braided river depositional profile, the conglomerates are crudely bedded longitudinal bar deposits, while the sandstone and mudstone lenses represent a filling of channels and scour hollows during low water. Rapid subsidence must have accompanied deposition of the Montgomery Creek basal conglomerates for such large thicknesses to be obtained. Also, normal faulting at basin margins is commonly associated with thick conglomerate sequences (Heward, 1978; Fig. 19, this report).

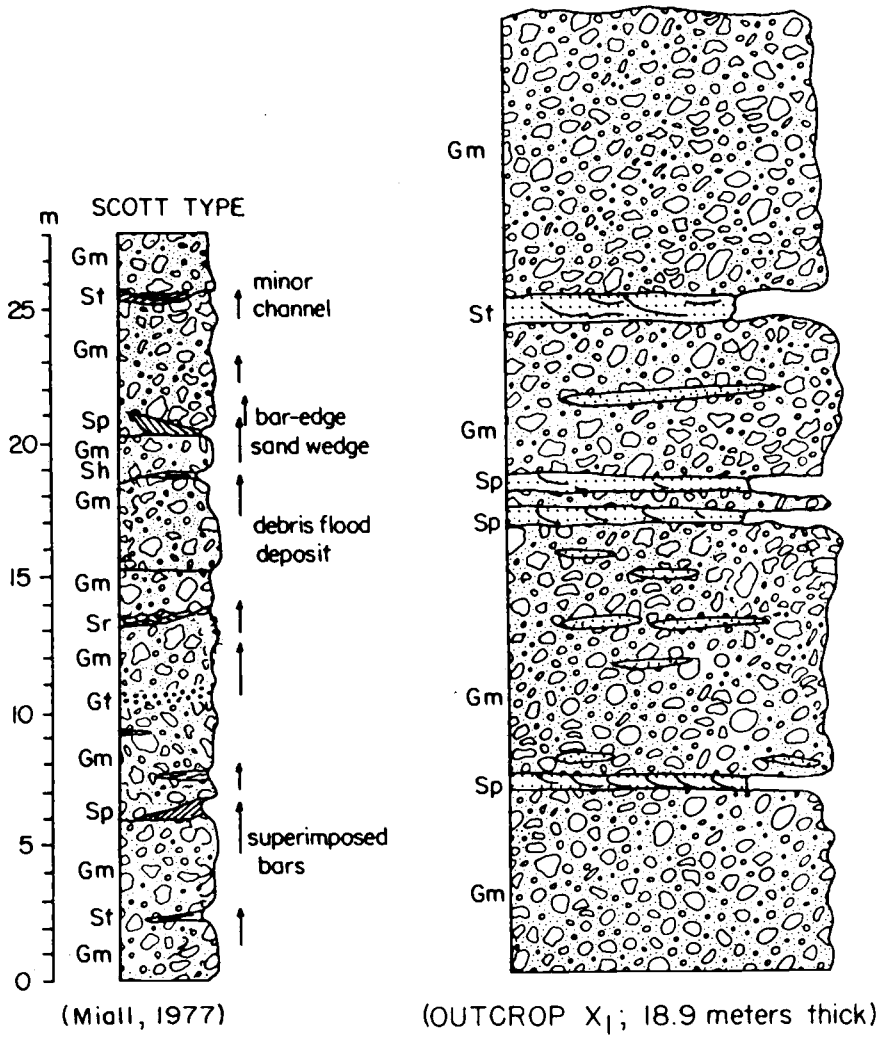

Figure 18. Stratigraphic columns of Scott-type braided river model (Miall, 1977) and outcrop X_1 (right). Both sequences are dominated by thick congomerates, and are interpreted to be proximal braided river deposits. An explanation of the symbols used by Miall (1977) is given as follows: Gm = Massive or crudely bedded gravel; longitudinal bar or channel-lag deposits. St = trough cross-bedded sandstones deposited by migrating dunes. Sp = planar cross-bedded sandstones; linguoid bar deposits. Sh = horizontally bedded sandstones; deposited by planar bed flow. Fl = siltstones and shales; overbank deposits.

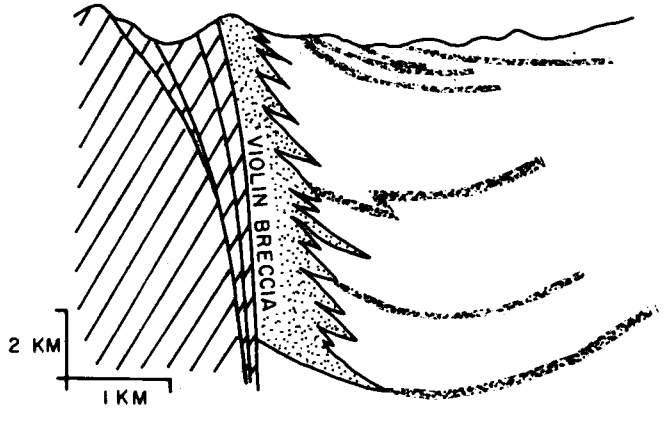

Figure 19. Thick conglomerate sequence associated with basin margin faulting (from Heward, 1978).

Montgomery Creek Formation Eocene Strata (Northern Section)

Directly overlying the Upper Cretaceous-lower Eocene conglomerates are 48 feet of tan to light gray, medium-grained arkosic wackes which probably make up the base of the upper Eocene section (outcrop X_2). These sandstones were deposited in channels cut into the underlying conglomerates, and represent a distinct lower flow regime. The sandstones have foreset bedding and low-angle trough cross-bedding. These sedimentary structures are common in strata higher in the northern section.

An offset of three miles northward along strike was taken to encounter strata estimated to be immediately higher in the Eocene section. These outcrops are found at the junction of Iron Canyon Reservoir Road and Arvison Flat Road (T37N, R1W, Sec. 24), and can be traced northward along strike for 1.25 miles, subparallel to Kosk Creek. Immediately north of the junction, outcrops consist of planar bedded siltstones and shales overlain by medium-grained, light gray arkosic wackes. The strata dip nearly due east in this area. Small-scale normal faulting is common. In one outcrop (X_4), the sandstones form a large channel 130 feet deep and 300 feet wide (Fig. 20). The channel margins dip shallowly toward each other. The sandstones are dotted with calcareous concretions,

Figure 20. Large sandstone outcrop, dotted with calcareous concretions. The geometry of this sandstone body is similar to that of a channel cross-section.

ranging from one to six feet in diameter. Well-defined foreset beds are common. Some foresets are characterized by pebbly lag deposits. On the channel margin, the weight of the overlying sandstone has penecontemporaneously steeply tilted the siltstones and shales (Fig. 21). Proceeding northward, the outcrops become less frequent, and are dominantly siltstones and shales. Some of the shales are carbonaceous, as observed near the junction of Kosk Creek and Baker Creek (outcrops X_{12} and X_{13}, Fig. 22).

To the southeast of the Iron Canyon Reservoir Road - Arvison Flat Road intersection, the Eocene strata are very poorly exposed. Shales and siltstones are exposed for 1.5 miles in several small, isolated outcrops along the road to the town of Big Bend (T37N, R1W, Sec. 27). Many of these shales are carbonaceous, with local lignites. Some of these strata strike southeast-northwest and dip to the northeast, as opposed to the due east dip of the sediments along Kosk Creek. Perhaps faulting, slumping or landslides have altered the orientation of these sediments.

About 0.5 miles northwest of Big Bend (T37N, R1W, Sec. 36), a 66 foot sequence of gray to dark gray shales, carbonaceous shales, lignite, and thin, tan arkosic wacke is exposed (outcrop X_{21}, Fig. 23). These sediments occupy a structural position 399 feet higher than the strata

Figure 21. Margin of channel shown in Figure 20. The weight of the overlying sandstone has tilted the underlying carbonaceous shales.

Figure 22. Carbonaceous shales are exposed along Arvison Flat Road near the confluence of Kosk Creek and Baker Creek.

Figure 23. Relatively steeply dipping carbonaceous shales and lignite, overlying a thin sandstone interbed. This sequence crops out along Big Bend Road, about 0.5 miles northwest of the town of Big Bend.

along Kosk Creek (Fig. 14b). The sequence dips steeply to the southeast, suggesting that it has been tilted due to local faulting. The shales are planar bedded and laminated; some of them have been buckled by soft sediment deformation. About 0.25 miles to the north (Sec. 25), 92 feet of tan arkosic wackes are exposed (outcrop X_{10}). These sandstones overlie the shales and form a fining upward sequence. The basal 22 feet are coarse-grained pebbly sandstones with well-defined planar bedding. These sandstones are overlain by 60 feet of medium- to very fine-grained arkosic wackes, which fine upward. These sandstones have well-defined foreset and trough cross-bedding and laminae. This is overlain by 10 feet of planar bedded and laminated siltstones and very fine-grained sandstones, completing the fining-upward sequence. The outcrop is mottled with calcareous concretions one to seven feet in diameter; some are elongated parallel to the bedding.

Southeast of this outcrop, the Eocene strata again strike nearly north-south and dip eastward. About 0.25 miles due north of the town of Big Bend, 44 feet of tan colored arkosic wacke crop out (outcrop X_6). This se quence is 199 stratigraphic feet higher than outcrop X_{10}. These sandstones have abundant low-angle trough cross- and foreset bedding. The bedding is well defined by differ-

ential weathering of pebbly layers. Southeast of this outcrop, the Eocene strata are poorly exposed for 0.6 miles before reappearing along the Pit River, about 0.5 miles east of Big Bend. This outcrop (X_7 and X_8) is 618 feet higher stratigraphically than strata to the west. The outcrop is laterally extensive, paralleling the Pit River for about 400 yards (Fig. 24). The sequence coarsens upward from planar bedded very fine-grained sandstones and siltstones to 30 feet of medium- to coarse-grained, gray to brown arkosic wackes. These cliff-forming sandstones have large-scale foreset bedding, pebbly horizons, and inclusions of carbonized wood fragments. Overlying these sandstones with sharp contact are 90 feet of brown, planar bedded shales, siltstones and isolated fine-grained arkosic wackes. The siltstones and shales form several fining-upward cycles within this sequence.

About 0.6 miles to the northeast of this outcrop, 117 feet of shales, siltstones, and arkosic wackes are exposed along the south bank of Nelson Creek (outcrop X_3). This sequence is 808 feet higher stratigraphically than the previous outcrop. The basal 25 feet consists of tan, medium-grained arkosic wacke, with large-scale planar cross-beds, foreset beds, and planar beds. Some of the bedding is well defined by pebbly layers. This arkosic wacke is overlain by 92 feet of siltstone and shale, with

Figure 24. This cliff-forming sandstone is exposed for about 400 yards along the Pit River, east of Big Bend. These sandstones have large-scale foreset beds and inclusions of carbonized wood fragments.

local fine-grained sandstones. The siltstones and shales form several coarsening upward cycles. A 6 inch thick silicified layer lies at the base of one of the fine-grained sandstones. Within this layer, silicified and carbonized plant remains are found (Fig. 25).

Southeast of the study area, two small Eocene arkosic wacke outcrops were observed along the Pit River. One outcrop is 0.5 miles east of Tunnel Reservoir (T36N, R1E, Sec. 8), and the other is farther southeast at Hagen Flat (Sec. 9). These outcrops are small and weathered, and accurate orientation of the bedding could not be obtained. If these sandstones have a similar easterly dip, an additional 2,368 stratigraphic feet could be added to the thickness of the Montgomery Creek Formation northern section.

Discussion of the Eocene Northern Section
Depositional Environment

Several lines of evidence suggest that the Montgomery Creek Formation northern section strata were deposited in a nonmarine, fluvial environment. This fluvial environment was active in a subsiding basin, as implied by the relatively large thickness of the sequence. The strata are thought to be nonmarine because (1) invertebrate marine fossils are absent; (2) evidence of fluvial deposition is abundant. Cyclic sedimentation is a feature

Figure 25. Silicified and carbonized plant fragments found in outcrop along Nelson Creek.

common to fluvial deposition (Beerbower, 1964; McLean and Jerzykiewicz, 1978). This cyclic sedimentation is represented by alternating sandstone, siltstone and shale units. It will be demonstrated that the sandstones are mainly river channel deposits, whereas the siltstones and shales are fine-grained overbank flood basin deposits (McLean and Jerzykiewicz, 1978).

(A) Sandstone Units

1. Primary Sedimentary Structures. Primary sedimentary structures found in the sandstones include large- and small-scale foreset bedding, planar bedding, trough cross-bedding (Fig. 26) and trough cross-laminae. Less commonly, planar cross-bedding (Fig. 26) and normal graded bedding were observed. The bedding is defined by pebbles or lithic-rich sands. Foreset beds develop by sand grains avalanching down the lee face of migrating dunes (Reineck and Singh, 1973). Trough cross-bedding consists of foresets separated from adjacent beds by surfaces of erosion, nondeposition, or abrupt change in lithology (Potter and Pettijohn, 1963). Therefore, both foreset bedding and trough cross-bedding can be attributed to deposition by migrating dunes. Both bedforms are deposited in the lower flow regime (Simons et al., 1965). The planar bedding is deposited in the lower part of the

Figure 26. (top) Low-angle trough cross-bedding in a northern section sandstone; (bottom) Planar cross-bedding, defined by heavy minerals and lithic fragments.

upper flow regime. McLean and Jerzykiewicz (1978) regard this type of bedding to have been deposited by flood events. The trough cross-laminae could have been deposited by migrating ripples (Reineck and Singh, 1973). These laminae are deposited in the lower flow regime.

2. Fining-upward Sequences. Some of the sandstone outcrops display a fining-upward sequence, indicative of point bar deposition on meandering rivers (Walker, 1976). Outcrop X_{10} (Fig. 27) has an upward change in sedimentary structures characteristic of point bar deposition: planar bedding passes upward into foreset and trough cross-bedding. Trough cross- and planar lamination complete the fining-upward sequence. This is analogous to a stratigraphic column described by Leeder (1973) (Fig. 27). Leeder interpreted these strata to be deposited by a highly sinuous meandering stream. A point bar is deposited on the inside of the meander loop, while erosion occurs on the outer parts of the loop (Walker, 1976).

Other northern section sandstone outcrops (X_{17}, X_6, X_8) show little or no fining upward. They also lack consistent upward change in bedding structures. These sandstone units typically have alternating foreset bedding, planar bedding, and trough cross-bedding. Such outcrops are more characteristic of low-sinuosity fluvial sedimentation, such as that described by Leeder (1973). However, the Montgomery Creek Formation sandstones were

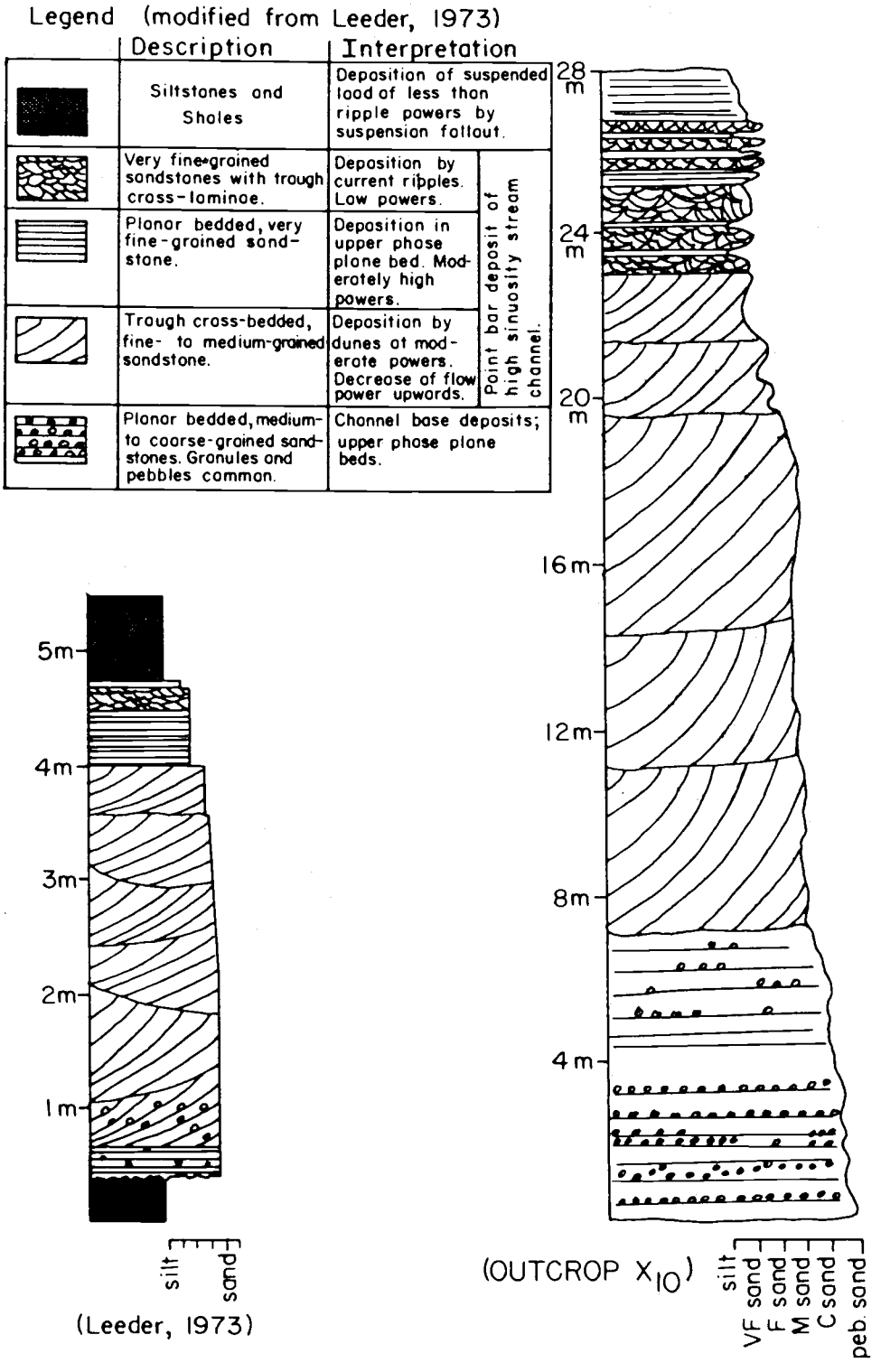

Figure 27. Stratigraphic columns showing fining-upward meandering river deposits of Leeder (1973) and outcrop X_{10} (right). The upward change in bedding structures is similar in the two columns.

probably deposited by meandering rivers. This interpretation is supported because they are adjacent to fine-grained siltstone and shale units of presumed flood basin deposition.

(B) Siltstone and Shale Units

Outside of the main channel, deposition in flood basins takes place by addition of sediment during flood stage when the river overtops its banks (Walker, 1976). Siltstones and shales are widespread in the northern section strata. Outcrops X_7 and X_3 have thick (90 foot) siltstone and shale units. These units are interpreted to be flood basin deposits on the following evidence: (1) X_7 has several fining-upward siltstone-shale cycles. This is indicative of multiple depositional events in flood basins (McLean and Jerzykiewicz, 1978). The low energy siltstones and shales were deposited from suspension during and after the declining phase of the flood; (2) both X_3 and X_7 have intercalated fine-grained sandstones, two to 14 feet thick. These planar bedded sandstones are similar to crevasse splay sands described by McLean and Jerzykiewicz (1978). These sands were deposited during the active phase of flooding in the flood basin. Reineck and Singh (1973) wrote that thick flood basin accumulations result when stream channels become relatively fixed in their position. Therefore, longer periods are avail-

able for deposition in flood basins.

Some outcrops (X_{13}, X_{21}) in the lower part of the northern section have large amounts of carbonaceous shale or lignite interbedded with the siltstones and shales. Gibson (1977) reported that luxuriant vegetation growing in low-lying swamps or marshes in the flood basin is responsible for the accumulation of carbonaceous strata. A high amount of rainfall can be inferred to contribute to this abundant vegetation.

In general, the relatively large thickness of fine-grained flood basin deposits in the northern section supports a meandering river sedimentation model. Braided rivers usually have thin, poorly preserved flood basin deposits. This is because: (1) silt and clay are transported through the system without significant accumulation (Walker, 1976); (2) the braided river has frequently shifted laterally, destroying any accumulation of flood basin deposits (Campbell, 1976). However, some braided rivers have considerable flood basin accumulation.

(C) Relation of Channel Sandstones to Flood Basin Deposits

In several outcrops, medium- to coarse-grained sandstones were observed to grade either laterally or vertically into flood basin siltstones and shales. In many cases, the transition is abrupt (outcrops X_5, X_3, X_7).

Walker (1976) explained this distribution of sediments: in a meandering river system, meander loops are cut off, and subsequently filled with silts and clays. These clay plugs are resistant to erosion. The clay plugs confine the meander belt, causing the channel sands to build up above the general level of the flood basin. This situation will persist until a catastrophic levee break results in the sudden switch of the entire river channel to a lower part of the flood basin. Thus, the sand body geometry should be channel sandstone lenticles interbedded with flood basin siltstones and shales. This is shown in Figure 28 from Allen (1965). Considering the evidence presented, this depositional model is applicable to the Eocene Montgomery Creek Formation northern section.

Southern Section

The Montgomery Creek Formation southern section is 4,596 feet thick. This thickness was calculated using the same procedure as for the northern section (Fig. 15). An easterly 16^{o} average regional dip was calculated for the southern section. The section is composed of a 100 foot thick basal conglomerate, overlain by 4,496 feet of sandstones, conglomerates, siltstones, shales, carbonaceous shales, and rare lignite and bituminous coal seams (Fig. 14 d-e).

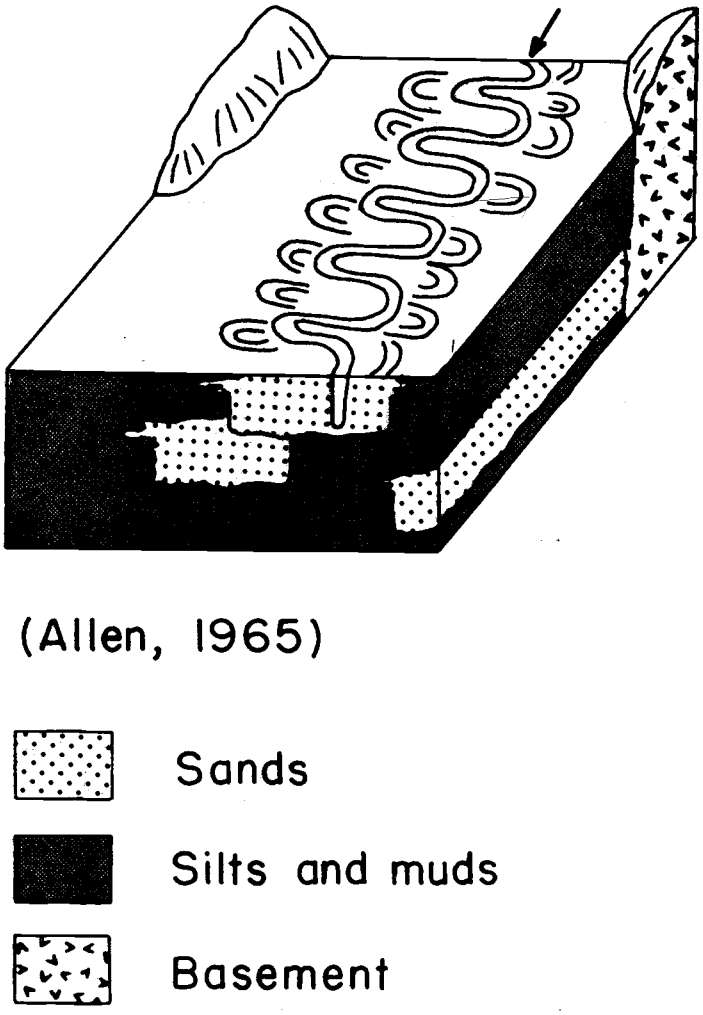

Figure 28. Facies model of a depositional basin dominated by meandering river sedimentation (from Allen, 1965). A model similar to this could be applied to much of the Montgomery Creek Formation northern section.

The basal conglomerate probably overlies the Middle Jurassic Bagley Andesite, although a basal contact was not observed. The Upper Cretaceous to Eocene strata are unconformably overlain by Cascade Range Pliocene basalts.

Basal Conglomerate

This conglomerate (outcrop X_{27}) is located near Marble Creek (Fig. 29), 0.25 miles northwest of the Roaring Creek Indian Ranchera (T25N, R1W, Sec. 10). This conglomerate is inferred to be Late Cretaceous to early Eocene(?) in age because: (1) appearance and composition are similar to the northern section conglomerate; (2) it is located about 300 yards north of exposed underlying Jurassic Bagley Andesite; (3) the conglomerate is 0.7 miles west of the nearest southern section Eocene outcrop. Taking into account the regional east dip, the conglomerate is considerably lower stratigraphically than the overlying Eocene southern section.

This conglomerate is very poorly sorted. Clasts range from 0.25 inches to 6 inches in diameter. The clasts are rounded to well rounded and are enclosed in a tan, fine-grained sandstone matrix. Tabular clasts are imbricated in subparallel fashion to assumed flow direction, dipping upstream (to the east). Andesite, basalt, chert, quartzite and argillite make up the frame-

Figure 29. Southern section Upper Cretaceous-lower Eocene(?) basal conglomerate, exposed along road near Marble Creek. The conglomerate has light colored sandstone interbeds.

work clast lithologies. Lens-shaped beds of arkosic wackes, 6 inches to 2 feet in thickness, are interbedded with the conglomerate. These conglomerates are interpreted to be proximal braided river deposits, as described for the northern section conglomerates.

Montgomery Creek Formation Eocene Strata (Southern Section)

An offset of 0.7 miles eastward from Upper Cretaceous-lower Eocene conglomerates was taken to encounter the overlying Eocene strata, located on Roaring Creek (T35N, R1W, Sec. 14). Tan to light gray fine-grained arkosic wackes, siltstones and shales crop out sporadically along this creek (outcrop X_{35}). These strata are stratigraphically higher than the conglomerates by about 832 feet (Fig. 14d) and are planar bedded (Fig. 30). Small-scale faulting was observed, resulting from sandstone slumping into the underlying shales and siltstones. Thirty feet of planar bedded gray to tan fine-grained sandstones, siltstones, and shales are exposed on Cove Road (Sec. 11, outcrop X_{19}), about 1.25 miles to the north along strike. Some of these strata contain plant remains, and some carbonaceous shale was found.

The next extensive Eocene outcrops are located 2.5 miles to the south, on the south side of Hatchet Creek (T35N, R1W, Secs. 24, 25; Fig. 12). These outcrops (X_{24},

Figure 30. Eocene strata exposed along Roaring Creek. This planar bedded, fine-grained sandstone grades upward into siltstones and shales.

X_{32}, X_{34}) are separated from the underlying sediments to the north by 632 stratigraphic feet. The strata are dominantly medium- to coarse-grained, tan to light gray lithic-rich arkosic wacke. There also are minor shales, siltstones, and pebbly conglomerates. These sediments are exposed in a series of cliffy outcrops, totalling 364 feet in thickness. The lower part of the sequence is characterized by planar and foreset bedded arkosic wacke. The bedding is defined by pebbly layers. Spectacular large-scale planar cross-bedding is conspicuous in the sandstones higher in the sequence (Fig. 31). The bedding is well defined by alternating lithic-rich and quartzofeldspathic layers. This planar cross-bedded sandstone is laterally extensive. One outcrop parallels Hatchet Creek for about 600 yards. About 0.5 miles to the west of these outcrops, across a narrow valley, light gray, lithic-rich arkosic wackes are exposed (Sec. 26). These strata are unusual in that they dip nearly due west, opposite the regional dip direction.

The next significant Eocene exposure (outcrop X_{15}) is 1.5 miles to the southeast, located on a sharp bend of Highway 299 (T35N, R1E, Sec. 31; Fig. 32). This outcrop is stratigraphically higher than the previous strata by 1720 feet. This is a fining-upward sequence, 107 feet in thickness. The bottom 34 feet consist of two 11 foot conglomerate beds separated by a tan to gray arkosic

Figure 31. Sandstone outcrop on the south side of Hatchet Creek, displaying large-scale planar cross-bedding. The bedding is defined by alternating lithic-rich and quartzo-feldspathic layers (shirt for scale).

Figure 32. Alternating conglomerate and sandstone beds in an outcrop exposed along Highway 299, east of the town of Montgomery Creek.

wacke. The conglomerates are poorly sorted. The framework clasts range from 0.25 inches to 8 inches in diameter. Rhyolite, andesite, basalt, chert, quartzite, and granite represent the clast lithologies. Overlying this basal series are 32 feet of medium-grained arkosic wacke, fining upward to very fine-grained sandstone. Planar and foreset bedding are common here; planar bedding dominates upward. Overlying this part are 40 feet of planar bedded siltstones and shales, with one thin conglomerate bed. This outcrop is cut by a normal fault, which offsets bedding vertically by 10 feet. About 1.25 miles due east from this outcrop is a fining-upward sequence of arkosic wackes (outcrop X_{25}). This exposure is 0.25 miles northwest of the town of Montgomery Creek. This outcrop fines upward from coarse-grained pebbly sandstones to fine-grained sandstones. Large-scale planar cross bedding gives way to planar bedding upward. These strata dip due west, and are nearly on strike with the west-dipping strata 1.5 miles to the north. Therefore, a north-northwest-trending anticline may exist from the town of Montgomery Creek northward for at least 1.5 miles.

Southeast from the roadcut on Highway 299, a series of outcrops (X_{14}, X_{28}, X_{29}) is exposed along the east side of Montgomery Creek (Figs. 33 and 34; T34N, R1E, Secs. 5 and 6). These outcrops lie in the Montgomery Creek Forma-

tion type section described by Anderson and Russell (1939). These strata stratigraphically overlie outcrop X_{15} by 350 feet. The Eocene strata form a prominent strike ridge, with 276 feet of measured section. Some of the outcrops are laterally extensive, being exposed along strike for about 700 yards. The base of this section consists of 20 feet of light gray, medium-grained arkosic wacke. This sandstone has foreset and planar bedding, and bituminous stringers concentrated near the base (Fig. 35). The sandstone is overlain at a sharp contact by 85 feet of planar bedded siltstone, shale, and local carbonaceous shale. These sediments pass upward into 44 feet of interbedded medium-grained arkosic wackes and conglomerates. The conglomerate beds are about a foot thick, with clasts ranging from 0.25 inches to 5 inches in diameter. Basalt, andesite, rhyolite, chert, quartzite, and granite represent the clast lithologies. This unit is overlain by 29 feet of arkosic wackes, fining upward from medium-grained sandstone to siltstone. These sandstones have well developed planar to low-angle trough cross-beds (Fig. 35). The bedding is defined by very coarse-grained lithic fragments. Sharply overlying this series are 30 feet of strata, fining upward from conglomerate to fine-grained sandstone. These strata pass upward into 72 feet of interbedded conglomerates, sandstones, siltstones, and shales. The sandstones display well developed planar to

Figure 33. Montgomery Creek Formation type section strata forming ridge on the east side of Montgomery Creek.

Figure 34. Outcrop X_{14} in type section area, showing large concretions up to six feet in diameter. These concretions are crudely parallel to the bedding.

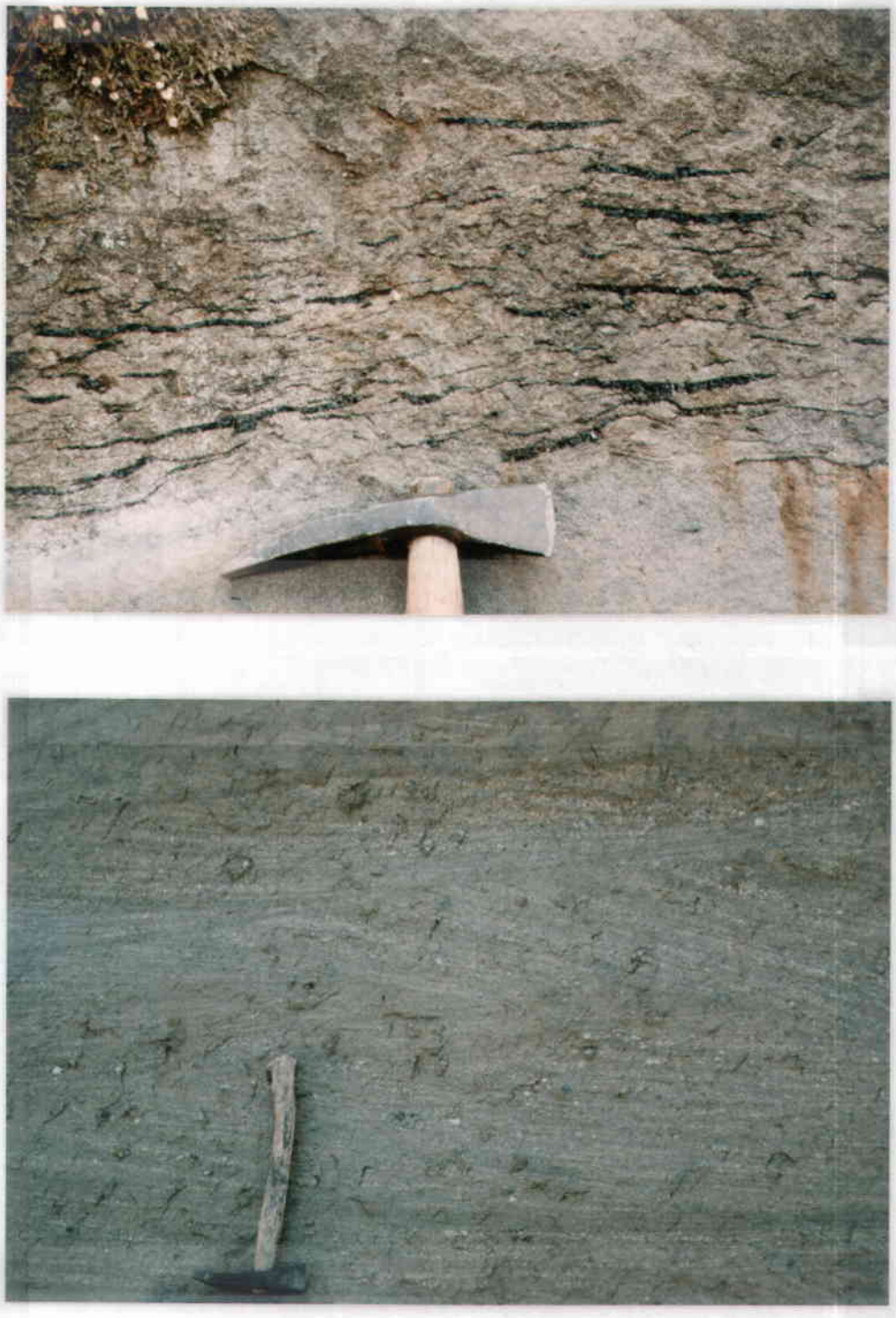

Figure 35. (top) Carbonaceous stringers in sandstone in the type section area; (below) Sandstones in type section area displaying planar to low-angle trough cross-bedding.

low-angle trough cross-bedding, similar to that in the underlying strata.

Discussion of the Southern Section Depositional Environment

The Eocene southern section strata were deposited in a nonmarine, fluvial environment, but differ from the northern section in the following ways: (1) presence of pebbly to cobbly conglomerate interbeds (in outcrops X_{15}, X_{14}, X_{24}, X_{31}), up to 14 feet in thickness; (2) greater abundance of large-scale planar cross-bedded strata, especially in outcrops on the south side of Hatchet Creek (X_{32}, X_{24}); (3) the sandstone outcrops on the south side of Hatchet Creek and the east side of Montgomery Creek (X_{14}) are both thick and laterally extensive. This sandstone body geometry was not observed in the northern section strata; (4) there are much less carbonaceous strata in the Eocene southern section. Only a few thin carbonaceous shale beds, bituminous stringers, and a thin bituminous seam (near outcrop X_{15}) were observed.

The relatively great thickness of the southern section implies that these strata were deposited in a subsiding basin, not unlike the northern section. However, the evidence given above points to a greater contribution by braided rivers. The sequence on the south side of Hatchet Creek has abundant large-scale planar cross beds,

some conglomerate beds, and rare flood basin siltstones and shales. These characteristics are consistent with the Platte-type braided stream model of Miall (1977) (Fig. 36). In outcrop X_{24}, the planar cross-beds could represent avalanche slope progradation in linguoid bar deposits (Miall, 1977). Mrakovich and Coogan (1974) suggest that planar cross-beds are formed when bed load is transported as large transverse bars. The conglomerates represent longitudinal bar deposits as described earlier.

The Eocene strata east and north of Montgomery Creek (outcrops X_{15}, X_{29}, X_{14}) are thick and laterally extensive, but differ from the Hatchet Creek outcrops in the following ways: (1) there are relatively thick flood basin siltstones, shales, and thin carbonaceous shales; (2) fining upward cycles occur in the sandstones; (3) trough cross-bedding predominates over planar cross-bedding. These characteristics imply a meandering river sedimentation model (Walker, 1976). On the other hand, the wide lateral extent of the sandstones with conglomerate interbeds favors the Donjek-type braided river model (Miall, 1977; Fig. 37). McLean and Jerzykiewicz (1978) observed thick flood basin deposits associated with sandy braided river deposits. These workers suggest that other factors such as river flooding, tectonics, and climate, in addition to channel type,

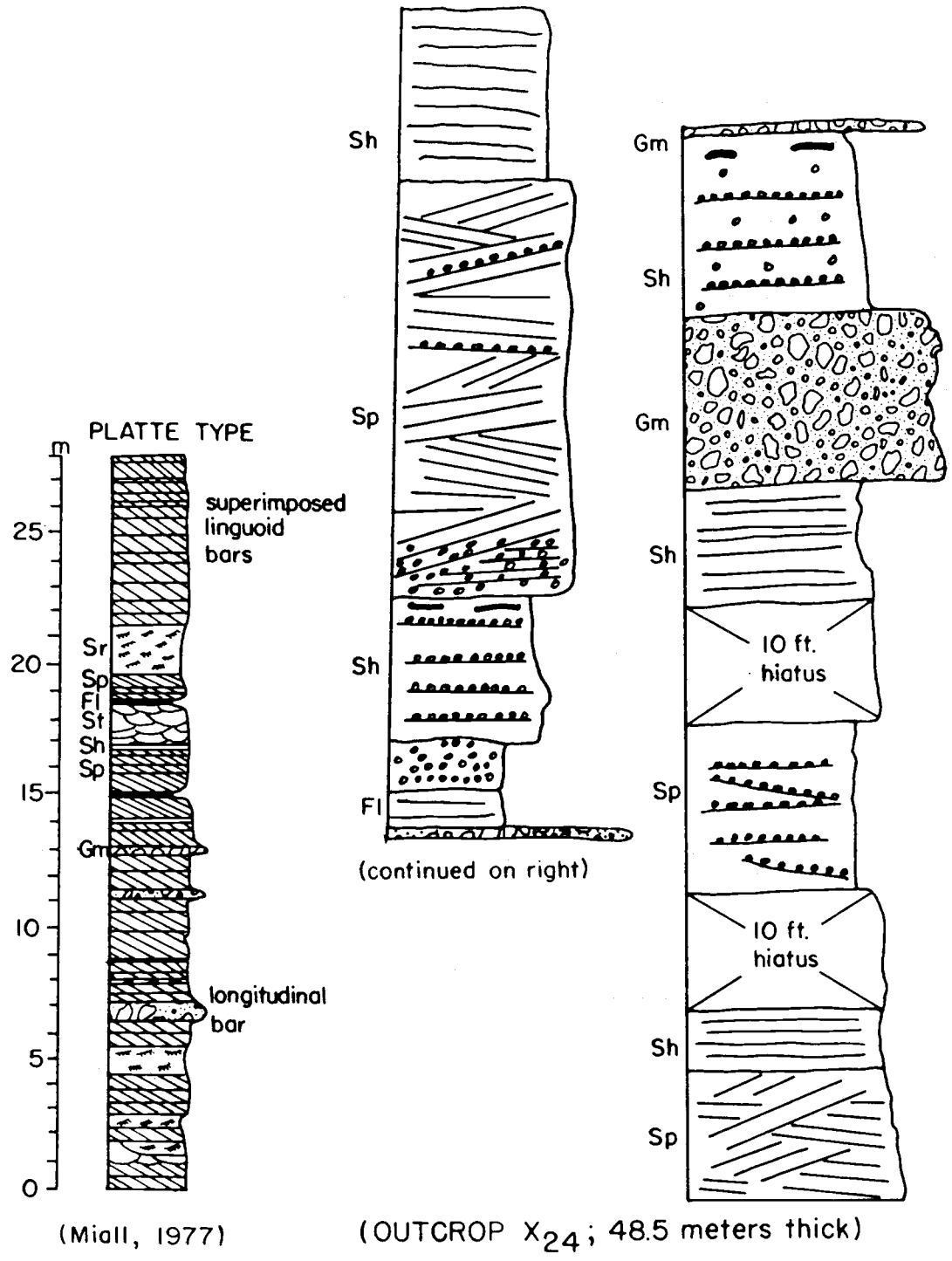

Figure 36. Sketch showing the Platte-type braided river model (Miall, 1977) and outcrop X_{24} (right). Both columns show an abundance of planar cross-bedding and thin flood basin deposits. An explanation of the symbols used by Miall (Sp, Sh, etc.) is given in Figure 18.

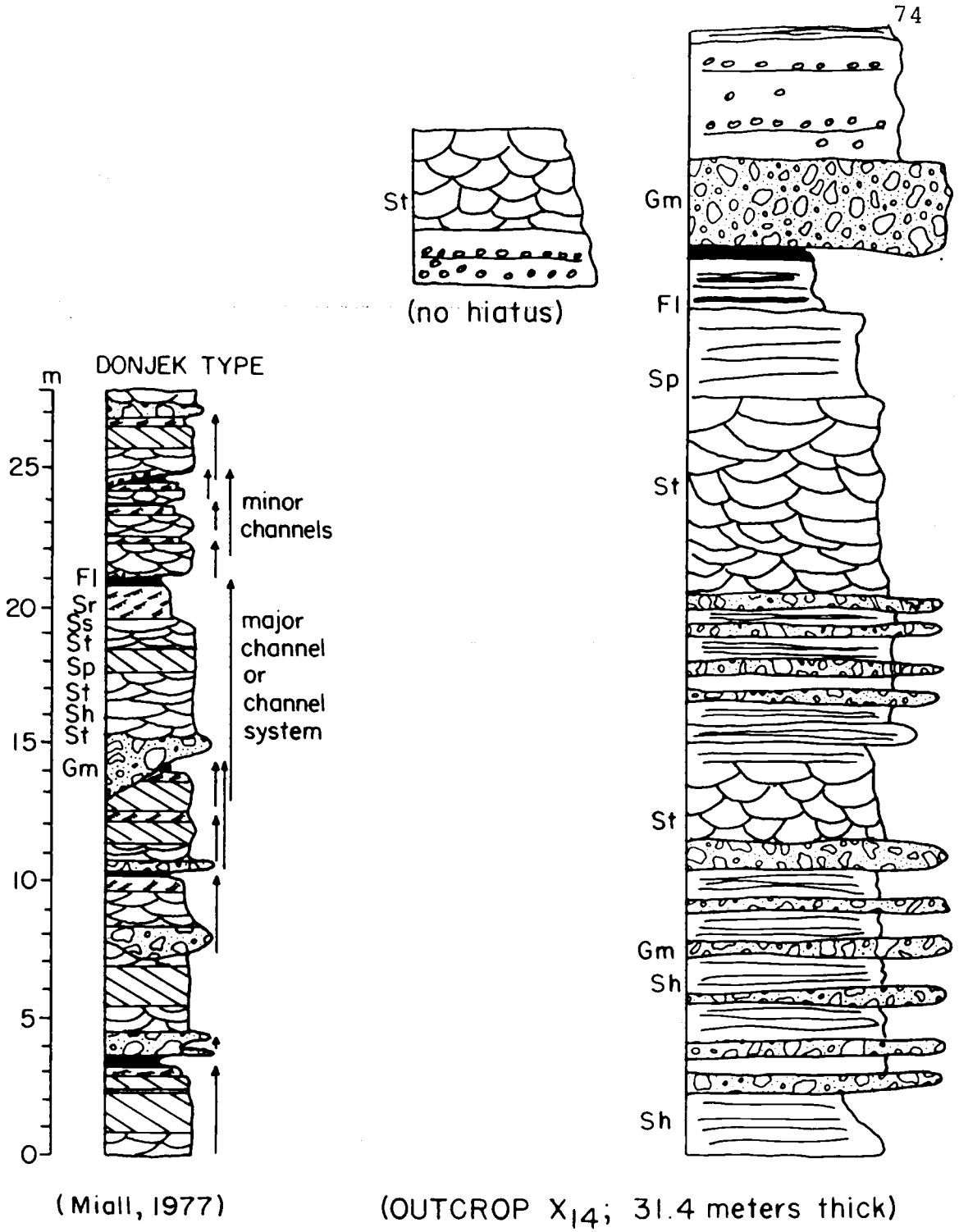

Figure 37. Sketch showing the Donjek-type braided river model (Miall, 1977) and outcrop X_{14} (right). Note similarity in lithofacies, especially the trough cross-bedded sandstone and conglomerate interbeds.

should be investigated to account for the thick flood-basin deposits.

The thick and areally extensive southern section sandstone strata probably were deposited by numerous laterally migrating braided streams. Gibson (1977) and Mrakovich and Coogan (1974) interpreted laterally extensive sandstones to have such an origin. Braided streams carry less fine-grained material than meandering streams, and are contained in less cohesive sandy banks (Schumm, 1960, 1968). Such rivers thus are prone to frequent lateral shifting, producing areally extensive sand deposits. Such deposits will form a sand-body geometry as shown by Allen (1965) (Fig. 38).

The lower part of the Eocene southern section, located in the north part of The Cove, is poorly exposed. The limited outcrops observed are composed of sandstone, siltstone, shale, and minor carbonaceous shale. The sandstone units do not exceed 15 feet in thickness, and contain planar and foreset bedding. In places, the sandstone has slumped into the underlying shales and siltstones. These strata resemble some outcrops in the northern section, and were likely deposited by a meandering river system.

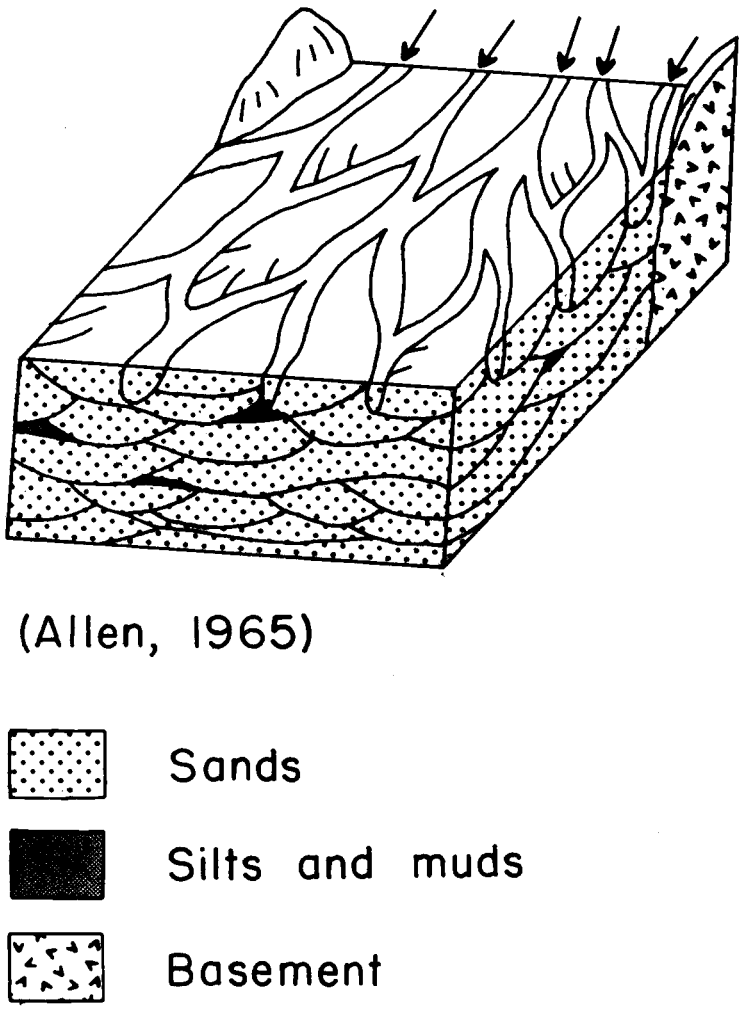

Figure 38. Facies model of a depositional basin dominated by braided river sedimentation (from Allen, 1965). A model similar to this could be applied to much of the Montgomery Creek Formation southern section.

Comparison of the Northern and Southern Section Depositional Environments

It has been shown that the Eocene northern section was deposited by meandering rivers, whereas braided river deposition was characteristic of the southern section. McLean and Jerzykiewicz (1978) and Adeleye (1974) have applied both meandering and braided-river depositional models to explain strata in their studies. Adeleye (1974) reported that a change from braided to meandering river sedimentation represents a decrease in stream power, caused by a decrease in slope in the depositional basin. This slope decrease may be associated with aggradation and geomorphic maturity of the basin. Steel (1974) suggested that a change from low sinuosity (braided) to high sinuosity (meandering) deposition was the result of both climatic change and lowering of relief. The greater abundance of carbonaceous strata in the northern section may reflect a more humid climate.

Applying these studies, it appears that the strata of the northern section were deposited in a basin with lower relief (and slope) than the southern section. Also, a more humid climate may have prevailed in the northern section. The presence of conglomerate interbeds in the southern section points to high discharge rates. Walker (1976) reports that braided systems are favored by rapid discharge fluctuations. Petrographic data later in this

report also will reveal compositional differences between the northern and southern section sandstones.

Outcrops on Upper Kosk Creek and Coal Creek

About 4.5 miles northeast of the northern section strata, Eocene rocks are exposed. These strata crop out near the confluence of Kosk Creek and Coal Creek, and for about 0.5 mile upstream on Coal Creek (T38N, R1E, Sec. 22). An abandoned coal prospect is located on Coal Creek. These rocks are designated "Eocene nonmarine" on the Alturas Sheet (Gay and Aune, 1958), and belong to the Montgomery Creek Formation. The east-dipping strata are dominated by shale, carbonaceous shale, and siltstone. Minor thicknesses of sandstone, lignite, and bituminous coal also crop out. The Eocene strata are bordered on the west by Triassic lavas, volcanic breccias, and metasedimentary rocks of the Klamath Mountains geologic province. Tertiary Cascade Range volcanics overlie the sedimentary rocks to the north, east, and south. The Eocene strata occur as isolated outcrops in a remote and heavily forested area. The incompetent fine-grained sedimentary rocks have undergone extensive slumping, forming numerous conspicuous pullaway scarps in the terrain.

Description of the Outcrops

Near the confluence of Kosk Creek and Coal Creek, 78 stratigraphic feet of shales, carbonaceous shales, siltstones, and fine-grained sandstones crop out (outcrop X_{30}; Fig. 39). The basal 20 feet consist mainly of gray, planar bedded siltstones and shales. These pass upward into 14 feet of light gray, fine-grained sandstone. This sandstone displays large-scale cross-bedding. The sandstone is overlain by 45 feet of planar bedded shale, carbonaceous shale, and siltstone.

About 0.3 miles to the northwest on Coal Creek, a 30-foot sequence of interbedded siltstone, shale, carbonaceous shale, lignite, and thin bituminous coal seams crops out (Fig. 40). The outcrop is laterally extensive, paralleling Coal Creek for some 200 yards. This site is an abandoned coal prospect. These strata are stratigraphically higher than the outcrop at the Kosk Creek-Coal Creek confluence by about 140 feet. About 200 yards to the west, a 10 foot thickness of lignite and carbonaceous shale is exposed in a slump scarp. Several slump scarps expose minor thicknesses of shale and carbonaceous shale both east and west of Coal Creek.

Discussion of the Depositional Environment

The Eocene strata near the confluence of Kosk Creek

Figure 39. Cross-bedded sandstone overlain by siltstones, shales, and carbonaceous shales, near the confluence of Kosk Creek and Coal Creek.

Figure 40. Sequence of carbonaceous shales, lignite, and thin bituminous coal seams at the site of an abandoned coal prospect along Coal Creek.

and Coal Creek were deposited in a nonmarine, fluvial environment. No marine invertebrate fossils were found. These sediments differ significantly from the Eocene strata to the south in the following ways: (1) Sandstone outcrops are much rarer. Where found, the sandstone unit is thin in comparison to the interbedded siltstone and shale; (2) There are larger amounts of carbonaceous shale, lignite, and bituminous coal; (3) The strata lie topographically 400 to 600 feet higher than the Eocene strata to the south. These rocks also occur farther to the east. By extrapolating the regional east dip and adding the topographic difference, these units occupy a structural position 2,843 stratigraphic feet above strata to the south. This difference could be accounted for by: (1) invoking uplift of the northern region; (2) presuming the northern strata are younger and stratigraphically overlie the southern sediments; (3) assuming the northern strata were deposited in a separate basin, topographically higher than the basins to the south.

The latter explanation is most likely, as demonstrated by the distribution of lithofacies. Flood basin siltstones, shales, and carbonaceous shales dominate the sequence in this area. Luxuriant vegetal growth was converted into large amounts of carbonaceous shale, lignite and lesser bituminous coal. These carbonaceous strata were deposited in low-lying flood basin swamps or marshes.

Gibson (1977) reports that deposition of carbonaceous sediments occurs when detrital input is at a minimum. This takes place when flood basin channels are sparse or distant from the carbonaceous deposits. Therefore, the paucity of channels in this region has promoted the deposition of large amounts of carbonaceous strata. The sparse, small-channel sandstones reflect a smaller sediment discharge than the depositional basins to the south. This suggests that the paleoslope and relief were even lower in this region.

AGE OF THE MONTGOMERY CREEK FORMATION

The age of the Montgomery Creek Formation basal conglomerate along Pit 5 Powerhouse Road has been determined to be somewhere between Late Cretaceous (Albian) and early Eocene (?) by Tenneco (1984). A carbonaceous mudstone lens within the conglomerate includes rare nonmarine palynomorphs which are almost entirely Classopollis classoides and coniferous bisaccate pollen. Common Classopollis spp. are characteristic of Cretaceous and Jurassic rocks (Tenneco, 1984). Other pollen species present include Nyssapollenites sp., Quadripollis krempii, Rugubivesiculatus reductus and Cicatricosisporites annulatus. These pollen species support a Cretaceous age (Tenneco, 1984). A Paleogene age is not ruled out, because some of the species listed above range into the Paleogene (Tenneco, 1984). However, no species diagnostic of the Paleogene were observed.

Sanborn (1960) regarded these conglomerates as Eocene in age. The conglomerates are also designated "Eocene nonmarine" on the Geologic Map of California Westwood Sheet (Lydon, et al., 1960). In Sanborn's generalized section of the Big Bend area, he determined the conglomerate to be near the top of the Montgomery Creek Formation. This interpretation is incorrect because: (1) the conglomerate was observed to rest directly on the Jurassic

Bagley Andesite; (2) the conglomerate makes up the westernmost exposures of the Montgomery Creek Formation. Accounting for the regional east dip and topographic differences, the conglomerate must be at the base of the formation. A Late Cretaceous to early Eocene age is the most reasonable for the conglomerate.

Flora in the overlying Montgomery Creek Formation was determined to be late-middle Eocene in age by R. W. Chaney (Hinds, 1933). Axelrod (1985) observed a collection of Montgomery Creek Formation flora, and reported the following taxa:

Lastraea, a fern
Salix, a willow
Hamamelites sp. (witch hazel)
Magnolia and lauraceous leaves, 6-7" long
Aralia whitneyi (aralia)

Diller (1906) reported the following flora from near the headwaters of Kosk Creek (the Coal Mine area):

Sabalites californicus Lesq. (palmetto)
Ulmus californica Lesq. (elm)
Ficus tiliaefolia Al. Br. (fig)
Populus zaddachi Heer. (poplar)
Quercus convexa Lesq. (oak)
Fagus antipofii abich (beech)
Persea pseudo-carolinensis Lesq. (persea)
Laurus sp. (laurel)

Magnolia californica Lesq. (magnolia)

Rhus mixta Lesq. (sumac)

These flora indicate a middle Eocene age, similar to the middle Eocene Chalk Bluffs flora on the west slope of the central Sierra Nevada Range (MacGinitie, 1941).

Nearly all of the above genera are characteristic of the Mixed Mesophytic Forest (Wolfe, 1977). These forests grow in moist, warm-temperate climates and are floristically diverse. Not until the Eocene did significant numbers of mixed mesophytic genera become recognizable (Wolfe, 1977).

HYDROCARBON SOURCE-ROCK EVALUATION

Hydrocarbon source-rock evaluation was performed by Tenneco (1984) on 10 samples from the Montgomery Creek Formation. The samples consist of carbonaceous mudstone and shale, shaly coal, and coal. Results of the evaluation are shown on Table 1.

Analytical Techniques

Some of the analytical techniques involved in source rock evaluation are as follows: (1) thermal maturation indicators: kerogen (organic residue) in source rocks must undergo heating at sufficient temperatures and time to produce gas or oil. Thermal maturation, a measure of the temperature/time history of rocks, was determined at Tenneco (1984) by vitrinite reflectance and spore/pollen coloration. Vitrinite is an organic component (maceral) found in carbonaceous sediments. Vitrinite, on thermally maturing, will yield volatiles and harden, thus increasing the ability to take polish and reflect light (Ruffin, 1980). Spore/pollen, on thermally maturing, will yield volatiles and darken as the fixed carbon content increases (Ruffin, 1980); (2) Rock-Eval pyrolysis: Rock-Eval pyrolysis is an analytical method used by Tenneco (1984) for evaluation of source-rock potential. The following discussion of Rock-Eval pyrolysis is paraphrased from Law

Table 1

Results of Source Rock Evaluation Performed by Tenneco (1984).

			TENNECO LABORATORIES				BROWN & RUTH LABORATORIES						
Lithology	Sample	Location	Spore Coloration	Vitrinite (R_o) Reflectance	Total Organic Carbon (%)	Extractable (ppm) Hydrocarbons	Total Organic Carbon (%)	S_1 (mg/g)	S_2 (mg/g)	S_3 (mg/g)	T_{max} °C	Hydrogen Index	Oxygen Index
Shaley Mudstone	HB-E-8	Big Bend Quadrangle T37N R1W Sect 36 NE¼	-	-	-	-	12.87	1.48	11.80	15.68	396	92	122
Carbonaceous Shale	HB-E-17	Big Bend Quadrangle T37N R1W Sect 24 NW¼	-	-	-	-	20.65	0.44	17.82	26.65	429	86	129
"Waxy" black Mudstone	HB-E-116A	Montgomery Creek Quad. T36N R1W Sect 11 NE¼	2	0.56	2.67	240	2.84	≤0.1	0.73	0.32	-	26	15
Black Mudstone	HB-E-117A	Big Bend Quad. T37N R1E Sect 31 SE¼	-	-	11.64	420	-	-	-	-	-	-	-
Gray Mudstone	HB-E-117B	Big Bend Quad. T37N R1E Sect 31 SE¼	-	0.43	0.30	120	0.51	≤0.1	≤0.1	0.32	-	-	63
Coal (?)	Eocene Coal Core	Montgomery Creek Quad. T35N R1E Sect 29(?)	-	-	-	-	18.68	0.39	24.46	9.40	420	131	50
Carbonaceous Shale	HB-E-C_{18}	Big Bend Quad. T38N R1E Sect 22 SW¼	4	0.90	26.40	240	23.92	0.35	8.28	11.16	444	35	47
Carbonaceous Shale	HB-E-C_{20}	Big Bend Quad. T38N R1E Sect 22 SW¼	-	0.65	59.0	580	35.44	0.56	39.90	16.90	433	113	48
Carbonaceous Shale	HB-E-C_{21}	Big Bend Quad. T38N R1E Sect 22 SW¼	5	-	55.4	0	25.66	0.19	0.25	2.76	441	1	11
Carbonaceous Shale	HB-E-C_{21}	Big Bend Quad. T38N R1E Sect 22 SW¼	-	-	-	-	25.66	0.19	0.12	2.86	-	-	11
Bituminous Coal	HB-E-C_{23}(b)	Big Bend Quad. T38N R1E Sect 22 SW¼	-	0.73	59.0	2380	71.1	1.59	109.1	3.08	424	152	4

et al. (1984): Referring to Table 1, the S_1 peak represents the amount of volatile hydrocarbons expelled from rocks held at 250°C for 5 minutes. The S_2 peak is a measurement of the quantity of hydrocarbons released from a sample during heating from 250° to 550°C, programmed at 25°C per minute. The S_3 peak is the amount of pyrolitic carbon dioxide released during the heating interval of 250° to 390°C. Thermal maturity is indicated by the temperature of maximum pyrolitic yield (T_{max} °C). Other Rock-Eval measurements include the oxygen and hydrogen indices.

Interpretation of Results

Tenneco and Rock-Eval standards for hydrocarbon source-rock evaluations are given in Figure 41. The samples are generally very rich in total organic carbon (see Table 1), ranging from 0.43 to 71.1 weight percent organic carbon. According to Dickey and Hunt (1972), a rock must have a minimum organic carbon content of 0.5 weight percent to be considered an effective hydrocarbon source rock. Rock-Eval S_2 values also indicate that most of the Eocene samples have good source potential.

Rock-Eval S_2/S_3 values and hydrogen indices are indicators of petroleum type. The samples are nearly all gas-prone according to these indicators. Vitrinite reflectance and spore coloration values also indicate gas as the

TENNECO STANDARDS

Maturation Level	Spore Color Index	Vitrinite R_o	Probable Hydrocarbon
Immature	1 (Yellow-Stains)	< 0.55	Gas
Transitional	2 (Yellow Brown)	0.55-0.7	Gas & Minor Oil
Mature	3 (Brown)	0.7-1.0	Gas & Oil
Very Mature	4 (Dark Brown)	1.0-1.5	Wet Gas/ Condensate
Advanced	5 (Drk. Brown to Black)	> 1.5	Gas

Total Organic Carbon (T.O.C.) (% of Rock)

	Shales	Carbonates
Poor	<0.5	<0.2
Fair	0.5-1.0	0.2-0.5
Rich	1.0-2.0	0.5-1.0
Very Rich	>2.0	>1.0

Extractable Hydrocarbons (H.C.) (ppm. of Rock)

	Shales	Carbonates
Poor	<500	<100
Fair	500-1000	100-500
Rich	1000-2000	500-1000
Very Rich	>2000	>1000

ROCK-EVAL STANDARDS

SOURCE POTENTIAL	PETROLEUM TYPE		THERMAL MATURITY
S_2	HYDROGEN INDEX	S_2/S_3	T_{max}
<2.0 Poor	<200 Gas Prone	<2.5 Dry Gas	<440 Immature
2.0-5.0 Marginal	200-300 Mixed	2.5-5.0 Wet Gas	440-470 Oil
>5.0 Good	>300 Oil Prone	>5.0 Oil	>470 Gas

Figure 41. Hydrocarbon source-rock evaluation standards (Tenneco, 1984).

probable hydrocarbon. The organic matter type is indicated by a plot of the oxygen index versus the hydrogen index on a modified van Krevelen diagram (Tissot and Welte, 1978; Fig. 42). Nearly all of the Eocene samples plot near the type III kerogen path. Type III kerogen is primarily derived from terrestrial plant debris and is associated with both nonmarine and marine sediments (Law et al., 1984). During catagenesis, type III kerogens generally produce gas with minor amounts of oil (Law et al., 1984).

In regard to thermal maturity, nearly all of the Eocene samples are immature. This is based on Rock-Eval (T_{max} ^{o}C) values. However, vitrinite reflectance and spore coloration data indicate maturation levels ranging from immature to advanced. The coal mine area samples have the highest maturation values. The maturation level for gas generation is not as critical as for oil (Ruffin, 1980). Gas can be generated in immature maturation environments via bacterial-fungal breakdown of organic matter and in mature to advanced environments via heat degradation (catagenesis) (Ruffin, 1980).

Conclusions

The following conclusions may be drawn as a result of hydrocarbon source-rock analysis of the Eocene samples:

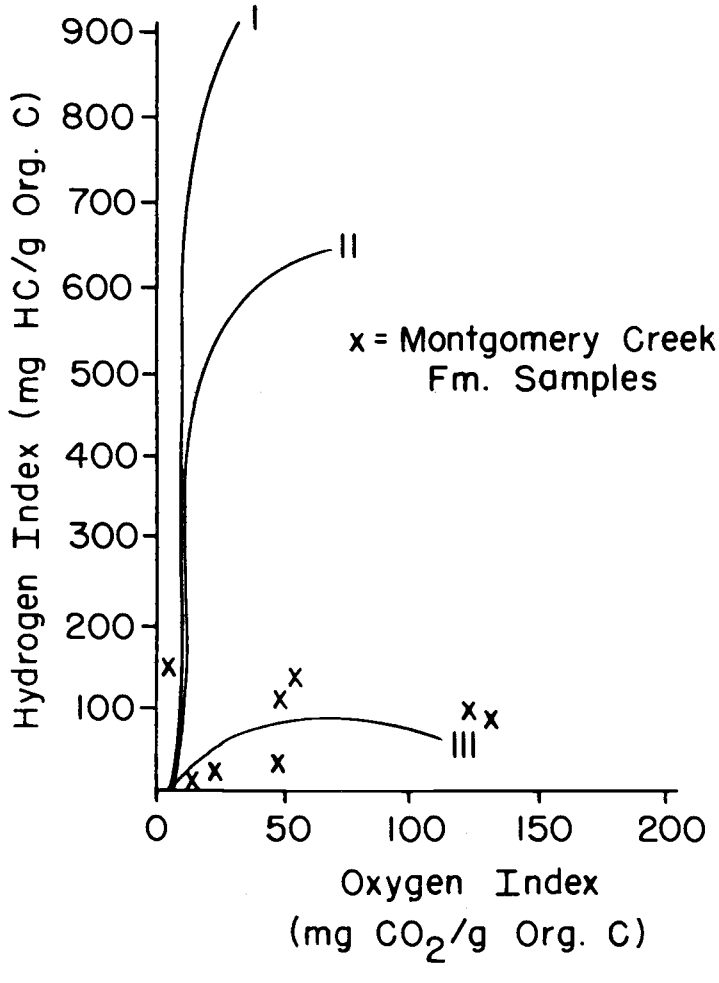

Modified Van Krevelen diagram
(Tissot and Welte, 1978)

Figure 42. Selected Montgomery Creek Formation samples plotting along trend for Type III kerogens on a modified Van Krevelen diagram.

(1) the samples are rich enough in organic carbon to be effective hydrocarbon source rocks; (2) various source rock indicators suggest that gas would be the probable hydrocarbon produced upon heating of the rock; (3) most of the analyzed rocks are not thermally mature. Only two samples from the coal mine area are mature to advanced in rank. Under proper conditions (previously mentioned), however, even the immature samples are capable of generating gas at depth.

POROSITY AND PERMEABILITY OF THE EOCENE SANDSTONES

Porosity and permeability values for selected Eocene sandstone samples are given in Table 2 (Tenneco, 1984). Porosity ranges from 11.9 to 33.1 percent, averaging 22.7 percent. Permeability is from 0.7 to 1,985 millidarcies, averaging 635.3 millidarcies. Sandstones that form petroleum reservoirs commonly have porosities of 5 to 20 percent, and permeabilities of a few to a few hundred millidarcies (Pettijohn et al., 1973). Most of the Montgomery Creek Formation sandstones sampled appear to have sufficient porosity and permeability to be petroleum reservoirs.

These sandstones are commonly underlain or overlain by impermeable siltstones and shales. These fine-grained sediments commonly act as barriers to fluid flow (Pettijohn et al., 1973), trapping the hydrocarbons within the sandstone bodies. Many of the carbonaceous shales are potential source rocks for gas, as revealed in the previous section. Some of these carbonaceous shales were observed in close proximity to the sandstone bodies.

The Cut Bank field of northern Montana and southern Alberta produces oil from strata deposited by meandering rivers (Cant, 1982). Hydrocarbons are trapped against the updip edge of channel sandstones truncated against floodplain shales and siltstones. This type of hydrocarbon

Table 2

Reservoir Properties

(Goode Laboratories, Bakersfield, California)

Sample #	Location	Porosity (%)	Permeability (millidarcies)
SX_{25}	T35N R1W Sect. 36 NW 1/4	24.6	1985
SX_{5}	T37N R1W Sect. 24 SW 1/4	21.3	208
SX_{24}	T35N R1W Sect. 24 SW 1/4	22.4	1516
SX_{17}	T37N R1W Sect. 25 NE 1/4	18.8	67
SX_{4}	T37N R1W Sect. 25 NW 1/4	20.6	130
SX_{13}	T37N R1W Sect. 24 NW 1/4	23.6	1041
MC_{16}	T35N R1W Sect. 36 NW 1/4	29.4	1341
SX_{2}	T36N R1W Sect. 11 NE 1/4	20.7	131
SX_{18}	T37N R1W Sect. 25 NW 1/4	33.1	1721
SX_{22}	T35N R1W Sect. 23 NE 1/4	21.9	597
SX_{10}	T37N R1W Sect. 25 SE 1/4	11.9	6.7
SX_{28}	T34N R1E Sect. 5 SW 1/4	22.5	193
HB-E-11	T37N R1W Sect. 36 NE 1/4	14.7	0.7
HB-E-13	T37N R1W Sect. 25 NW 1/4	22.1	33
HB-E-14	T37N R1W Sect. 25 NW 1/4	22.2	175
HB-E-16	T37N R1W Sect. 24 SW 1/4	28.2	1651
HB-H-1010	T37N R1E Sect. 31 NW 1/4	17.3	4.4

entrapment may exist in the Montgomery Creek Formation, especially in the northern section and coal mine area. These areas have strata deposited by meandering rivers, with desirable source rocks adjacent to channel sandstones.

PETROGRAPHY OF THE MONTGOMERY CREEK FORMATION SANDSTONES

Introduction

Petrographic analysis was made on 33 sandstones from within and south of the study area. Six of these samples are of probable Cretaceous to early Eocene (?) age, while the remaining rocks are Eocene in age. These sandstones were impregnated and made into thin sections, and subsequently point-counted. Two hundred and fifty counts were made on most of the samples. A few slides were of poor quality, and only 100 to 150 counts were made. The mineral point-count results are shown in Appendix 2 (Table 7). The location of samples within the study area is shown on the geologic map (Plate 1).

Sandstone Classification

Figures 43 and 44 show the distribution of point-counted sandstones on QFL diagrams. These classification diagrams are modified from Dott (1964). Of the 33 sandstone samples, 21 are wackes (feldspathic and lithic graywackes). The remaining sandstones are arkosic and lithic arenites. Most of the southern section sandstones plot in the lithic-rich portion of the diagrams. The northern section and coal mine area samples nearly all plot in the feldspathic half of the diagrams.

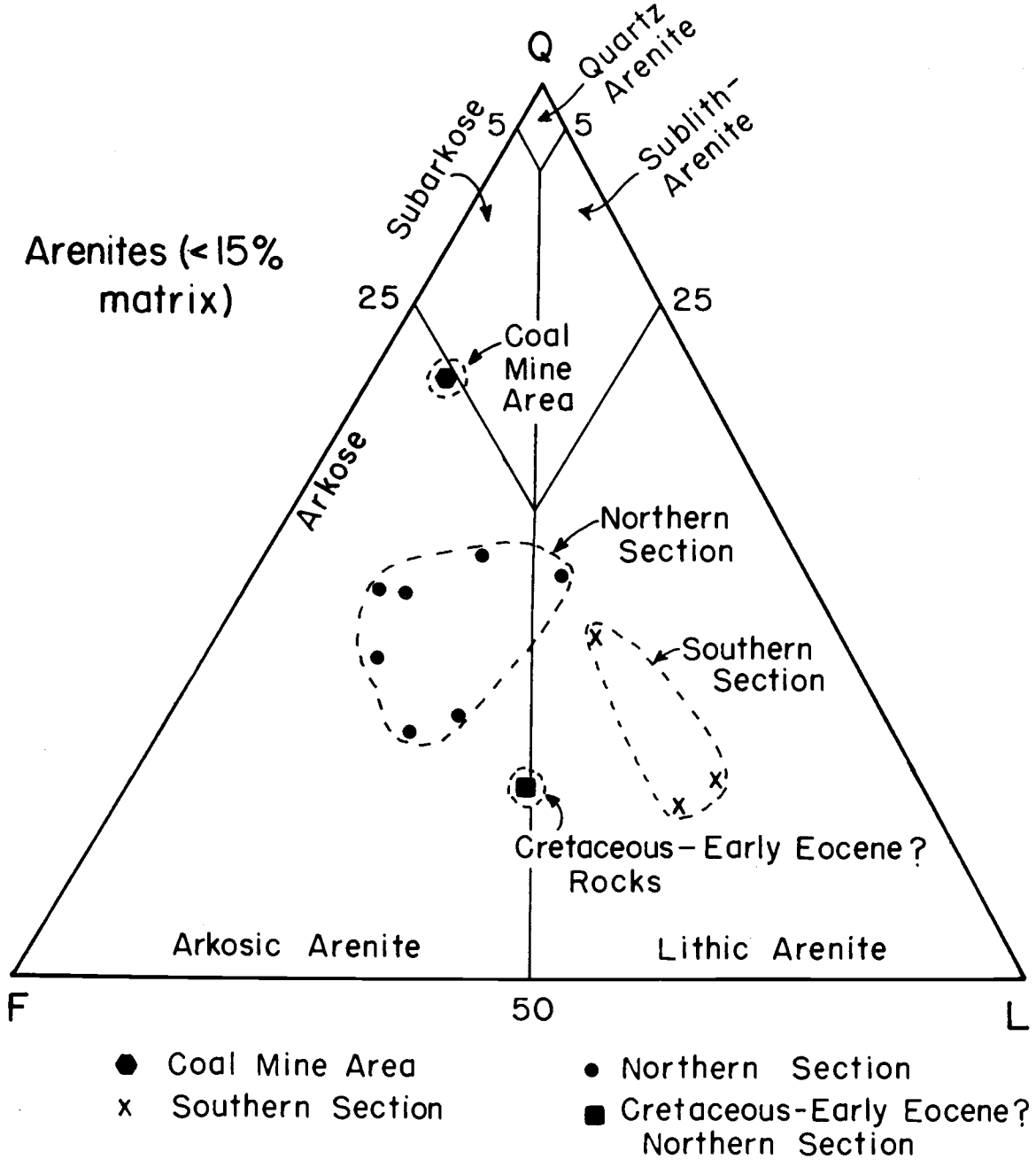

Figure 43: QFL diagram showing distribution of selected Montgomery Creek Formation arenites. Diagram modified from Dott (1964). Q = Quartz, quartzite, and chert. F = Potassium feldspar and plagioclase feldspar. L = fine-grained rock fragments.

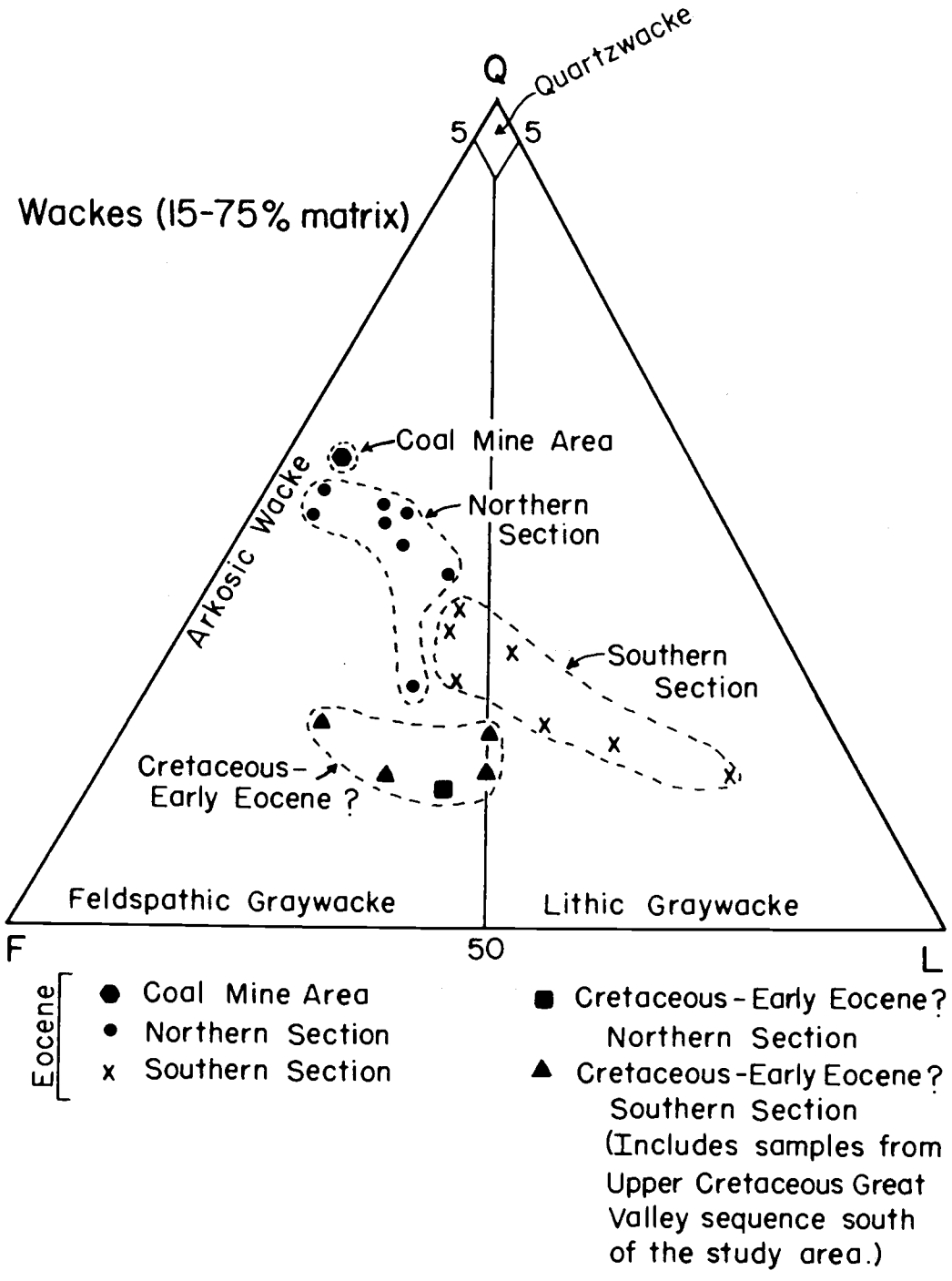

Figure 44. QFL diagram showing distribution of selected Montgomery Creek Formation wackes. Diagram modified from Dott (1964). QFL end members are the same as Figure 43.

Compositional Trends

Figure 45 shows compositional trends and groupings for the 33 sandstone samples. The northern and southern Eocene sections both show a general increase in lithic fragments upsection. This trend reflects the increase in Cascade volcanism toward the end of Montgomery Creek Formation deposition. The upsection increase in volcanic lithic fragments is also shown in Figure 46. A similar upsection trend can be seen in plots for the nonmarine Eocene Payne Cliffs Formation (McKnight, 1971, Fig. 47). This formation is about 85 miles to the northwest of the study area in southwestern Oregon.

The following observations can also be made about Figure 45: (1) the northern section sandstones maintain a more quartzo-feldspathic composition than the southern section. This is partly due to a higher input of volcanic rock fragments into the southern section; (2) the coal mine area and Cretaceous sandstones have mineral distributions distinct from the other Eocene rocks. These sandstones probably originated from different source areas than the other rocks. However, the low quartz content of the Cretaceous samples may be due to climatic conditions. Dickinson et al (1979) reported an upward increase in quartz content at the expense of both feldspar and lithic fragments from upper Cretaceous to lower Eocene strata in

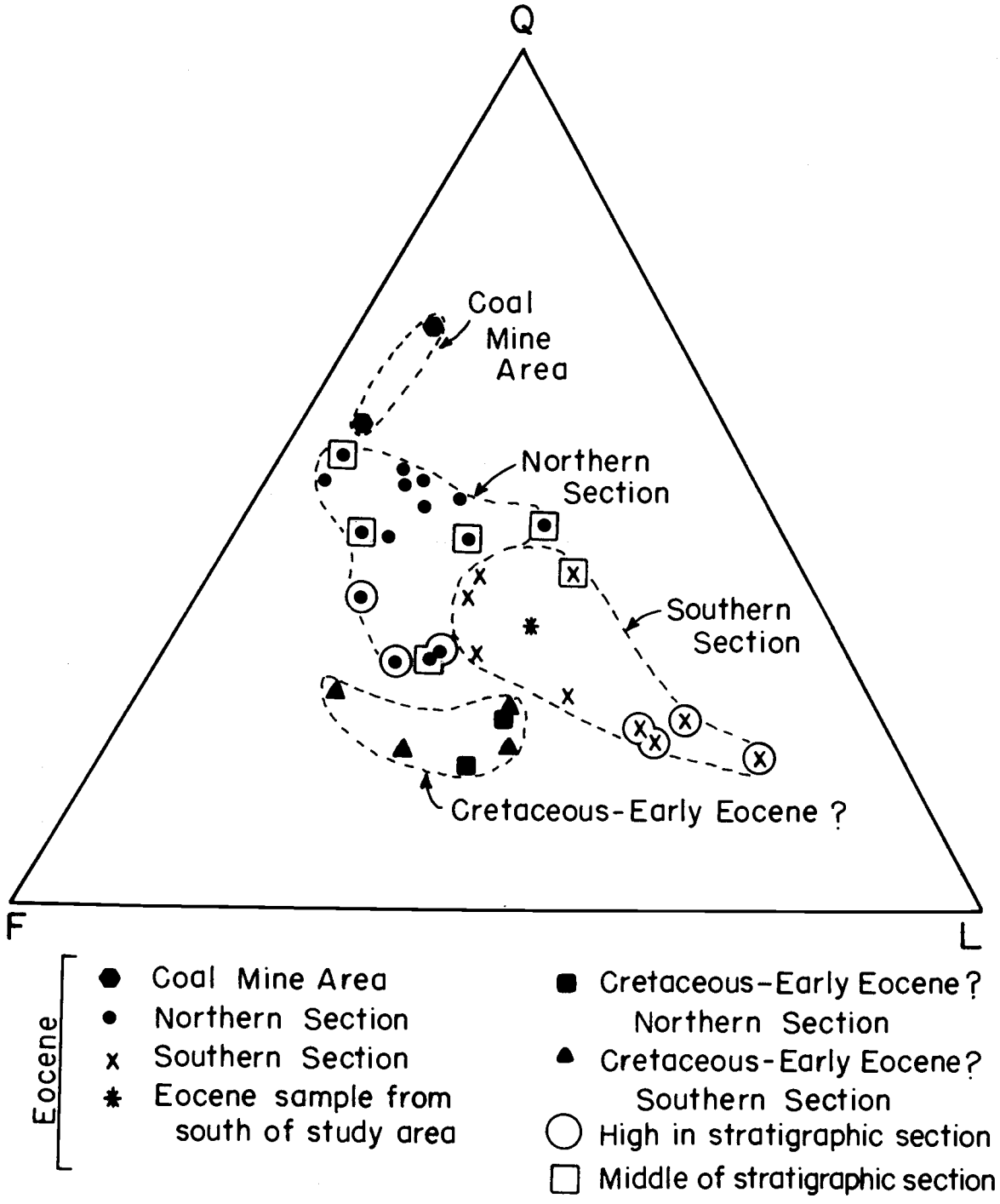

Figure 45. All sandstone samples from the Montgomery Creek Formation are grouped on this QFL diagram to show change in composition upward in the section.

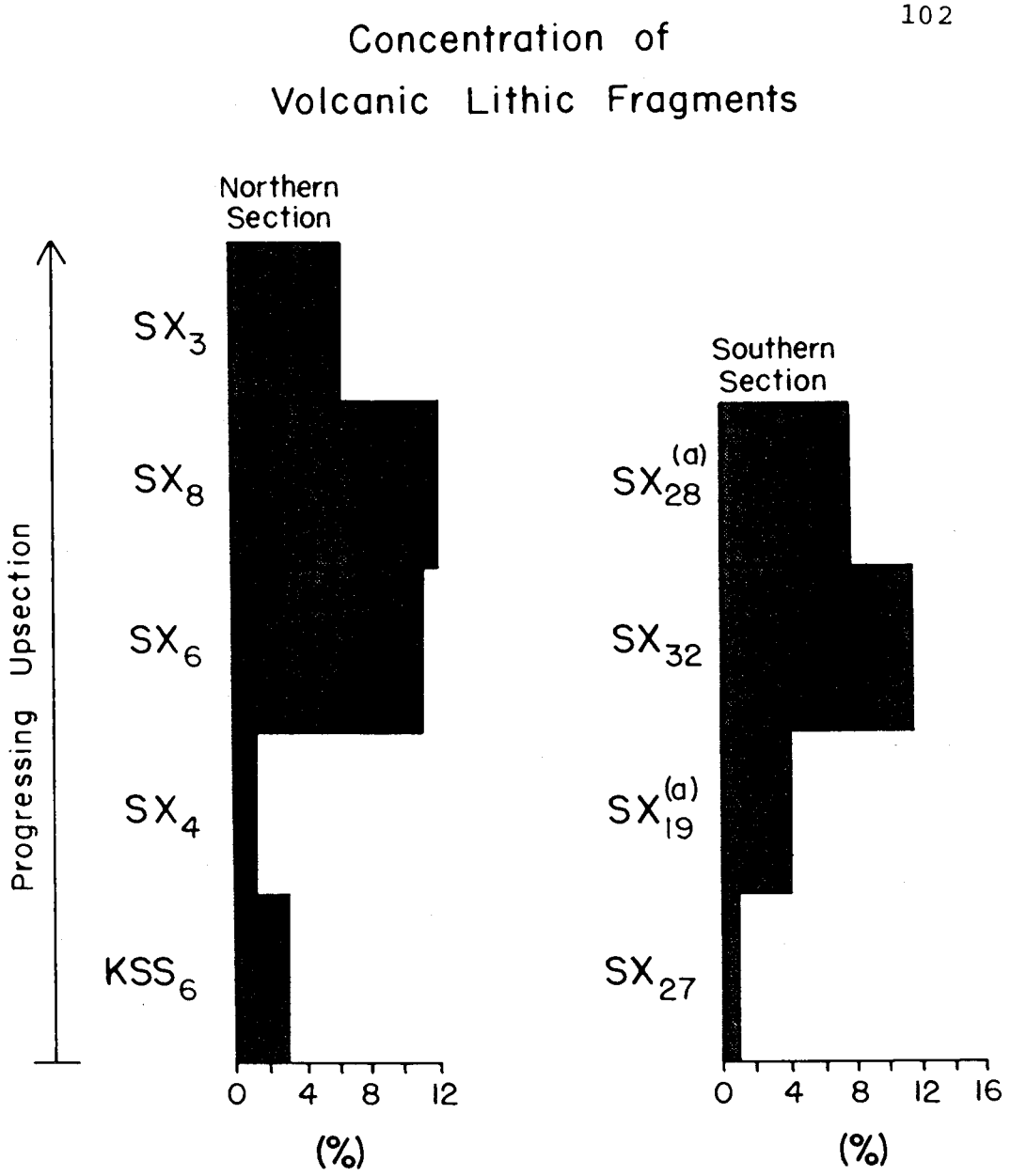

Figure 46. Diagram showing a general upsection increase in volcanic lithic fragments in the Montgomery Creek Formation northern and southern sections.

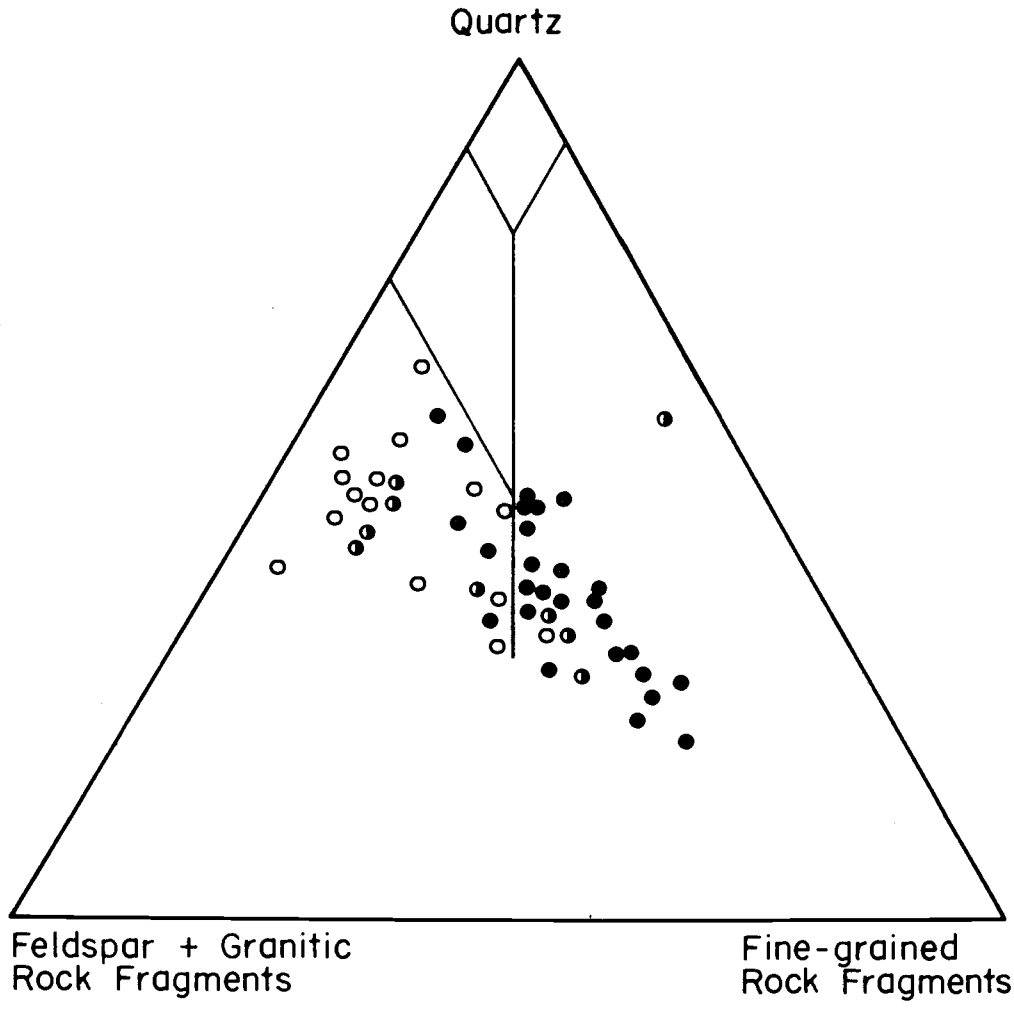

Figure 47. Samples from the Payne Cliffs Formation (McKnight, 1971) are plotted on this QFL diagram. The upsection increase in lithic fragments is similar to the Montgomery Creek Formation compositional trend.
○ = low in stratigraphic section,
◐ = middle of section,
● = high in section.

the Sacramento basin. This was due to warmer and moister conditions during the Eocene.

Distribution and Petrography of the Framework Minerals and Lithic Fragments

Introduction

During point counting of thin sections of sandstone and heavy mineral mounts, 25 species of minerals and lithic fragments were observed. Lithic fragments were further subdivided into specific groups. Figures 48, 49, and 50 show some typical Cretaceous and Eocene sandstones and their framework clast distributions. Quartz, plagioclase feldspar, orthoclase, biotite, and lithic fragments are the most frequently observed framework constituents. These framework clasts are typically set in an argillaceous or chloritic matrix. Less commonly, the clasts are imbedded in a carbonate or iron oxide cement.

Description of the Framework Clasts

Quartz: Quartz is a framework mineral in all 33 sandstone samples observed. Angular to well-rounded grains occur, but most quartz is subangular to subrounded. Grains range from .05 to 1.7 mm in diameter, averaging .4 mm. Most of the quartz is equant to subequant, although some elongate grains occur. Unstrained quartz is slightly more abundant than strained quartz. Monocrystalline quartz greatly

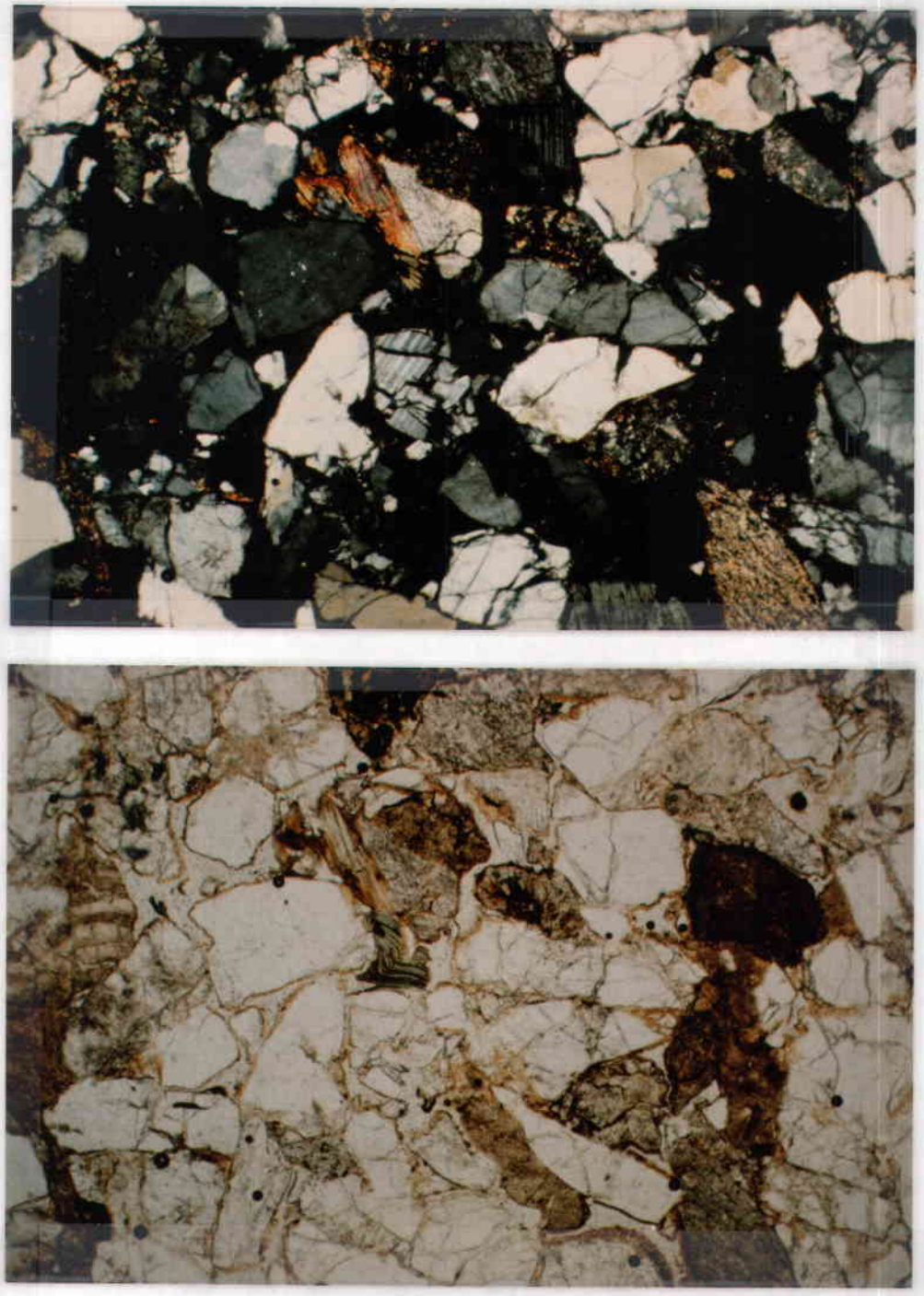

Figure 48. (top) Northern section Eocene sandstone (crossed nichols, 40 X). A moderately sorted feldspathic graywacke, with angular to sub-rounded clasts of quartz, plagioclase feldspar, orthocloase, and muscovite; (bottom) same field in plain light. Note the darker colored, slightly deformed shaly lithic fragments.

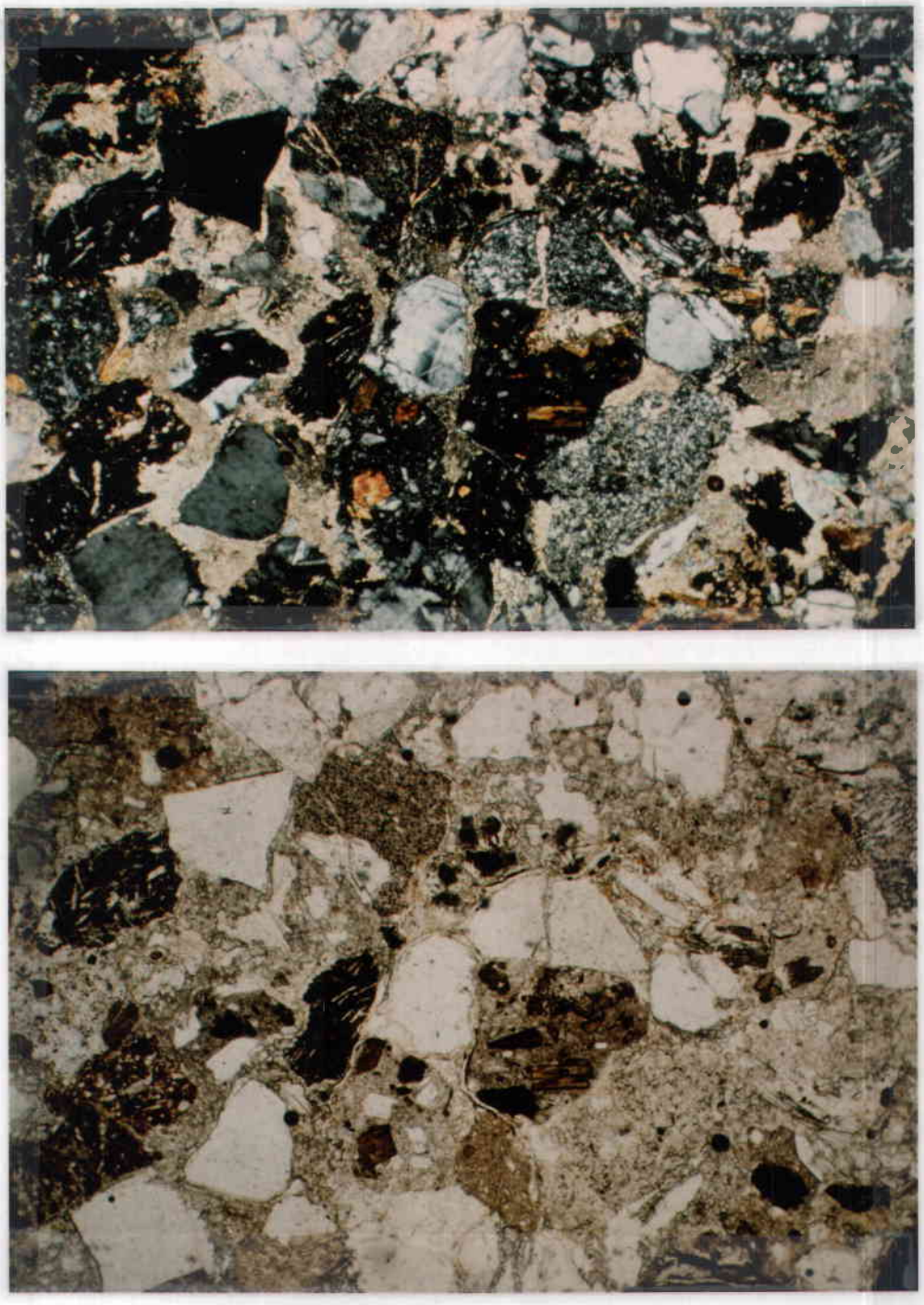

Figure 49. (top) Southern section Eocene sandstone (crossed nichols, 40X). A moderately sorted, calcite-cemented lithic graywacke. The calcite has corroded many of the framework clasts. Note the abundance of volcanic and silty lithic fragments compared to the northern section sandstone. Other framework clasts are quartz, zoned plagioclase feldspar and chert; (bottom). Same field in plain light.

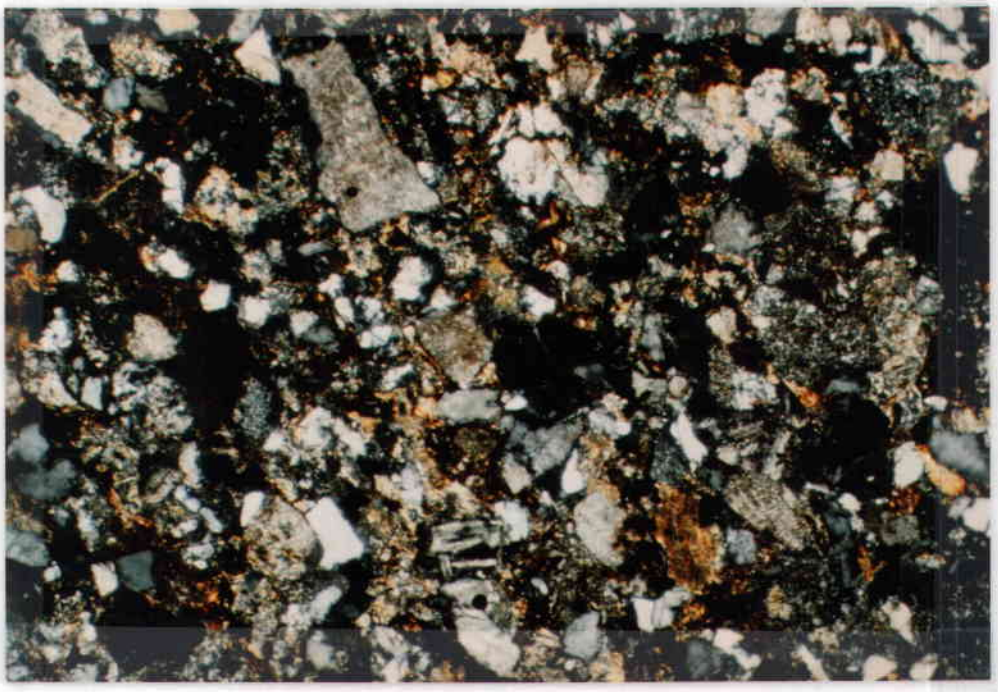

Figure 50. Cretaceous marine sandstone from south of the study area (crossed nichols, 40X). Framework grains include quartz, plagioclase feldspar, chert, and biotite. These sandstones are generally finer-grained than the younger Eocene samples.

outnumbers polycrystalline varieties. The polycrystalline quartz has roughly equant subunits. This differs from the elongated quartz subunits in metamorphic quartzite. Most of the quartz is inclusion-free, but some contains minute zircon inclusions. Less common mineral inclusions are epidote, sphene, rutile, hornblende, magnetite, and biotite. Some quartz is ridden with vacuoles and tiny dust specks. This gives the quartz a cloudy appearance.

Feldspars: Plagioclase feldspar, orthoclase and microcline were the feldspar varieties observed in the sandstones. Plagioclase feldspar and orthoclase are present in all 33 samples, while microcline is in 15. The feldspars are angular to rounded, but most are subangular to subrounded. Plagioclase feldspar and orthoclase are similar in size, ranging from .05 to 1.9 mm in diameter. Microcline grains are smaller, ranging only up to .7 mm. Tabular and elongated grains of plagioclase and orthoclase are more common than equant forms. In microcline, equant grains predominate over more elongate varieties. Plagioclase and orthoclase are generally more extensively altered than microcline. The plagioclase has altered to sericite, while the orthoclase and microcline have altered to kaolinite. The feldspars in the older samples show a greater degree of alteration. Polysynthetic twinning is ubiquitous in the plagioclase, although sometimes obscured

by alteration. Microcline is readily identified by its quadrille twinning. Inclusions are fairly rare in the feldspars. Minute amounts of zircon, apatite and biotite are present in the plagioclase, while only epidote is in the orthoclase. Oligoclase and andesine predominate as the plagioclase varieties. Occasionally, the plagioclase grains display normal zoning. This zoning is more common among fresh grains high in the stratigraphic section. Many of these unaltered grains are also sheared or slightly disaggregated. Myrmekite was also observed in some plagioclase grains.

Micas: Biotite and muscovite are present as mica varieties. Biotite is a framework mineral in 30 of 33 samples, while muscovite is in 18 of 33. The micas are generally angular and elongate, displaying well-defined cleavage parallel to the long dimension. The mica grains are .2 to 2.2 mm in length, averaging about .5 mm. Many grains are bent into undulated forms, deformed under pressure by surrounding framework clasts. In some samples, the micas are subparallel to each other. These grains were probably aligned by depositional currents. In some fine-grained sandstone samples, coarse-grained micas are abundant. This demonstrates the hydrodynamic equivalence of the micas to less buoyant, finer-grained framework clasts. The micas sometimes have quartz and magnetite concentrated

along cleavage traces. The biotite is commonly pleochroic from light brown to dark brown. In Cretaceous marine samples south of the study area, the biotite displays a lighter red-brown color and weaker pleochroism. This may be due to the leaching of ferromagnesian elements contained within the biotite. Occasionally, magnetite has rimmed or completely replaced the biotite. The biotite rarely has inclusions; minute sphene, zircon, and quartz blebs were observed. Some zircon is surrounded by pleochroic halos.

Chert: Chert was observed in 27 of 33 samples. Angular to rounded chert occurs, but most grains are subangular to subrounded. The grains are equant to elongate in form. The chert ranges from .3 to 1.8 mm in diameter, averaging .5 mm. The chert consists of microcrystalline quartz subunits. Sometimes this quartzose groundmass is cut by veins or pods of coarser quartz. Some chert is dusted with tiny opaque matter, probably carbonaceous material.

Volcanic Rock Fragments: Volcanic rock fragments were found in 30 of 33 samples. These clasts are subrounded to well rounded. Both the volcanic and sedimentary rock fragments show a higher degree of rounding than the surrounding framework minerals. The volcanic grains are usually slightly elongate. The grains range from .3 to 2.7 mm in diameter, averaging about .5 mm. The following

volcanic fragments are commonly observed: (1) Porphyritic andesite; this volcanic rock has phenocrysts of hornblende and magnetite in a pilotaxitic groundmass of plagioclase feldspar microlites; (2) Porphyritic andesite: this andesite has phenocrysts of plagioclase feldspar and clinopyroxene in a holohyaline groundmass of dark gray to black glass. This volcanic rock is similar to the Jurassic Bagley Andesite; (3) Porphyritic dacite(?): this volcanic rock has phenocrysts of clinopyroxene, hornblende, quartz, plagioclase feldspar, and magnetite in a holohyaline groundmass of light gray glass.

Hornblende andesites are particularly abundant as volcanic rock fragments. This lithology is conspicuously absent in the Cascade volcanic rocks that overlie the Montgomery Creek Formation. The quantity of volcanic rock fragments increases sharply near the top of both the northern and southern sections. This increase in volcanic fragments reflects the onset of Cascade volcanism during the latter stages of Montgomery Creek Formation deposition.

Sedimentary Rock Fragments: Sedimentary rock fragments are present in all 33 sandstone samples. Fine-grained siltstones and shales predominate, while sandstone fragments are relatively rare. These grains are subrounded to well rounded, and are usually slightly elongate. The

fragments are .3 to 2.4 mm in diameter, averaging about .5 mm. The following sedimentary rock fragments were commonly observed: (1) Siltstone: silt-sized quartz, magnetite and plagioclase feldspar in a brown argillaceous groundmass; (2) Shale: silt-sized quartz in a dark gray carbonaceous groundmass. Minute pyrite grains were observed under reflected light. This fragment closely resembles the Triassic Kosk member of the Modin Formation; (3) Siltstone: silt-sized quartz and feldspar in a gray-green micaceous groundmass. Subparallel carbonaceous stringers are seen in some fragments.

Many of these sedimentary rock fragments are petrographically similar to samples taken from silty and shaly units of the Montgomery Creek Formation. Therefore, many of these fragments probably were intraformationally derived.

Metamorphic Rock Fragments: Metamorphic rock fragments are present in 24 of 33 samples, and are generally the least abundant of the lithic fragments. The grains are subangular to rounded, and are slightly elongate. These fragments are .3 to 1.2 mm long, averaging about .5 mm. The following metamorphic rock fragments were observed: (1) Metamorphic quartzite: elongate, subparallel, strained quartz subunits. Some of these fragments contain epidote or hornblende intergrowths; (2) Schistose frag-

ments: intergrown combinations of subparallel quartz-biotite, muscovite-biotite, or quartz-muscovite; (3) Phyllite (?) fragments: fine-grained rock containing subparallel subunits of quartz and muscovite.

Granitic Rock Fragments: These fragments were observed in 24 of 33 sandstone samples. These grains are subangular to rounded, and are equant to slightly elongate. These composite grains are .3 to 1.9 mm in diameter, averaging about .5 mm. Quartz, orthoclase, plagioclase feldspar, biotite, and muscovite are present as mineral subunits. A single granitic fragment contains two or three of these minerals. The plagioclase feldspar was determined to be oligoclase in one fragment.

Heavy Minerals

Actinolite: Actinolite was observed in 14 of 33 sandstone samples. It occurs as small, slightly elongate grains. The actinolite is .05 to .2 mm in length, and is angular to subangular. The actinolite displays a 5-10^{o} extinction angle and has ragged ends. The grains have fair cleavage parallel to the long dimension.

Hornblende: Both hornblende and oxyhornblende were observed. Hornblende is in 18 of 33 sandstone samples, while oxyhornblende was observed in only 2 of 33. Both hornblende varieties occur as elongate, prismatic grains.

The grains range from .1 to 1.0 mm in length. The hornblende extinguishes at angles from 9^{o}-24^{o}, while oxyhornblende has parallel extinction. The hornblende grains are pleochroic in hues of yellow-green, green-brown, and dark brown. The oxyhornblende is pleochroic from yellow-brown to red-brown. Occasionally, the hornblende is rimmed or replaced by magnetite. Often, the grains are fractured or disaggregated.

Orthopyroxene: Orthopyroxene was observed in 3 of 33 samples. These grains are elongate, and from .1 to .5 mm in length. The orthopyroxene is faintly pleochroic from yellow-green to light green, has high relief, and displays parallel extinction.

Clinopyroxene: Clinopyroxene was seen in 10 of 33 samples. These grains are usually subangular and elongate. The clinopyroxene ranges from .2 to .5 mm in length. The grains are gray-green in color, and have high relief. Extinction angles range from 20^{o} to 44^{o}. Some clinopyroxene is rimmed by magnetite.

Sphene: Sphene was observed in 6 of 33 samples. Sphene occurs as equant, fractured grains, about .2 to .3 mm in diameter. The grains are brown in color, and have high

relief. Many grains have been altered in varying degrees to ilmenite or luecoxene.

Garnet (Almandite): Garnet was observed in 3 of 33 samples. It occurs as equant, subangular to rounded grains. The grains are .1 to .3 mm in diameter. The garnet is light gray, light orange, pink, and near colorless. The garnet is isotropic, and sometimes is fractured or slightly disaggregated.

Tourmaline: Tourmaline was observed in 3 of 33 samples. The grains are small and tabular, ranging from .1 to .3 mm in length. The tourmaline is strongly pleochroic from pink-orange to dark gray or blue-black.

Glaucophane: Glaucophane was seen in 3 of 33 samples. The grains are small and subequant, ranging from .1 to .2 mm in diameter. The glaucophane is pleochroic from light blue to gray-blue.

Apatite: Apatite was seen in 2 of 33 samples. It occurs as small, subequant grains ranging from .05 to .1 mm in diameter. These grains are colorless, and display moderate relief.

Ilmenite and Magnetite: These opaque heavy minerals were observed in 22 of 33 samples. The two minerals often were difficult to distinguish from each other. Magnetite some-

times has a square form, and often replaces hornblende, biotite, or clinopyroxene. Ilmenite sometimes replaces sphene, or is itself altered to luecoxene. The opaque minerals are angular to well-rounded, and range from .05 to .5 mm in diameter. Occasionally, the opaque minerals are concentrated in thin laminations. The laminations are indicative of strong winnowing forces often found in fluvial systems.

Fluorite: Fluorite was not found in the 33 thin sections observed, but was seen in a few heavy mineral grain mounts. The fluorite is colorless and isotropic, but displays a lower relief than garnet.

Zircon: Zircon also was not observed in the thin sections, but was a common mineral seen in the heavy mineral mounts. The zircon displays high relief and parallel extinction. Most of the zircon is slightly elongate and subangular, although rare rounded varieties were seen. Many grains have distinct bipyramidal terminations.

Rutile: Rutile also was only observed in heavy mineral grain mounts. Rutile is distinguished by its brilliant red-brown color and high relief. The rutile sometimes is partially altered to ilmenite.

Heavy Mineral Analysis

Technique For Separating Heavy Minerals

The heavy minerals were separated from sieved sand samples in which the grains were from 60 to 200 microns in diameter. The sieved sand samples were put into a heavy liquid (tetrabromoethane-specific gravity 2.92). The heavy minerals that settled to the bottom of the liquid were put on grain mounts for petrographic analysis.

Significance of the Nonopaque Heavy Minerals

Table 3 shows the distribution of nonopaque heavy minerals of selected samples from the Montgomery Creek Formation. The heavy minerals are sensitive indicators of source rocks for the sandstones. The following observations were made on the heavy mineral distribution: (1) The coal mine area sample (MC 18) is high in zircon, rutile, tourmaline, and glaucophane relative to the other Eocene sandstone samples. It is probable that this sandstone was eroded from different source rocks than the Eocene samples to the south. Alternatively, the ultrastable zircon, rutile, and tourmaline could have been concentrated in this sample by selective removal of less stable heavy minerals in a warm, moist climate. The high quartz content of this sandstone is also indicative of such climatic conditions. The sandstone was likely

Table 3

Distribution of Nonopaque Heavy Minerals in
Selected Montgomery Creek Formation Sandstone Samples

	Zircon	Sphene	Rutile	Tourmaline	Epidote	Glaucophane	Garnet	Actinolite	Apatite	Hornblende	Fluorite	Clinopyroxene	Orthopyroxene	Oxyhornblende	Volcanic glass	Counts & Total
Coal Mine Area																
MC 18	32.0	20.5	15.0	22.5	0.5	8.5	1.0	-	-	-	-	-	-	-	-	200/100.0
Cretaceous Great Valley (Marine)																
KSS 3	13.0	39.0	2.0	7.0	7.0	2.0	12.0	-	16.0	-	2.0	-	-	-	-	100/100.0
Northern Sect. (up sect at top)																
SX_7	3.0	9.0	-	-	10.5	-	2.5	2.5	2.0	53.0	-	0.5	2.0	11.5	3.5	200/100.0
SX_{10}	8.0	26.5	-	6.0	24.5	-	18.0	3.0	3.5	6.5	1.0	1.5	-	1.5	-	200/100.0
SX_4	9.0	42.0	-	1.0	17.0	-	24.0	-	2.0	1.0	-	1.0	-	3.0	-	100/100.0
SX_2	8.0	27.0	1.0	1.5	19.5	0.5	25.5	4.0	5.0	5.0	1.5	1.5	-	-	-	200/100.0
KSS6 (Cretaceous)	1.0	64.5	1.0	0.5	5.5	-	2.0	8.5	0.5	1.5	-	7.0	8.0	-	-	200/100.0
Southern Sect. (Up sect. at top)																
SX_{28}	-	3.5	-	-	4.0	-	1.0	2.5	1.0	57.0	-	16.0	1.0	14.0	-	200/100.0
SX_{32}	2.0	4.0	-	-	2.0	-	-	2.5	0.5	62.5	-	12.5	-	12.0	2.0	200/100.0
SX_{19} (b)	5.5	41.5	1.5	1.0	6.0	1.0	2.0	13.0	2.5	16.5	-	5.0	4.5	-	-	200/100.0

derived from granitic rocks and crystalline schists (including glaucophane schists); (2) The Cretaceous marine sample (KSS 3) was collected several miles south of the study area. This rock is high in zircon, apatite, and tourmaline relative to the Eocene sandstones. This suggests these Cretaceous rocks originated from different sources. The mineral distribution again suggests that granitic rocks and crystalline schists were the source materials; (3) Near the base of both the northern and southern Eocene sections, particularly high amounts of sphene and actinolite are found. Moving up in the northern section, epidote, garnet and zircon become abundant. This suggests a change in source material, due possibly to progressive erosion of the source area. The heavy minerals indicate crystalline schists and granitic rocks as source material for the sandstones; (4) Near the top of both the northern and southern sections, large amounts of hornblende, oxyhornblende, and clinopyroxene are found. These heavy minerals are indicative of a volcanic rock source, probably andesite. The heavy minerals reflect the onset of Cascade volcanism near the end of Montgomery Creek Formation deposition.

Petrographic Description of The Klamath Province Rocks

Locations of selected Klamath province rocks are

shown in Table 4 and are also on the geologic map (Plate 1).

Kosk Member of the Modin Formation (Late Triassic; Sample Tr 1)

This rock is an argillite, with alternating micrite-rich and carbonaceous-rich laminations. Silt sized detrital sparry calcite and micrite predominate as framework clasts. Smaller amounts of silty plagioclase feldspar, quartz, and chert also occur. Pyrite was observed under reflected light. The pyrite and carbonaceous material suggest that the argillite was deposited under reducing conditions. Sanborn (1960) also supports such an origin for the argillites.

Arvision Formation (Early Jurassic; Sample Jarv 1)

This Arvison Formation sample is a porphyritic andesite. The andesite has subhedral phenocrysts of altered plagioclase feldspar, clinopyroxene, and chlorite. Phenocrysts are set in a hyalopilitic groundmass of randomly oriented plagioclase feldspar microlites and black volcanic glass. Nearly all of the ferromagnesian minerals have been altered to chlorite. Plagioclase feldspar phenocrysts are altered to sericite. The plagioclase phenocrysts are large, ranging up to 9 mm in length. The

Table 4

Location of Klamath Province and Sierra Nevada Samples

(See Plate 1)

	Sample No.	Quadrangle	Location
Gabbroic Intrusion (Jurassic ?)	Ja_1	Big Bend	T37N R1W Sec. 26 SE¼
	Ja_2	Big Bend	T37N R1W Sec. 26 SE¼
Granitic pebble in Eocene sandstone	Cgl_2	Montgomery Creek	T34N R1E Sec. 5 NW¼
Sierra Nevada Granite near Susanville, California	SNGR1	Susanville	T29N R12E Sec. 18 SE¼
	SNGR3	Susanville	T29N R12E Sec. 18 SE¼
Klamath Province Granite (Shasta Bally Batholith)	KGR1	Redding	T32N R5W Sec. 31 NW¼
	KGR2	Redding	T32N R5W Sec. 31 NW¼
Bagley Andesite (Jurassic)	Ja^v3	Montgomery Creek	T34N R1W Sec. 1 NW¼
	Ja^v4	Montgomery Creek	T35N R1W Sec. 23 NW¼
	Ja^v5	Big Bend	T36N R1W Sec. 3 SE¼
Arvison Formation Andesite	Jarv 1	Big Bend	T37N R1W Sec. 24 NW¼
Triassic Argillite (Kosk Member of Modin Formation)	Tr 1	Big Bend	T37N R1W Sec. 12 SW¼

rock is petrographically similar to the Jurassic Bagley Andesite.

Bagley Andesite (Early and Middle Jurassic; Samples Jav 3-5)

This rock is a porphyritic andesite (Fig. 51), with subhedral phenocrysts of plagioclase feldspar, clinopyroxene, orthopyroxene, and magnetite. The phenocrysts are set in a hyalopilitic groundmass of randomly oriented plagioclase feldspar microlites, clinopyroxene, magnetite, and dark grey volcanic glass. Some of the pyroxene phenocrysts are altered to chlorite. The plagioclase feldspar is altered to sericite. The plagioclase phenocrysts are large, ranging up to 6 mm in length.

Potem Formation (Early and Middle Jurassic)

For this report, samples from the Potem Formation were not microscopically examined. Sanborn (1960) provided a detailed description of the Potem Formation. The formation is made up of argillite, tuffaceous sandstone, and limestone. Microscopic examination of the limestone showed it to be a calcarenite (Sanborn, 1960). Fine-grained particles of calcite, fossil fragments, microfossils, and calcite cement constitute 75 percent of the rock (Sanborn, 1960). The remainder of the rock is made

Figure 51. Jurassic Bagley Andesite (crossed nichols, 40X). Large plagioclase feldspar and clinopyroxene phenocrysts set in a hyalopilitic groundmass of plagioclase feldspar microlites and volcanic glass.

up of tuffaceous fragments, quartz, and black organic material.

Gabbroic Intrusion (Jurassic (?); Samples Ja_1 and Ja_2)

The intrusive body is found at the confluence of the Pit River and Kosk Creek. This gabbro has a fine-grained, hypidiomorphic granular texture (Fig. 52). Average grain diameter is about 0.8 mm. Euhedral plagioclase feldspar, clinopyroxene, and orthopyroxene are often embayed by anhedral quartz and magnetite. Some of the pyroxenes are slightly to extensively altered to chlorite. The plagioclase feldspar is slightly altered to sericite. Point-count results for this gabbro and the following granites are given in Fig. 53.

Shasta Bally Batholith (Late Jurassic; Samples KGR_1 and KGR_2)

This granitic body is located about 34 miles southwest of the study area, immediately west of Redding, California. The Shasta Bally batholith is one of many granitic bodies that intruded the Klamath Province during the Late Jurassic Nevadan orogeny (Irwin, 1966). The granite has a medium-grained, hypiomorphic granular texture (Fig. 54). Subhedral to euhedral plagioclase feldspar and orthoclase are often embayed by anhedral strained quartz and chlorite. Magnetite and hornblende

Figure 52. Jurassic(?) gabbroic intrusive rock (crossed nichols, 40X). The rock is composed of subhedral to euhedral plagioclase feldspar, clinopyroxene, and othopyroxene. Anhedral quartz and magnetite fill interstices between these minerals.

Sample %	$SNGR_3$	KGR 1	Ja_2	Cgl_2
Quartz	27.0	40.0	9.0	33.0
Plagioclase feldspar	21.7	24.7	67.4	34.3
Orthoclase	32.3	21.3	-	25.7
Microcline	8.6	-	-	-
Hornblende	2.3	1.0	0.3	2.7
Chlorite	0.7	6.7	1.7	1.7
Epidote	1.0	2.3	-	-
Orthopyroxene	-	-	7.3	-
Clinopyroxene	-	-	10.6	-
Magnetite	-	-	3.0	0.7
Biotite	6.3	-	-	0.3
Sphene	-	-	-	1.7
Calcite	-	-	0.7	-
Kaolinite, Sericite	-	4.0	-	-

Figure 53. Modes of igneous rocks, based upon 300 points counted per thin section.

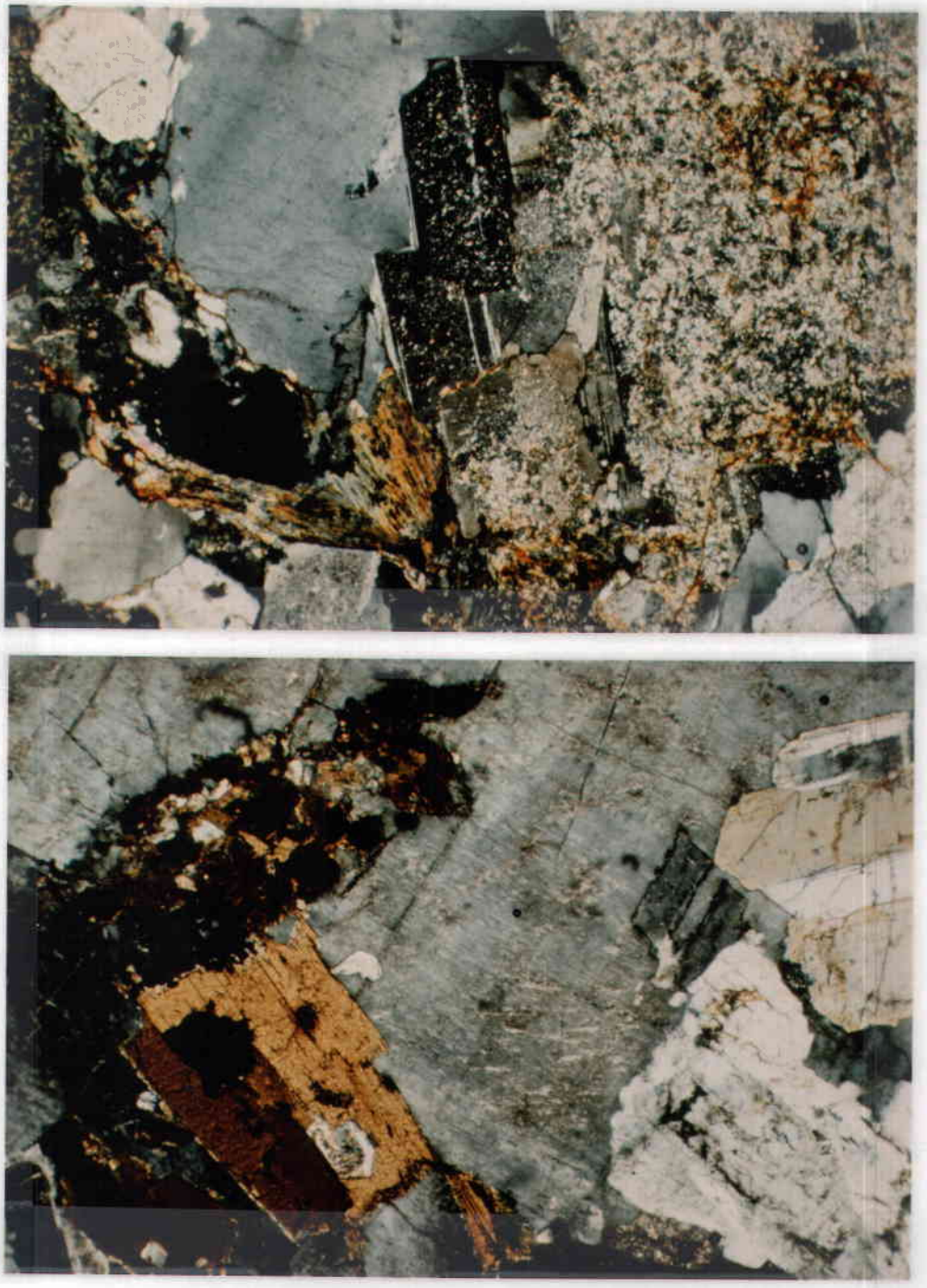

Figure 54 (top): Late Jurassic Shasta Bally batholith granite (crossed nichols, 40X). Subhedral, altered plagioclase feldspar and orthoclase are embayed by anhedral strained quartz; (bottom); Cretaceous Sierra Nevada Range granite (crossed nichols, 40X). Subhedral plagioclase feldspar and biotite are bordered by anhedral orthoclase.

are present in minor amounts. The feldspars have been extensively altered to kaolinite and sericite, while the ferromagnesian minerals have altered to chlorite.

Sierra Nevada Range Granite
(Cretaceous; Samples $SNGR_1$ and $SNGR_3$)

This granite was collected 74 miles southeast of the study area, near Susanville, California. The granite has a medium-grained, hypidiomorphic granular texture (Fig. 54). Subhedral to euhedral plagioclase feldspar, biotite, hornblende, and magnetite are embayed by anhedral quartz, orthoclase, and microcline. Some hornblende is partly replaced by magnetite. The feldspars are slightly altered to sericite and kaolinite. Some of the plagioclase feldspar is zoned.

Granite Pebble (In Eocene Sandstone;
Sample Cgl_2)

This is a well rounded pebble, about two inches in diameter. The pebble was collected from an Eocene sandstone outcrop high in the Montgomery Creek Formation southern section. This is a porphyritic granite, with corroded, subhedral to anhedral phenocrysts of quartz, hornblende, plagioclase feldspar, and biotite (Fig. 55). Phenocrysts are set in a fine-grained, hypidiomorphic granular groundmass of quartz, orthoclase, plagioclase

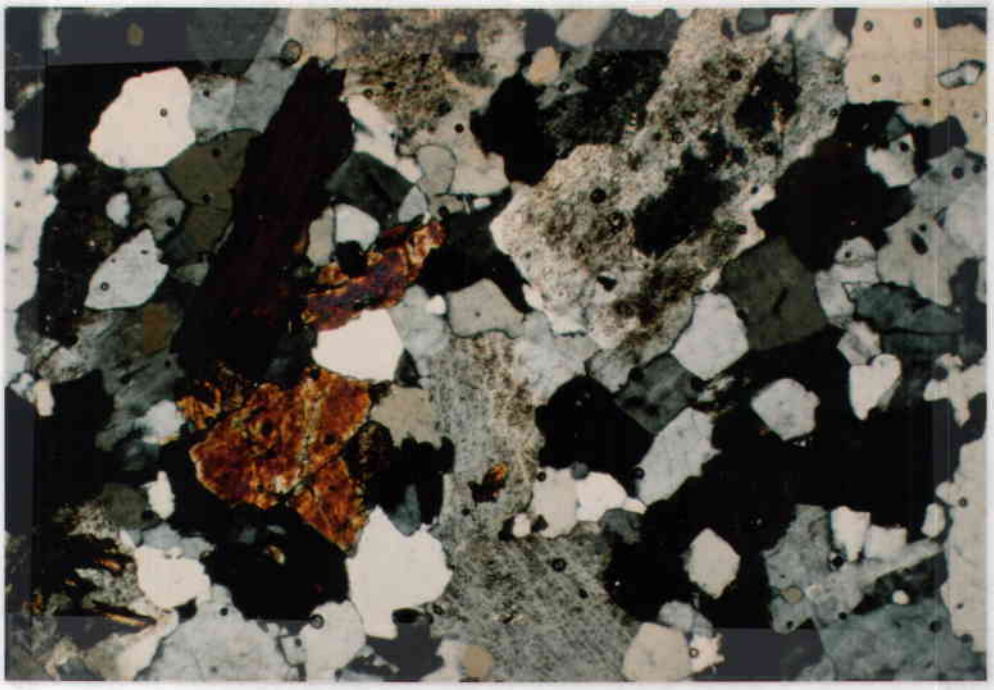

Figure 55. Granite pebble in Eocene sandstone (crossed nichols, 40X). Subhedral to anhedral phenocrysts of orthoclase, plagioclase feldspar, and hornblende are set in a finer-grained groundmass of anhedral orthoclase and quartz.

feldspar, magnetite, and sphene. The biotite and hornblende are partially altered to chlorite. Plagioclase feldspar and orthoclase are slightly altered to sericite and kaolinite.

Petrographic Description of the Cascade Range Volcanic Rocks

The locations of the following samples are shown in Table 5 and Plate 1.

Northern Section Andesite, Pliocene(?); Samples $Tva_{5, 7, 10, 13, 14}$

This is a porphyritic pyroxene andesite (Fig. 56). The andesite has randomly arranged, euhedral to subhedral phenocrysts of plagioclase feldspar, clinopyroxene, and orthopyroxene. Phenocrysts are set in a hyalopilitic groundmass of plagioclase feldspar microlites, pyroxene, magnetite, and gray glass. Some plagioclase phenocrysts display normal zoning. The plagioclase is fresh or slightly altered to sericite. Occasional glomerophenocrysts composed of plagioclase feldspar, clinopyroxene, and orthopyroxene were observed.

Northern Section Basalt, Pliocene(?); Samples Tva_4 and Tva_{20}

This is a porphyritic basalt, with euhedral to subhedral phenocrysts of plagioclase feldspar, clinopyroxene,

Table 5

Location of Cascade Province Volcanic Rock Samples

(See Plate 1)

	Sample No.	Quadrangle	Location
Northern Section Andesites Miocene(?)-Pliocene	Tva 5	Big Bend	T37N R1E Sec. 29 NE¼
	Tva 7	Big Bend	T37N R1E Sec. 33 NW¼
	Tva 10	Big Bend	T37N R1E Sec. 32 NE¼
	Tva 13	Montgomery Creek	T36N R1E Sec. 9 NW¼
	Tva 14	Montgomery Creek	T36N R1E Sec. 9 NW¼
Northern Section Basalts Miocene(?)-Pliocene	Tva 4	Big Bend	T37N R1W Sec. 25 NE¼
	Tva 20	Big Bend	T37N R1E Sec. 29 NW¼
Basalt dike Pliocene(?)	Tvb 2	Montgomery Creek	T36N R1W Sec. 11 NE¼
Southern Section Basalts Pliocene(?)	Tvb 3	Montgomery Creek	T35N R1E Sec. 19 SE¼
	Tvb 4	Montgomery Creek	T35N R1E Sec. 19 SE¼
	Tvb 11	Montgomery Creek	T35N R1W Sec. 25 NW¼
	Tva 11	Montgomery Creek	T35N R1W Sec. 14 SE¼
	Tva 18	Montgomery Creek	T35N R1W Sec. 26 NE¼
	Tvb (5-8)	Montgomery Creek	T35N R1W Sec. 11 NW¼

Figure 56. Pliocene northern section andesite (crossed nichols, 40X). Subhedral to euhedral phenocrysts of plagioclase feldspar, clinopyroxene, and orthopyroxene are set in a hyalopilitic groundmass of glass and plagioclase feldspar microlites.

and olivine (Fig. 57). Subparallel arranged phenocrysts are set in a hyalopilitic groundmass of plagioclase feldspar microlites, pyroxene, magnetite, and dark gray glass. The plagioclase phenocrysts are sometimes zoned, and occasionally are altered to sericite. The olivine phenocrysts are frequently rimmed and mottled by iddingsite. Glomerophenocrysts composed of clinopyroxene, olivine, and plagioclase were sometimes observed.

Northern Section Basalt Dike, Pliocene(?); Sample Tvb_2

This basalt dike cuts through the Cretaceous-early Eocene conglomerate on Pit 5 Powerhouse Road. This is an altered porphyritic basalt (Fig. 58). The basalt has subparallel phenocrysts of plagioclase feldspar in a pilotaxitic groundmass of plagioclase microlites, pyroxene, and chlorite. The chlorite is probably an alteration product of pre-existing ferromagnesian minerals. Plagioclase phenocrysts are moderately altered to sericite. The rock is slightly vesicular, with calcite partly filling some void spaces. This dike rock resembles the northern section basalt, but any former olivine has been altered to chlorite.

Southern Section Basalts, Pliocene(?)

Two main varieties of basalt were observed in the

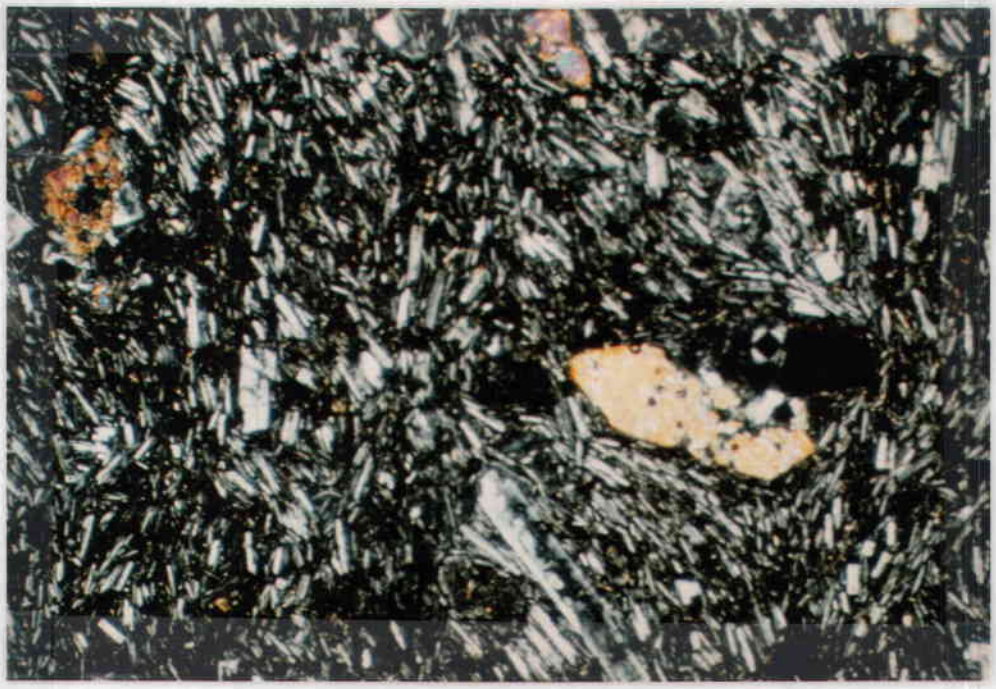

Figure 57. Pliocene northern section basalt (crossed nichols, 40X). Euhedral to subhedral phenocrysts of plagioclase feldspar and olivine in a hyalopilitic groundmass of glass and plagioclase feldspar microlites.

Figure 58. Pliocene northern section basalt dike (crossed nichols, 40X). Subhedral to euhedral phenocrysts of plagioclase feldspar in a pilotaxitic groundmass of plagioclase feldspar microlites and chlorite.

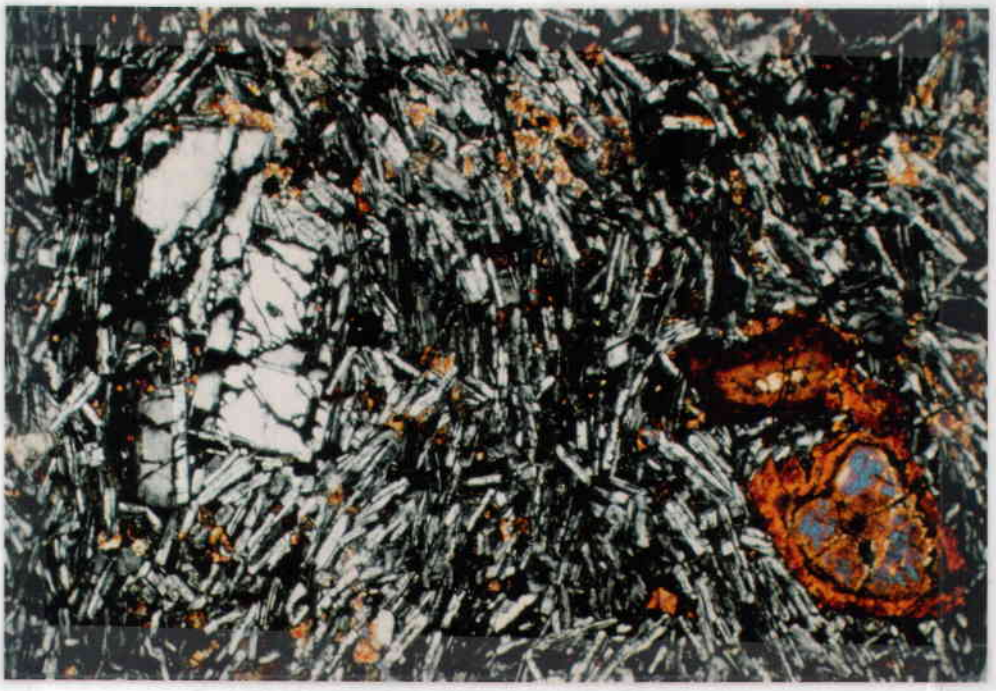

Figure 59. Pliocene southern section basalt (crossed nichols, 40X). Phenocrysts of plagioclase feldspar are olivine (altered to iddingsite) and set in a groundmass of plagioclase feldspar microlites and clinopyroxene. The clinopyroxene has subophitically enclosed some of the plagioclase microlites.

Conclusions

Petrographic examination of the Montgomery Creek Formation, Klamath Province, and Cascade Range rocks has revealed information on the source areas of the Montgomery Creek sandstones. The following observations and conclusions were made: (1) Clasts similar to the Bagley Andesite and Kosk member or the Modin Formation are present in minor amounts in some Eocene sandstones. Therefore, nearby Klamath Province rocks probably contributed detritus to the Montgomery Creek Formation; (2) Fresh volcanic lithic clasts high in the Eocene section do not resemble overlying Cascade Range volcanic rocks. The clasts were evidently derived from a Cascade volcanic arc that has been covered by younger volcanics; (3) Many fine-grained sedimentary lithic fragments in the sandstones resemble samples taken from silty and shaly units of the Montgomery Creek Formation. These clasts were probably intraformationally derived; (4) A granite pebble high in the Eocene section does not resemble samples taken from Klamath province and Sierra Nevada range plutons. However, this pebble could have been derived from an unsampled pluton or a pluton buried beneath younger deposits; (5) The distribution and composition of mineral and lithic clasts in the Eocene sandstones reveal that the sediments were derived

from: (a) plutonic and metamorphic rocks of the Klamath Province; (b) volcanic rocks of the Cascade Range, probably buried under younger lava flows.

Post-Depositional Alteration of the Montgomery Creek Formation Sandstones

The Montgomery Creek Formation sandstones are generally porous and friable rocks. However, these sandstones have undergone varying degrees and forms of post-depositional alteration. They are as follows:

Compaction

The Eocene sandstones have undergone a small degree of compaction. The deformation of incompetent framework grains such as the micas and fine-grained lithic fragments reflect this compaction. In many sandstones, biotite and muscovite have been bent; surrounding framework grains frequently indent the micas (Fig. 60). Likewise, some volcanic and sedimentary lithic fragments have been deformed into irregular shapes (Fig. 60). The degree of compaction lessens slightly upsection, due to decreasing overburden. For instance, sandstones high in the southern section have lithic fragments that remain relatively undeformed. Some of these rocks are very friable in hand sample. Porosity and permeability (Tenneco, 1984, Table 2) show no obvious increase with depth in the northern

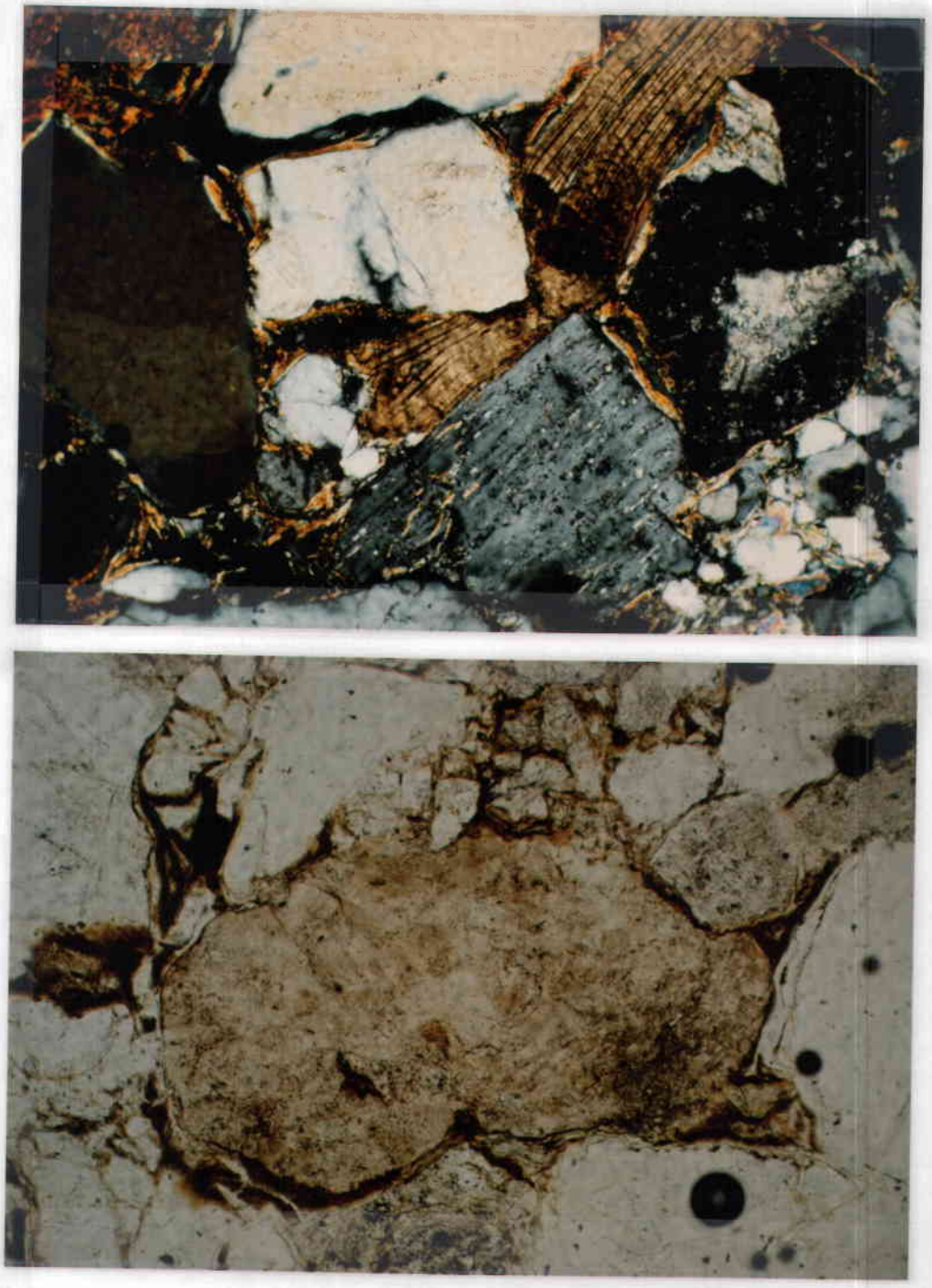

Figure 60. (top): Southern section Eocene sandstone (crossed nichols, 100X). The biotite has been indented by a more competent quartz grain; (bottom): Northern section Eocene sandstone (plain light, 100X). This incompetent lithic fragment has been slightly deformed by surrounding framework minerals.

section. Apparently no significant change in porosity and permeability has occurred due to compaction.

Matrix Formation

Much of the matrix in the Eocene sandstones has been formed from the framework constituents. The following observations and interpretations were made concerning the formation of matrix: (1) Some matrix has a similar texture and composition to volcanic and sedimentary lithic fragments found in the sandstone. The conversion of lithic fragments to matrix appears to be largely a mechanical process. For example, some deformed lithic fragments have oozed into the cracks between surrounding framework grains. Often, part of the original outline of the lithic fragment remains intact; (2) Chlorite-rich matrix has formed from the chemical breakdown of ferromagnesian minerals such as biotite, hornblende, and clinopyroxene. Biotite and hornblende were observed in varying degrees of alteration to chlorite, sometimes merging with a green-brown chlorite-rich matrix (Fig. 61); (3) In some volcanic-rich sandstones, chlorite rims many of the framework clasts (Fig. 61). The chlorite grows radially into the void space between the clasts. The chlorite was probably formed from the diffusion of iron and magnesium ions from the volcanic rock fragments and ferromagnesian minerals.

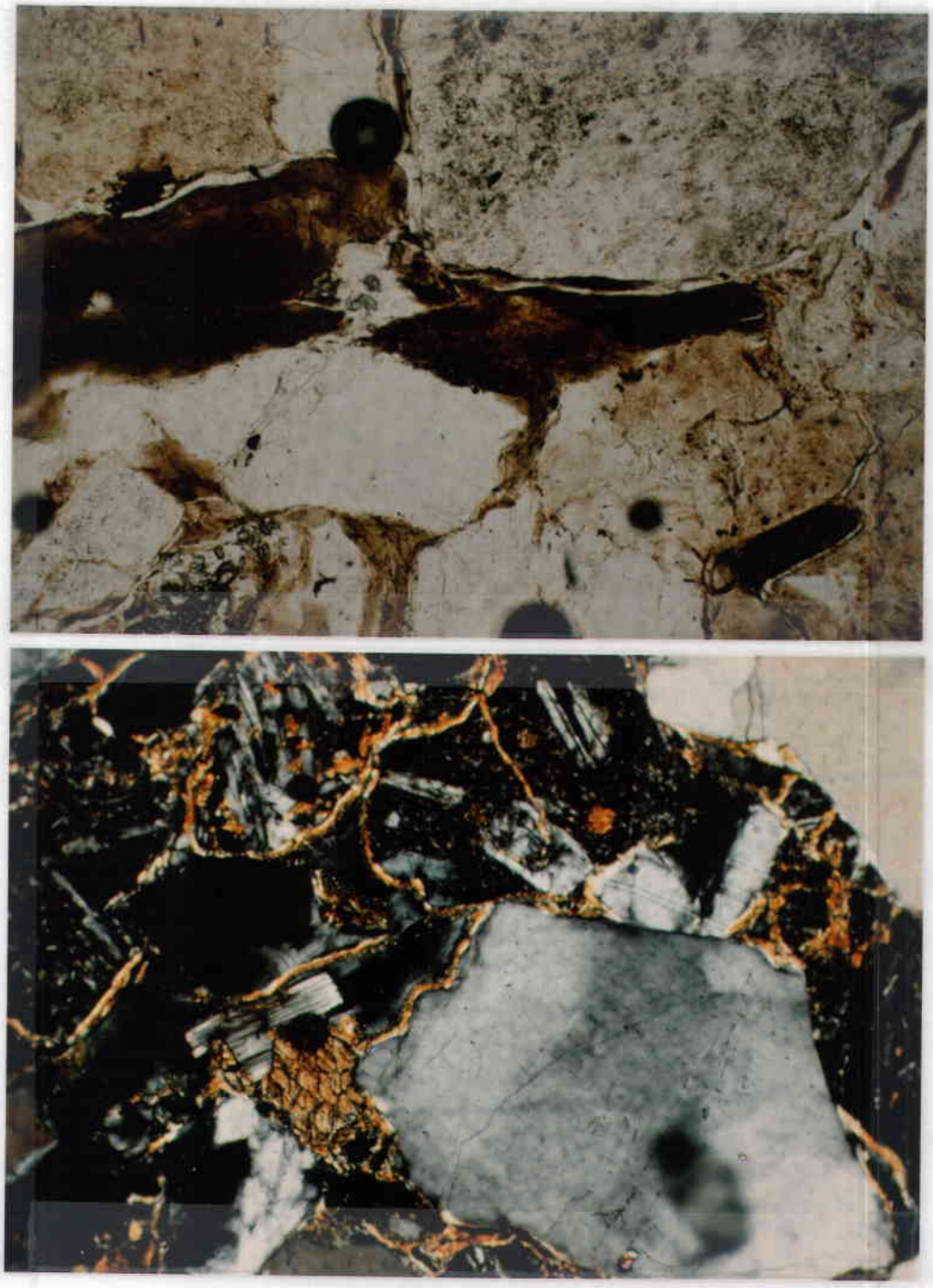

Figure 61. (top): Northern section Eocene sandstone (plain light, 100X). The biotite grain has altered to chlorite, which fills some void space between the framework clasts; (bottom): Southern section Eocene sandstone (crossed nichols, 100X). Chlorite has surrounded many detrital clasts and radiated into the void space between the clasts.

Many of the framework grains are corroded where they are in contact with the surrounding matrix. These grains evidently reacted chemically with the newly formed matrix.

Calcite Cement

Calcite cement is present in 7 of 33 sandstone samples. Nearly all of this cement is sparry calcite, with minor amounts of micrite. Where found, the calcite forms 5 to 30 percent of the rock. When there is a significant amount of calcite, relatively small amounts of clay matrix are present. This could be due to abundant matrix inhibiting carbonate cementation because of reduced porosity.

Apparently, the calcite was precipitated out of a carbonate-rich solution. When the solution crystallized and expanded, it disrupted some of the framework clasts. Some biotite has been invaded along cleavage traces and expanded by the calcite (Fig. 62). The calcite also intruded lithic fragments and other framework minerals along fractures and wedged the clasts apart. The calcite also has replaced or reacted with many framework clasts. Many lithic fragments and framework minerals have undulatory, corroded outer boundaries where in contact with the calcite cement. A few grains have been nearly replaced by the calcite, with only remnant fragments defining the

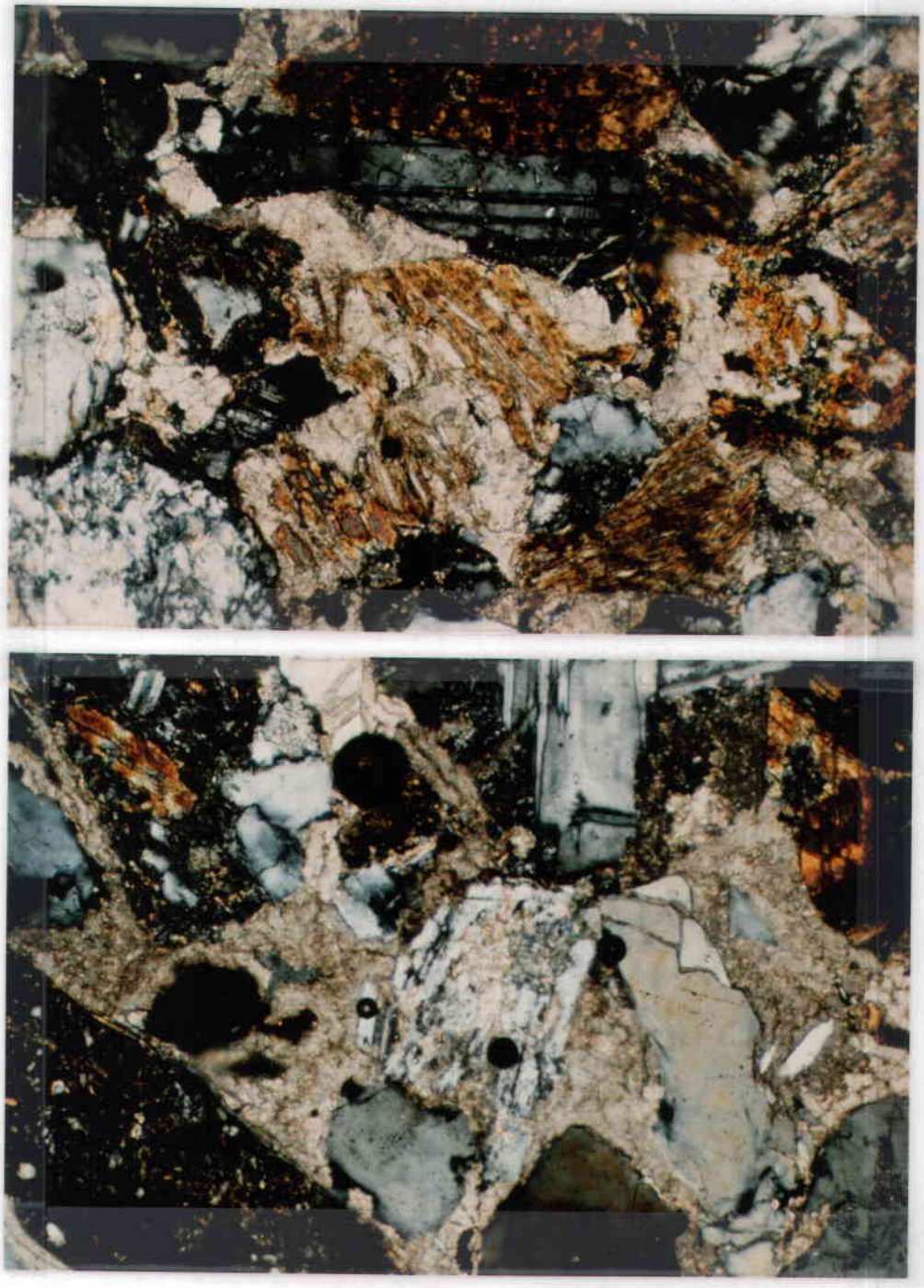

Figure 62. (top): Northern section Eocene sandstone (crossed nichols, 100X). Calcite cement has dilated the biotite grain, and corroded some framework minrals; (bottom): Southern section Eocene sandstone (crossed nichols, 100X). Calcite cement has fractured and partially replaced a plagioclase feldspar grain.

original grain (Fig. 62). Fine-grained lithic fragments, ferromagnesian minerals, and the feldspars were most susceptible to reaction with the calcite. Quartz was less reactive with the calcite cement.

Iron-oxide Cement

Many sandstone samples display a pervasive, opaque red-brown stain, interpreted to be an iron-oxide cement. The cement rims some framework clasts and fills void spaces in the rock. In the Cretaceous(?) samples collected within and south of the study area, this cement is particularly abundant. In hand sample, the Cretaceous rocks are finer grained, darker colored (reddish brown to yellow brown), and generally much more indurated than the Eocene sandstone samples. It is probable that the iron-oxide cement contributed to the higher degree of induration. The leaching of iron from ferromagnesian minerals likely contributed some of the ions for the iron-oxide cement. Most of the biotite grains present are faded and weakly pleochroic, possibly due to depletion of iron ions. Many Eocene sandstones have small amounts of iron-oxide cement, but are relatively friable. One fine-grained Eocene sandstone sample from the coal mine area has abundant iron-oxide cement. This sample is as well-indurated as the Cretaceous samples.

Zeolite and Quartz Overgrowths

Zeolites were occasionally observed in the Eocene sandstone samples. The zeolites occupy parts of the void spaces between framework minerals. This mineral appears mostly in the volcanic-rich sandstones.

Quartz overgrowths were observed rarely in the Cretaceous sandstone samples, and even less in the Eocene samples. The overgrowths are probably insignificant as a cementing agent in the sandstones.

Textural Analysis

Method

Textural analysis was performed on 16 sandstone samples. The average grain diameters were measured from thin sections on the petrographic microscope. Orthoclase, microcline, plagioclase feldspar, and quartz grains were measured. These grains were point counted as to Phi size and plotted on histograms (Appendix 3). Most samples had 250 grains measured. Only 100 to 150 counts were made on two poor slides. The selected minerals have similar form and specific gravity, making the minerals hydrodynamically equivalent. Therefore, the textural data on these grains should accurately reflect flow conditions that existed during deposition of the sandstones.

Results of the Textural Analysis

The results from the histograms were plotted on cumulative frequency graphs (Appendix 4). From these graphs, the median, mean grain diameter, standard deviation (sorting), and skewness of the sandstones were calculated (Table 6). These statistical measures were done using formulas from Folk and Ward (1957, Table 6). Standards for the mean, sorting and skewness are also shown in Table 6. The sandstones range from fine grained to coarse grained, according to mean grain diameter. Most of the sandstones are medium grained. A Cretaceous marine sandstone (KSS_1) from south of the study area is the finest-grained sample. All of the samples analyzed are moderately to moderately well sorted. Sandstones with these sorting values are characteristic of several depositional environments, including fluvial deposits (Friedman, 1962). Most of the samples have positive skewness values, indicating an enrichment in the fine-grained fraction. A plot of sorting versus skewness (Friedman, 1967, Fig. 63) indicates a fluvial depositional environment for the selected Eocene sandstone samples. The fluvial Eocene sands are less reworked by currents than typical beach sands, and are therefore more enriched in fines.

Table 6

Measures, Standards, and Results for the Sandstone Grain Size Distribution

Graphic Measures for Size Distribution Analysis

(from Folk and Ward, 1957)

Median = ϕ_{50}

$$\text{Graphic mean} = \frac{\phi_{16} + \phi_{50} + \phi_{84}}{3}$$

$$\underset{(S_1)}{\text{Sorting}} = \frac{\phi_{84} - \phi_{16}}{4} + \frac{\phi_{95} - \phi_5}{6.6}$$

$$\underset{(SK_1)}{\text{Skewness}} = \frac{(\phi_{84} + \phi_{16} - 2\phi_{50})}{2\,(\phi_{84} - \phi_{16})} + \frac{(\phi_{95} + \phi_5 - 2\phi_{50})}{2\,(\phi_{95} - \phi_5)}$$

Standards for Mean, Sorting, and Skewness

(From Folk, 1974; Pettijon et al, 1973; Friedman, 1962)

Mean:	Fine sand	3.0 ϕ - 2.0 ϕ
	Medium sand	2.0 ϕ - 1.0 ϕ
	Coarse sand	1.0 ϕ - 0ϕ

		S_1 Value
Sorting:	Well sorted	.35 - .50
	Moderately well sorted	.50 - .80
	Moderately sorted	.80 -1.40
	Poorly sorted	1.40 -2.00

		SK_1 Value
Skewness	Negatively skewed	-0.30 to -0.10
	Nearly symmetrical	-0.10 to +0.10
	Positively skewed	+0.10 to +0.30

Values of Selected Eocene and Cretaceous Samples

Sample	KSS_1	SX_2	SX_{32}	SX_3	SX_{28} (a)	SX_6	SX_{30}	MC_{15}	SX_4	SX_8	MC_{18}	KSS_6	SX_1	SX_{27}	SX_{10}	SX_{26}
Median (ϕ)	2.8	1.5	1.2	1.0	1.2	1.2	2.7	2.1	.8	.9	1.8	1.9	1.9	2.0	1.7	1.1
Mean (ϕ)	2.83	1.47	1.13	1.0	1.23	1.2	2.77	2.1	.83	.97	1.87	1.87	1.93	2.03	1.8	1.16
Sorting (S_1)	.738	.458	.498	.498	.673	.664	.79	.65	.56	.92	.82	.70	.73	.79	.84	.61
Skewness (SK_1)	.075	.06	-.09	.02	.11	.08	.14	0	.08	.14	.13	-.01	.07	.14	.16	.24

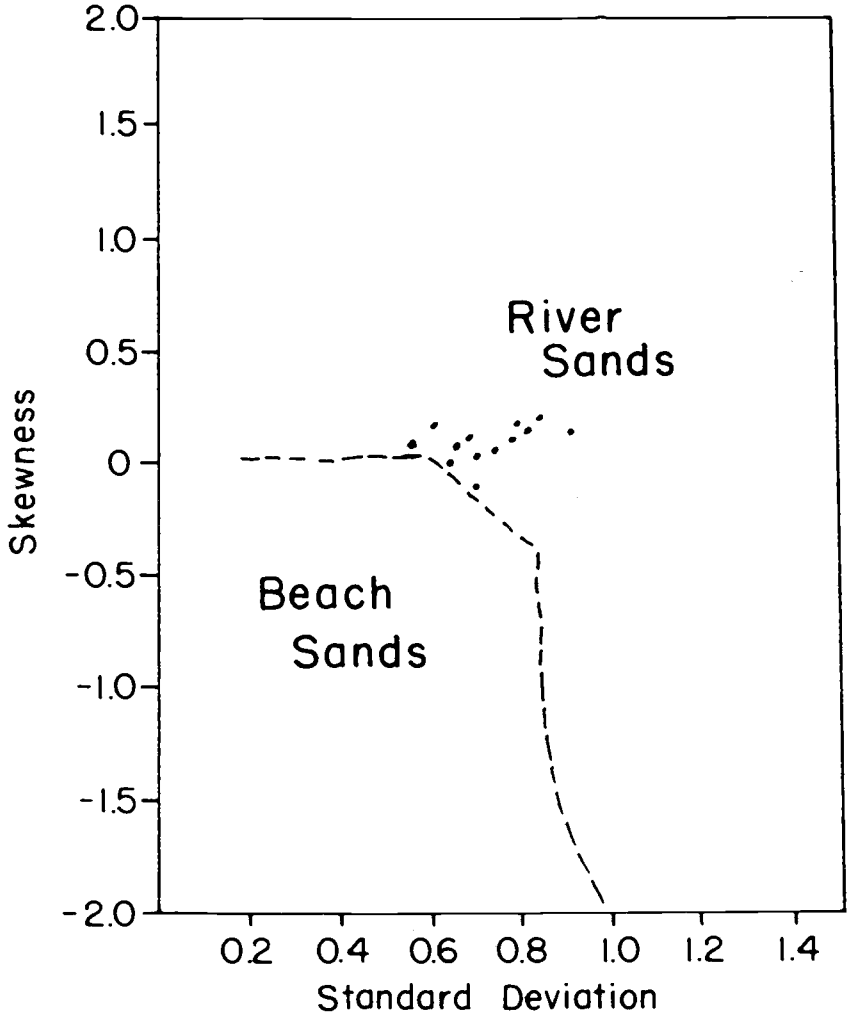

Figure 63. Samples from the Montgomery Creek Formation (dots), plot in section for river sands. Diagram modified from Friedman (1967).

CONGLOMERATE PEBBLE COUNT

Conglomerate clasts from three outcrops were counted, as shown on Figure 64. The lithologies represented include basalt, andesite, rhyolite, quartzite, argillite, chert, and intrusive rocks. A slight decrease in volcanics and argillite occurs from northeast to southwest, while chert, quartzite, and plutonic rocks increase. Only the argillite and some of the volcanics resemble observed Klamath province rocks. The argillite is similar to the Kosk member of the Modin Formation, and some porphyritic andesite clasts match the underlying Bagley Andesite.

The plutonic pebbles are granitic, as suggested by a point count on a single selected clast (Fig. 53). Therefore, a granitic body was relatively close to the Montgomery Creek Formation during deposition of this conglomerate. A granite body possibly now lies under the volcanic carapace of the Tertiary Cascade Range.

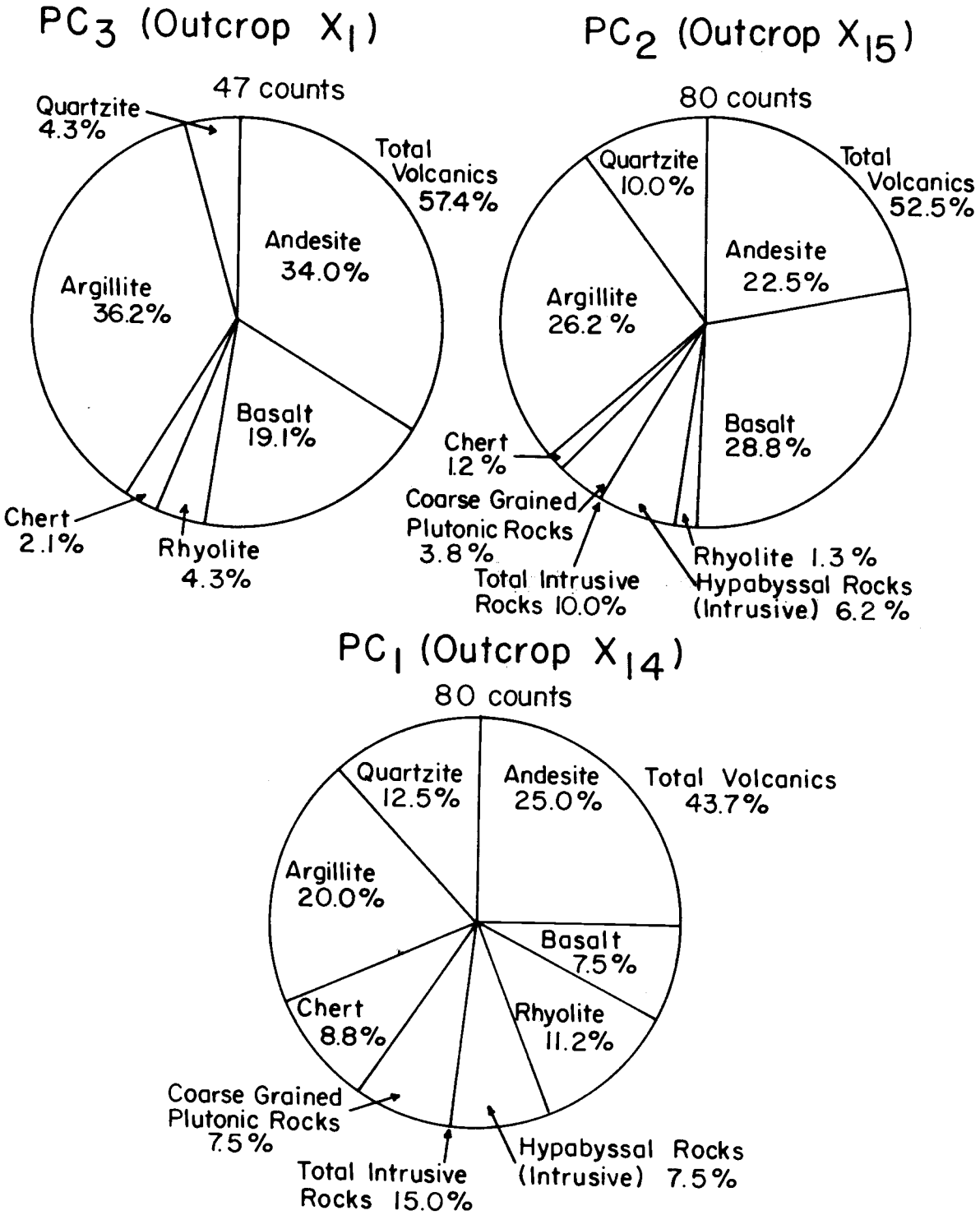

Figure 64. Results of conglomerate pebble counts as shown on pie diagrams. Locations of the conglomerates are shown in Figure 65.

PALEOCURRENT DATA

Paleocurrent readings were taken from several Montgomery Creek Formation outcrops in the study area. These measurements were made by Brunton Compass on foreset bedding and imbricated conglomerate pebbles. These orientations were then plotted on rose diagrams. It is assumed that the foreset bedding dips in a downstream direction, while the imbricated pebbles dip upstream. A mean vector was calculated for a grand rose diagram of the entire study area.

Imbricated Pebbles

Measurements were made on 91 pebbles from six outcrops (Fig. 65). The pebbles dip from near due north to due east. A direction of transport toward the southwest is therefore shown by the rose diagrams.

Foreset Bedding

Readings were taken on 23 foreset beds from eight outcrops (Fig. 65). A direction of transport toward the southeast is indicated by the rose diagrams.

Paleocurrent data point to a generally south transport direction. This flow direction is subparallel to the regional trend of the Cascade Range and Klamath province rocks. A northern source for the sandstones is also

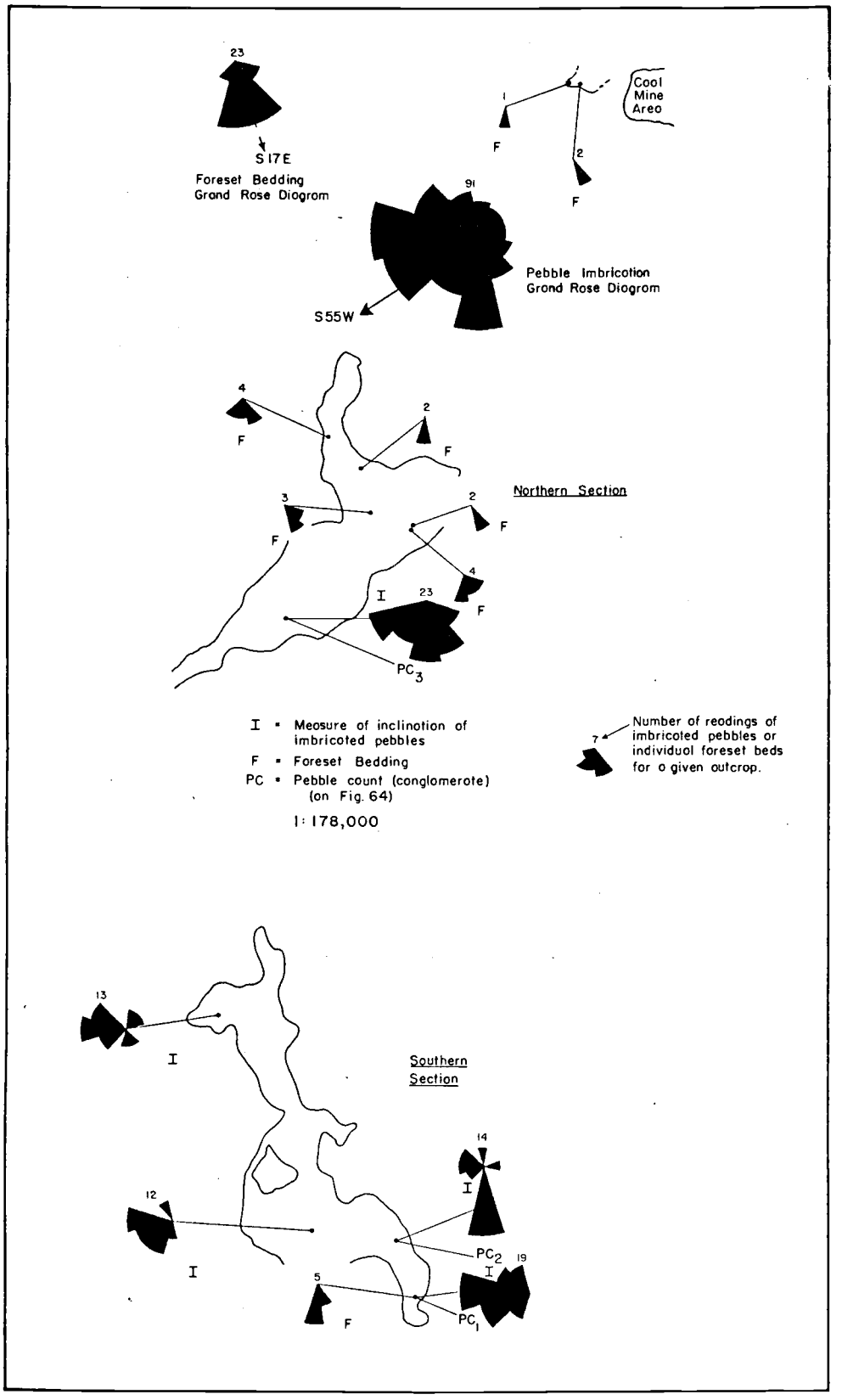

Figure 65. Sketch map of the study area showing paleocurrent directions.

implied. A paleoslope, downward from north to south, existed during deposition of the Montgomery Creek Formation.

SOURCE OF THE SANDSTONES

Petrographic and heavy mineral analyses of sandstones of the Montgomery Creek Formation reveal that these rocks were derived from two main sources:

(1) Granitic and metamorphic rocks: These rocks formed the main source materials for sandstones in the lower part of the section, and a partial source for the upper section sandstones. Typical sandstones derived from these granitic and metamorphic rocks include such framework grains as quartz, potassium feldspar, plagioclase feldspar (oligoclase), biotite, muscovite, and epidote. Granitic and metamorphic rock fragments are also observed. Many of the sandstone framework clasts are subangular, with very few grains rounded to well rounded. This suggests a relatively short transport distance for the sandstones. The plutonic-metamorphic source was located to the north of the study area, as demonstrated by the paleocurrent results. Mesozoic granitic plutons are exposed about 30 miles to the northwest of the study area in the Klamath Mountains (Weed Sheet, Strand, 1963). To the east, these plutons are buried beneath a carapace of Tertiary and Quaternary volcanics which includes Mount Shasta. It is possible that a large plutonic-metamorphic body lies beneath this volcanic cover, and was a source for the Montgomery Creek Formation sandstones.

The possibility of the sandstones being derived from a Sierra-Nevadan plutonic-metamorphic source must be discounted for the following reasons: (A) The paleocurrent results point to a northerly source, and only Klamath plutons are recognized to the north of the study area; (B) Triassic and Jurassic volcanic arc units of the Eastern Klamaths and Sierra Nevadas are broadly correlative (Schweikert and Cowen, 1975). However, the timing of subsequent plutonic activity is different for the Sierra Nevadas and Klamaths. Cretaceous plutons are found in the Sierra Nevadas, while Late Jurassic plutons are present in the Klamaths (Irwin, 1966). Therefore, it is unlikely that Sierra Nevadan Cretaceous plutonic activity ever extended as far north as the Klamath Mountains (or to the study area). Petrographic analysis was performed on a granitic pebble high in the Eocene section (Fig. 53). This sample resembled neither the Klamath nor the Sierra Nevadan samples analyzed.

(2) Volcanic Rocks: Volcanic rocks formed a major source for the upper section Eocene sandstones, and a minor source for sandstones in the lower section. The lower section sandstones sometimes contain volcanic fragments similar to adjacent Klamath province volcanics. Some of these fragments resemble the Jurassic Bagley Andesite or Arvison Formation. The upper section Eocene

sandstones contain abundant fresh volcanic rock fragments, especially in the southern section. These basaltic and andesitic clasts were probably derived from a developing Cascade volcanic arc to the north and east, as supported by paleocurrent readings. Abundant fresh plagioclase feldspar (andesine), hornblende, clinopyroxene, and oxy-hornblende typically accompany these volcanic rock fragments. Minerals such as potassium feldspar, biotite, and oligoclase indicate a continuing contribution from Klamath granitic source rocks.

GEOLOGIC HISTORY

The Montgomery Creek Formation is located between two large geologic provinces. The older Klamath Mountains border the Eocene sediments to the west, while the younger Cascade Mountains overlie the sediments to the east.

Klamath Mountains

The Klamath Mountains consist of four subprovinces. Only the eastern Klamath subprovince borders the Montgomery Creek Formation. Irwin (1981) concluded that the Paleozoic rocks of the eastern Klamath mountains formed a volcanic island arc built on ultramafic rocks. This volcanic arc was intermittently active from the early Paleozoic to the Jurassic. Burchfiel and Davis (1972) have suggested that this volcanic arc was separatd from the cratonic and continental miogeosynclinal area by some form of basin at least since the Silurian.

Petrographic studies of volcanic graywackes indicate that there were four episodes of increased volcanism in the eastern Klamaths from the Late Silurian to Jurassic (Murray and Condie, 1973). The Triassic and Jurassic rocks which border the Montgomery Creek Formation represent the youngest of these volcanic arc deposits. At this time, the western margin of the continent was largely submerged and the volcanic arc appeared as islands that

supplied clastic detritus to adjacent marine basins to the east (Burchfiel and Davis, 1981).

Paleomagnetic studies by Mankinen et al. (1984) reveal that the Triassic and Jurassic rocks adjacent to the study area rotated clockwise during and after their deposition. The Triassic rocks have rotated 100°, while Jurassic strata have rotated 60°. The strata began to rotate during Late Triassic or Early Jurassic, possibly in response to accretion of an eastern Klamath terrane to the continental margin (Mankinen, et al., 1984). The rotation was virtually completed by the Early Cretaceous, probably representing the end of accretion.

During the Late Jurassic, eastern Klamath subprovince rocks were involved in the Nevadan orogeny (Irwin, 1966). The eastern Klamath strata were tilted and folded by this orogeny, and intruded by granitic plutons. In addition, the strata were thrust westward over the adjacent Klamath central metamorphic belt (Irwin, 1966). The effect that the Nevadan orogeny had on the clockwise rotation of the Triassic and Jurassic strata is uncertain. Possibly the rotation was completed before inception of the orogeny.

Subsequent to the Nevadan orogeny, the Klamath Mountains basement complex was tectonically uplifted in the Early Cretaceous to form a major source for Cretaceous sediment which was shed northeastward into the Hornbrook basin and southward into the Great Valley forearc basin

(Nilsen, 1984; Fig. 66). Deposits in these two marine basins record transgression until the Late Cretaceous. The seas transgressed northeastward in the vicinity of Redding, and southward in the vicinity of Hornbrook near the California-Oregon border (Jones, 1960; Fig. 67). The presence of Cretaceous marine deposits in the study area is questionable, because no marine fossils were found. It is possible that any Cretaceous marine sandstones deposited in the study area were subsequently eroded away. The connection of the Hornbrook and Great Valley basins (Fig. 66) is uncertain, because the intervening area is covered with Tertiary and Quaternary volcanic rocks.

The Klamaths evidently formed a persistent positive element throughout Cretaceous and Tertiary time. Evidence for this is as follows: (1) Lower Cretaceous nonmarine and shallow marine facies indicative of strandline associations locally rest uncomformably on igneous and metamorphic rocks within the Klamath block (Jones and Irwin, 1971). By contrast, Lower Cretaceous strata to the south are entirely deep-water turbidites that display southerly paleocurrents essentially all the way to the San Francisco Bay area (Ojakangas, 1968); (2) The distribution of Upper Cretaceous turbidite facies and paleocurrents south of the Klamaths also imply northward shoaling of a deep trough, and its closure against submarine slopes and shelves along

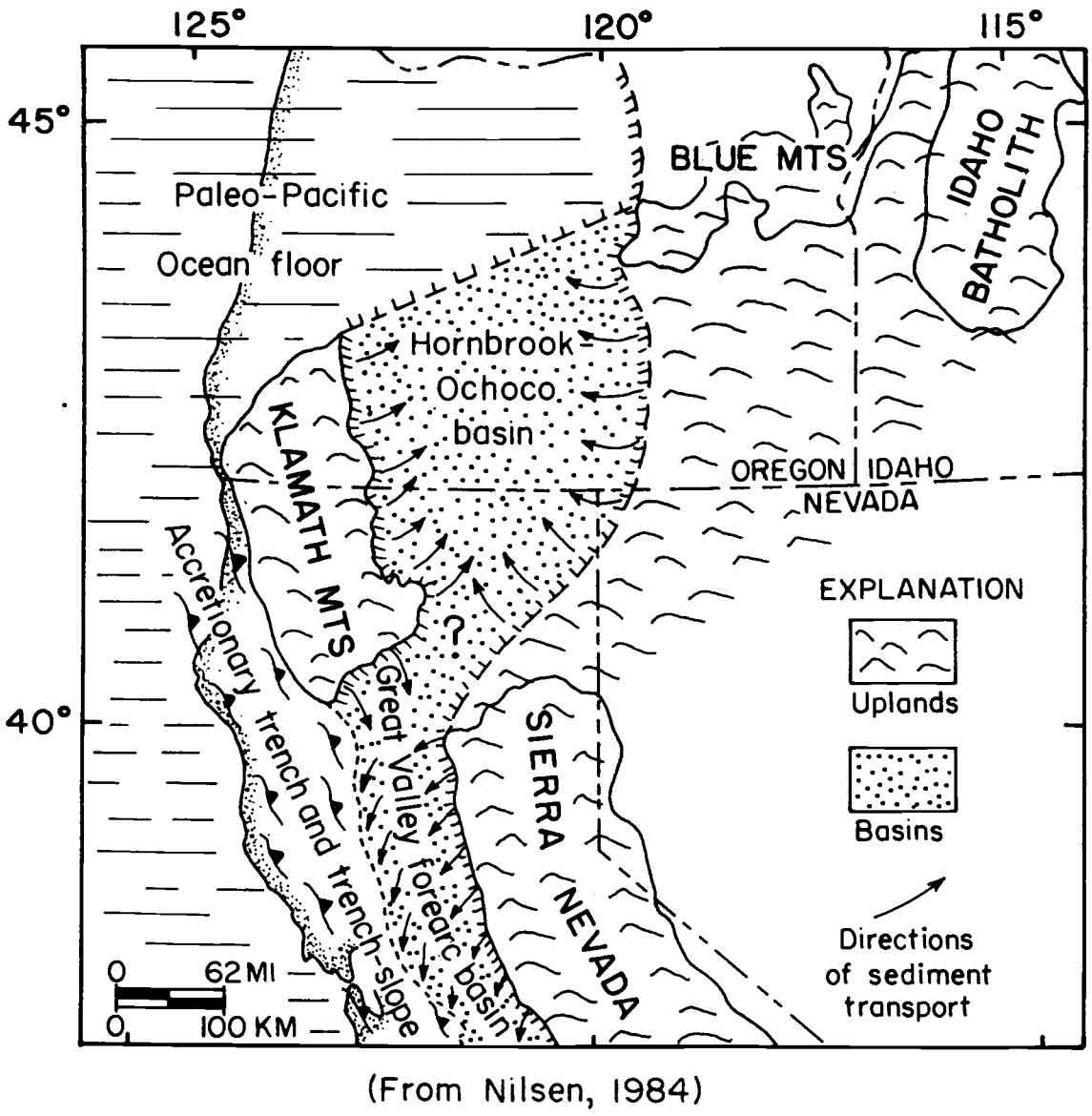

(From Nilsen, 1984)

Figure 66. The Klamath Mountains acted as a source area for Cretaceous marine sandstones of the Great Valley and Hornbrook-Ochoco basins. Diagram from Nilsen (1984).

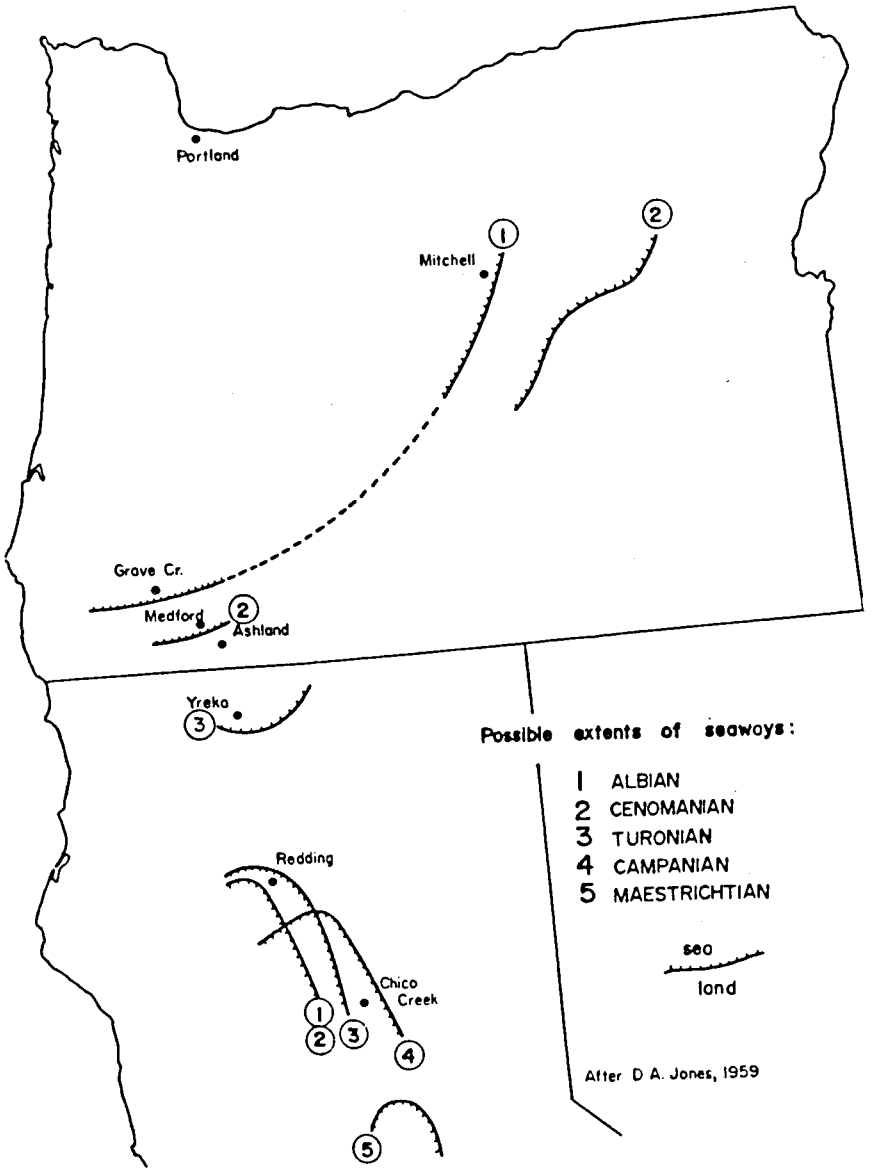

Figure 67. Map by Jones (1960) showing Cretaceous seas transgressing eastward in the Redding area and southward in the Yreka region.

the southern edge of the Klamath block (Ingersoll, 1979). Conversely, paleocurrents in Upper Cretaceous and Paleogene strata (Hornbrook and Payne Cliffs Formations) on the northeast side of the Klamath Mountains trend northward away from the Klamath block (Elliott, 1971; McKnight, 1971).

The Montgomery Creek Formation basal conglomerate, dated as Upper Cretaceous-lower Eocene, is indicative of renewed uplift in the eastern Klamath subprovince, within the time span of the Laramide orogeny. This orogeny was marked by crustal buckling and associated fracturing to form giant fault-bounded, basement cored uplifts separated by intervening basins in which sediment accumulated while deformation was in progress (Dickinson and Snyder, 1978). Although the orogeny occured far to the east in the central Rocky Mountains, some evidence of Laramide-style deformation might be expected to the west. The episode of early to middle Eocene folding and high-angle faulting in the northern Cascades (Misch, 1966) could have been a local effect of the Laramide tectonism (Dickinson and Snyder, 1978). Likewise, the Upper Cretaceous-lower Eocene Klamath uplift could be attributed to Laramide tectonics.

The late Eocene nonmarine Payne Cliffs Formation on the northeast edge of the southern Oregon Klamath Mountains contains a basal conglomerate and several

conglomerate lenses. Conglomerate clast lithologies include quartzite, chert, and plutonic rock fragments (McKnight, 1971, 1984). This suggests repeated Klamath Mountain uplifts during the late Eocene, somewhat later than the Montgomery Creek Formation basal conglomerate. However, conglomerate beds high in the Montgomery Creek Formation southern section may record a Klamath uplift history similar to that of the Payne Cliffs Formation. The uplifted Klamath Mountains served as a source for the middle Eocene Montgomery Creek Formation. The lower part of the formation was deposited by meandering rivers which flowed generally north to south across an extensive subsiding flood basin. Many of these deposits occur in the northern section, coal mine area, and lower southern section.

Cascade Range

The onset of Eocene Cascade volcanism is recorded in the sandstones of the Montgomery Creek Formation. Arc magmatism did not begin in the Oregon Cascades prior to the late Eocene (Peck, et al, 1964). Therefore, strata in the upper part of the formation may be late Eocene in age. Fresh andesitic and basaltic clasts are abundant in the upper part of the formation, especially in the southern section. Rivers choked with Cascade volcanic detritus

flowed into the Montgomery Creek Formation flood basin, soon dominating deposition in the basin. These were braided streams, influenced by high volcanic sediment discharge and steep gradients in the depositional basin. Braided streams usually require sharper gradients than meandering river systems. The steep gradients were probably aided by increased subsidence rates in the depositional basin. Klamath-derived sediments continued to contribute to the Montgomery Creek Formation, mixing with the Cascade volcanic detritus. The system of rivers which deposited the Montgomery Creek Formation strata flowed southward and delivered sediments to the Sacramento basin (Dickinson, et al, 1979; Fig. 68). An extensive Paleogene marine shelf about 75 km wide occupied much of the basin.

Following deposition of the Eocene sediments, the strata underwent erosion during the Oligocene and Miocene. The Klamath Mountains underwent regional structural doming at some time between middle Miocene and early Pliocene (Mortimer and Coleman, 1984). This doming affected rocks of the Klamath and Cascade Mountains, tilting Cretaceous to Miocene strata. The regional east dip and small normal faults found in the Montgomery Creek Formation probably were caused by this Klamath upwarping to the west.

During the late Miocene(?) and Pliocene, lava flows covered the study area. Andesite and basalt flows prevailed in the northern section, while only basalt blank-

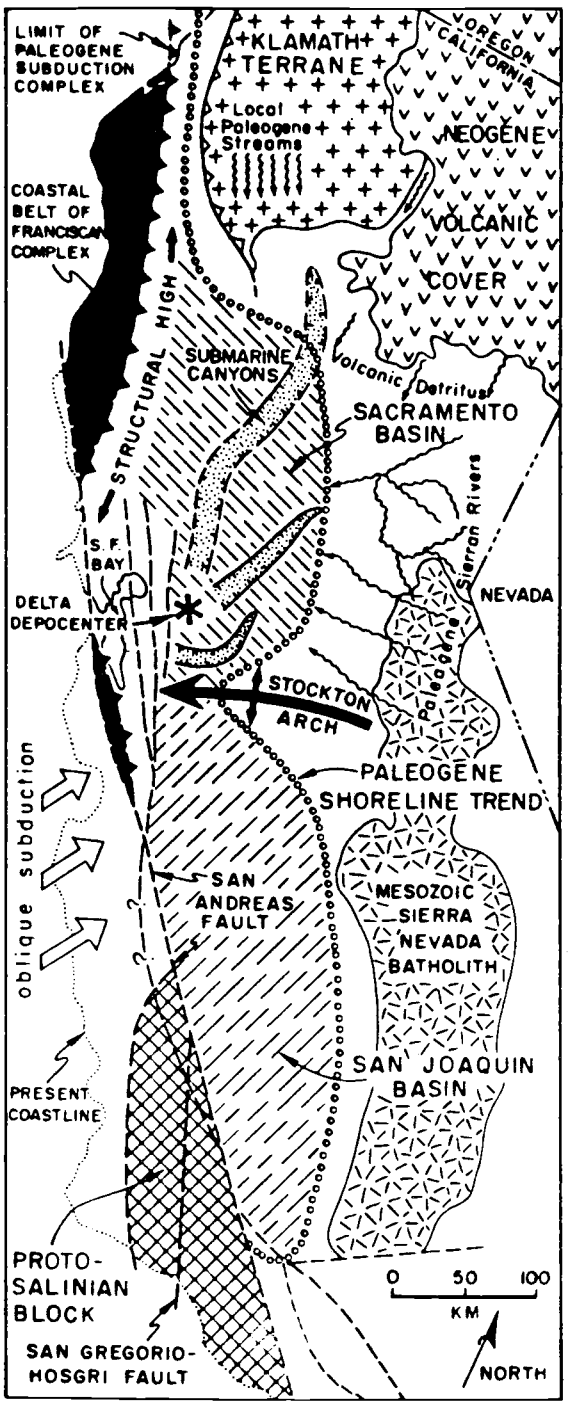

Figure 68. Sketch map of northern and central California during Paleogene time. In northern California, note sediment dispersal into Sacramento basin by fluvial systems draining Klamath, Cascades (volcanic), and Sierran provenances (from Dickinson, et al., 1979).

eted the southern section. The northern section volcanics may have experienced effects of the Klamath doming event, as they are tilted slightly eastward. The younger (?) southern section volcanics are nearly flat-lying, and probably were less affected by the doming. Streams have since cut through the volcanic cover, exposing the underlying strata and forming the present rugged topography in the study area. Small amounts of Quaternary alluvium were deposited by these streams, especially adjacent to the Pit River and Kosk Creek.

BIBLIOGRAPHY

Adeleye, D. R., 1974, Sedimentology of the fluvial Bida Sandstone (Cretaceous), Nigeria: Sedimentary Geology, v. 12, p. 1-24.

Allen, J. R. L., 1965, A review of the origin and characteristics of Recent alluvial sediments: Sedimentology, v. 5, p. 89-191.

Anderson, C. A., and R. D. Russell, 1939, Tertiary formations of northern Sacramento Valley, California: California Division of Mines Report 35, p. 219-253.

Aune, Q. A., 1964, A trip to Burney Falls: California Division of Mines and Geology Mineral Information Service, V. 17, n. 10, p. 183-191.

Axelrod, D. I., 1985, Botany Professor, University of California, Davis, personal communication: Department of Botany, Davis, California.

Beerbower, J. R., 1964, Cyclothems and cyclic depositional mechanisms in alluvial plain sedimentation, in Merriam, D. F., ed., Symposium on Cyclic Sedimentation: State Geological Survey of Kansas, Bulletin 169, p. 31-42.

Burchfiel, B. C., and G. A. Davis, 1972, Structural framework and evolution of the southern part of the Cordilleran orogen, western United States: American Journal of Science, v. 272, p. 97-118.

_____, and G. A. Davis, 1981, Triassic and Jurassic tectonic evolution of the Klamath Mountains - Sierra Nevada geologic terrane, in Ernst, W. G., ed., The Geotectonic Development of California: Englewood Cliffs, N.J., Prentice-Hall, Inc., p. 50-70.

Callaghan, E., 1933, Some features of the volcanic sequence in the Cascade Range in Oregon: American Geophysical Union Trans., 14th Annual Meeting, p. 243-249.

Campbell, C. V., 1976, Reservoir geometry of a fluvial sheet sandstone: AAPG Bulletin, v. 60, p. 1009-1020.

Cant, D. J., 1982, Fluvial facies models and their application, in Scholle, P. A., and D. Spearing, eds., Sandstone depositional environments: AAPG Memoir 31, p. 115-137.

Dickey, P. A., and J. M. Hunt, 1972, Geochemical and hydrogeologic methods of prospecting for stratigraphic traps: AAPG Memoir 16, p. 136-167.

Dickinson, W.R., and W.S. Snyder, 1978, Plate tectonics of the Laramide orgeny: GSA Memoir 151, p. 355-366.

_____, R.V. Ingersoll, and S.A. Graham, 1979, Paleogene sediment dispersal and paleotectonics in northern California: GSA Bulletin, Part II, v. 90, p. 1458-1528. (Summary of this article in Part I, v. 90, p. 897-898).

Diller, J. S., 1889, Geology of the Lassen Peak district: U.S. Geological Survey Annual Report 8, p. 401-432.

_____, 1906, Description of the Redding quadrangle (California): U.S. Geological Survey Geologic Atlas, Redding Folio, n. 138, 14 p.

Dott, R. L., Jr., 1964, Wacke, graywacke and matrix - What approach to immature sandstone classification?: Journal of Sedimentary Petrology, v. 34, p. 625-632.

Elliott, M.A., 1971, Stratigraphy and petrology of the Late Cretaceous rocks near Hilt and Hornbrook, Siskiyou County, California, and Jackson County, Oregon: Ph.D thesis, Corvallis, Oregon, Oregon State University, 171 p.

Fairbanks, H. W., 1893, Geology and mineralogy of Shasta County: California Mineral Bureau Report 11, p. 24-53.

Folk, R. L., and W. C. Ward, 1957, Brazos river bar: a study in the significance of grain size parameters: Journal of Sedimentary Petrology, v. 27, p. 3-26.

Friedman, G. M., 1962, On sorting, sorting coefficients, and the lognormality of the grain-size distribution of sandstones: Journal of Geology, v. 70, p. 737-753.

_____, 1967, Dynamic processes and statistical parameters compared for size frequency distribution of beach and river sands: Journal of Sedimentary Petrology, v. 37, p. 327-354.

Gay, T. E., Jr., and Q. A. Aune, 1958, Geologic map of California, Alturas Sheet, scale 1:250,000: California Division of Mines.

Gibson, D. W., 1977, Upper Cretaceous and Tertiary coal-bearing strata in the Drumheller-Ardley region, Red Deer River Valley, Alberta: Geological Survey of Canada, Paper 76-35, 41 p.

Heward, A. P., 1978, Alluvial fan sequence and megasequence models: with examples from Westphalian D - Stephanian B coalfields, northern Spain, in Miall, A. D., ed., Fluvial sedimentology, CSPG Memoir 5, p. 669-702.

Hilton, R. P., 1975, The geology of the Ingot-Round Mountain area, Shasta County, California: Master's thesis, California State University, Chico, p.

Hinds, N. E. A., 1933, Geologic formations of the Redding, Weaverville districts, northern California: California Journal of Mines and Geology, v. 29, n. 1, p. 76-122.

Ingersoll, R.V., 1979, Evolution of the Late Cretaceous forearc basin, northern and central California: GSA Bulletin, Part I, v. 80, p. 813-826.

Irwin, W. P., 1966, Geology of the Klamath Mountains province, in Bailey, E. H., ed., Geology of northern California: California Division of Mines and Geology Bulletin 190, p. 19-38.

_____, 1977, Review of Paleozoic rocks of the Klamath Mountains, in Stewart, J. H., and others, eds., Paleozoic paleogeography of the western United States: Pacific Section SEPM, Pacific Coast Paleogeography Symposium 1, p. 441-454.

_____, 1981, Tectonic accretion of the Klamath Mountains, in Ernst, W. G., ed., The Geotectonic Development of California: Englewood Cliffs, N.J., Prentice-Hall, Inc., p. 29-49.

Jones, D. L., 1960, Cretaceous stratigraphy of northern California and southern Oregon: Pacific Petroleum Geologist, v. 14, n. 5, p. 4.

_____, and W.P. Irwin, 1971, Structural implications of an offset Early Cretaceous shoreline in northern California: GSA Bulletin, v. 82, p. 815-822.

Law, B. E., D. E. Anders, and T. H. Nilsen, 1984, The petroleum source-rock potential of the Upper Cretaceous Hornbrook Formation, north-central California and southwestern Oregon, in Nilsen, T. H., ed., Geology of the Upper Cretaceous Hornbrook Formation, Oregon and California: Pacific Section SEPM, v. 42, p. 133-140.

Leeder, M., 1973, Sedimentology and palaeogeography of the Upper Old Red Sandstone in the Scottish Border Basin: Scottish Journal of Geology, v. 9, p. 117-144.

Lydon, P. A., T. E. Gay, Jr., and C. W. Jennings, 1960, Geologic map of California, Westwood Sheet, scale 1:250,000: California Division of Mines.

MacDonald, G. A., 1966, Geology of the Cascade Range and Modoc Plateau, in Bailey, E. H., ed., Geology of northern California: California Division of Mines and Geology Bulletin 190, p. 65-96.

MacGinitie, H. D., 1941, A middle Eocene flora from the central Sierra Nevada: Carnegie Institute of Washington Publication 534, 178 p.

Mankinen, E. A., W. P. Irwin, and C. S. Gromme, 1984, Implications of paleomagnetism for the tectonic history of the eastern Klamath and related terranes in California and Oregon, in Nilsen, T. H., ed., Geology of the Upper Cretaceous Hornbrook Formation, Oregon and California: Pacific Section SEPM, v. 42, p. 221-229.

McKnight, B. K., 1971, Petrology and sedimentation of Cretaceous and Eocene rocks in the Medford-Ashland region, southwestern Oregon: Ph.D thesis, Oregon State University, Corvallis, 177 p.

_____, 1984, Stratigraphy and sedimentology of the Payne Cliffs Formation, southwestern Oregon, in Nilsen, T. H., ed., Geology of the Upper Cretaceous Hornbrook Formation, Oregon and California: Pacific Section SEPM, v. 42, p. 187-194.

McLean, J. R., and T. Jerzykiewicz, 1978, Cyclicity, tectonics and coal: some aspects of fluvial sedimentology in the Brazeau-Paskapoo Formations, Coal Valley area, Alberta, Canada, in Miall, A. D., ed., Fluvial sedimentology: CSPG Memoir 5, p. 441-468.

Miall, A. D., 1977, A review of the braided-river depositional environment: Earth Science Review, v. 13, p. 1-62.

Misch, P., 1966, Tectonic evolution of the northern Cascades of Washington State: Canadian Inst. of Mining and Metallurgy Special Vol. 8, p. 101-148.

Mortimer, N., and R. G. Coleman, 1984, A Neogene structural dome in the Klamath Mountains, California and Oregon, in Nilsen, T. H., ed., Geology of the Upper Cretaceous Hornbrook Formation, Oregon and California: Pacific Section SEPM, v. 42, p. 179-186.

Mrakovich, J. V., and A. H. Coogan, 1974, Depositional environment of the Sharon Conglomerate member of the Pottsville Formation in northeastern Ohio: Journal of Sedimentary Petrology, v. 44, p. 1186-1199.

Murray, M., and K. C. Condie, 1973, Post-Ordovician to early Mesozoic history of the eastern Klamath subprovince, northern California: Journal of Sedimentary Petrology, v. 43, p. 505-515.

Nilsen, T. H., 1984, Stratigraphy, sedimentology, and tectonic framework of the Upper Cretaceous Hornbrook Formation, Oregon and California, in Nilsen, T. H., ed., Geology of the Upper Cretaceous Hornbrook Formation, Oregon and California: Pacific Section SEPM, v. 42, p. 51-88.

Ojakangas, R. W., 1968, Cretaceous sedimentation, Sacramento Valley, California: GSA Bulletin, v. 79, p. 973-1008.

Peck, D. L., A. B. Griggs, H. G. Schlicker, F. G. Wells, and H. M. Dole, 1964, Geology of central and northern parts of the western Cascade Range in Oregon: U.S. Geological Survey, Professional Paper 449, 56 p.

Pettijohn, F. J., P. E. Potter, and R. Siever, 1973, Sand and sandstone: New York-Heidelberg-Berlin, Springer-Verlag, 618 p.

Potter, P. E., and E. F. Pettijohn, 1963, Palaeocurrents and basin analysis: Berlin-Gottingen-Heidelberg, Springer, 296 p.

Powers, M. C., 1953, A new roundness scale for sedimentary particles: Journal of Sedimentary Petrology, v. 23, p. 117-119.

Reineck, H. E., and I. B. Singh, 1973, Depositional sedimentary environments: New York, Springer-Verlag, 439 p.

Ruffin, J. H., 1980, An explanation of hydrocarbon source-rock evaluation, contained in the Tenneco Oil Company personal communication.

Sanborn, A. F., 1960, Geology and paleontology of the southwest quarter of the Big Bend quadrangle, Shasta County, California: California Division of Mines Special Report 63, 26 p.

Schumm, S. A., 1960, The effect of sediment type on the shape and stratification of some modern fluvial deposits: American Journal of Science, v. 258, p. 177-184.

_____, 1968, Speculations concerning paleohydraulic controls of terrestrial sedimentation: GSA Bulletin, v. 79, p. 1573-1588.

Schweickert, R. A., and D. S. Cowan, 1975, Early Mesozoic tectonic evolution of the western Sierra Nevada, California: GSA Bulletin, v. 86, p. 1329-1336.

Simons, D. B., E. V. Richardson, and C. F. Nordin, 1965, Sedimentary structures generated by flow in alluvial channels, in Middleton, G. V., ed., Primary sedimentary structures and their hydrodynamic interpretation: SEPM Special Publication 12, p. 34-52.

Steel, R. J., 1974, New Red Sandstone floodplain and piedmont sedimentation in the Hebridean Province, Scotland: Journal of Sedimentary Petrology, v. 44, p. 336-357.

Strand, R. G., 1962, Geologic map of California, Redding Sheet, scale 1:250,000: California Division of Mines and Geology.

_____, 1963, Geologic map of California, Weed Sheet, scale 1:250,000: California Division of Mines and Geology.

Tenneco Oil Company, 1984, Personal communication containing reservoir properties, source-rock evaluation, and age determination of samples from the Montgomery Creek Formation.

Tissot, B., and D. Welte, 1978, Petroleum formation and occurrence: Berlin, Springer-Verlag, 527 p.

Walker, R. G., 1976, Facies models-3. Sandy fluvial systems: Geoscience Canada, v. 3, p. 101-109.

Williams, H., 1932, Geology of the Lassen Volcanic National Park, California: University of California Department of Geological Science Bulletin, v. 21, n. 8, p. 195-385.

Wolfe, J.A., 1977, Paleogene floras from the Gulf of Alaska region: U.S. Geological Survey, Professional Paper 997, 108 p.

APPENDICES

APPENDIX I

Montgomery Creek Formation
Outcrop Sketches

Legend for Outcrop Sketches in Appendix I
Vertical Scale: 1 Inch=10 Feet

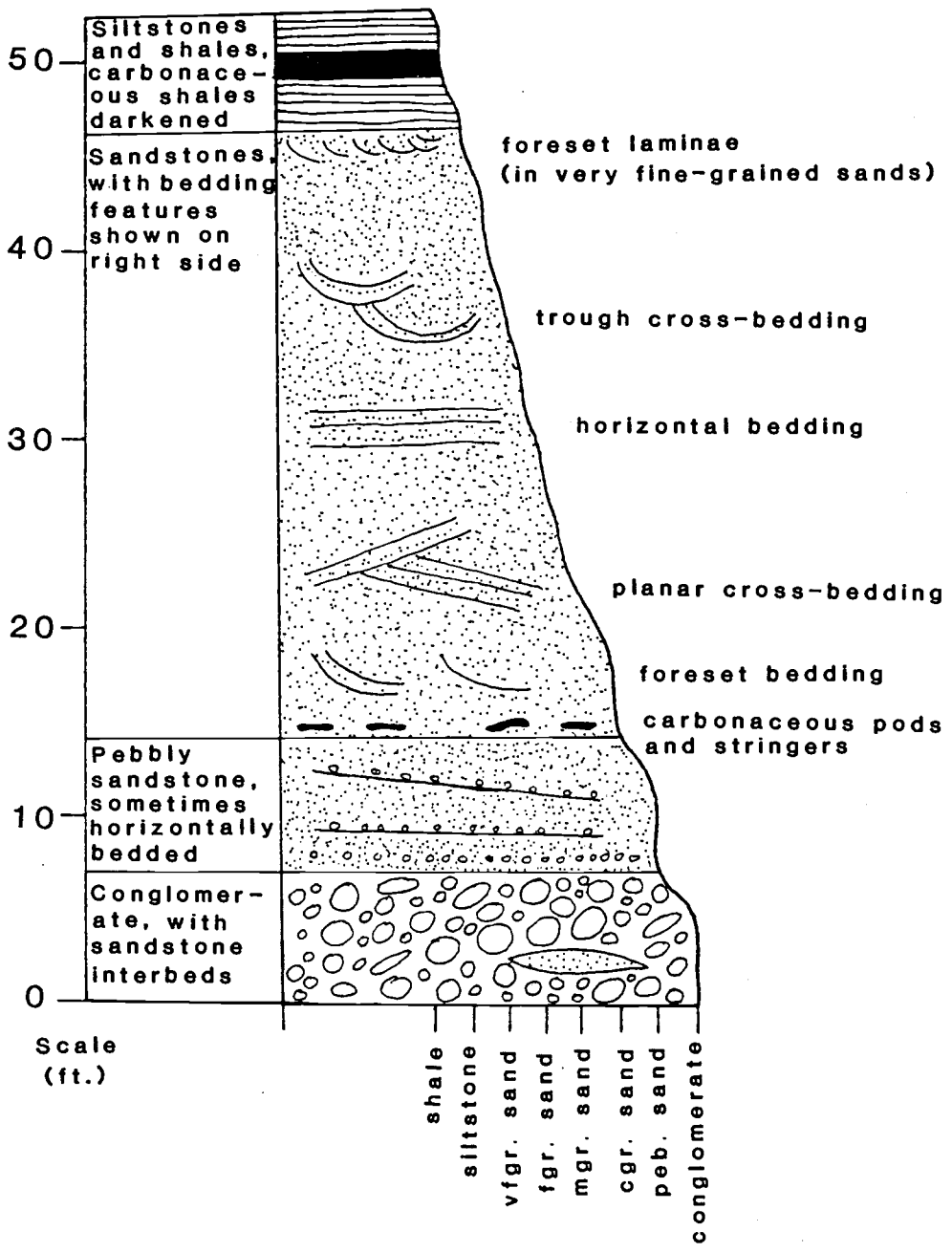

Northern Section Outcrops
(Beginning at base of section and proceeding upsection)

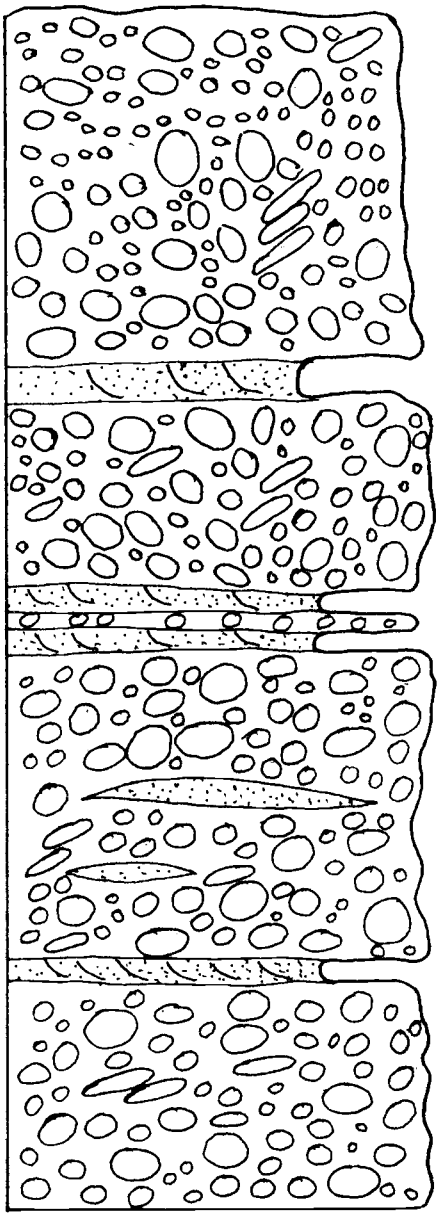

Outcrop X_1
(62 feet portion of
300 foot basal
conglomerate)

T3SN R1W
Sec. 11 NW 1/4

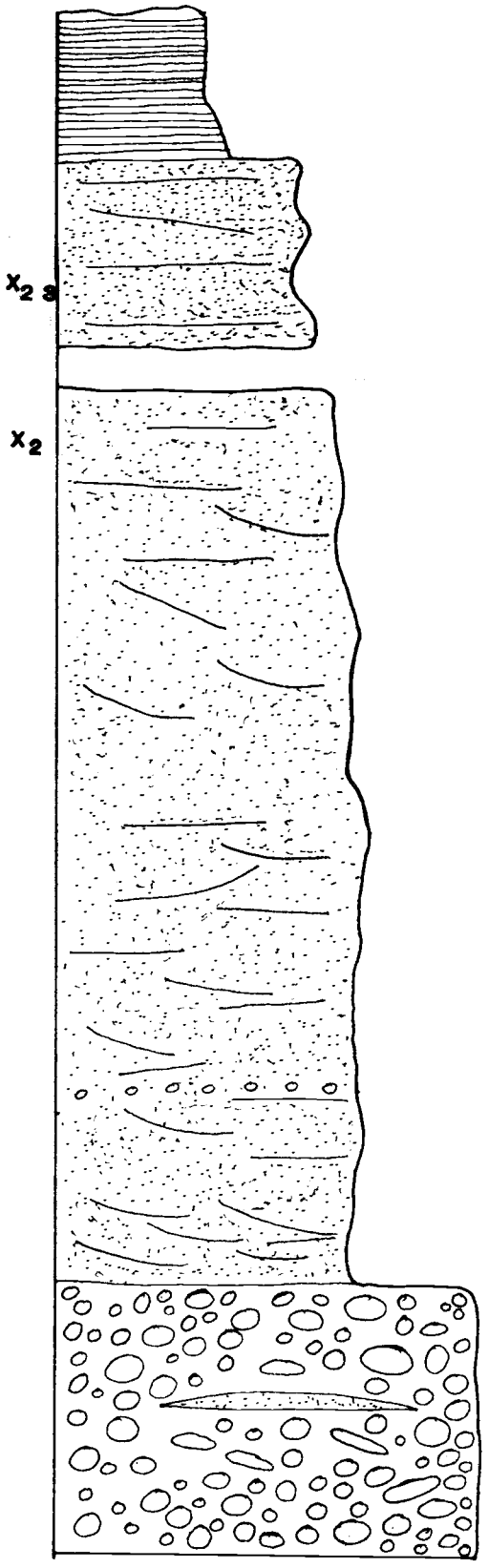

Outcrops X_2 and X_{23}
T36N R1W
Sec. 11 NE 1/4

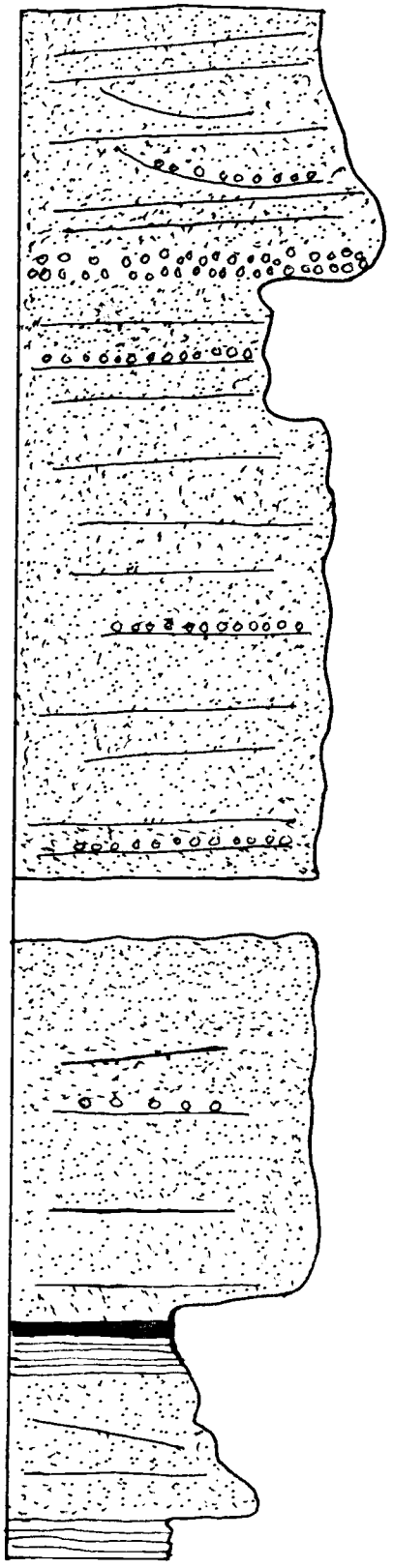

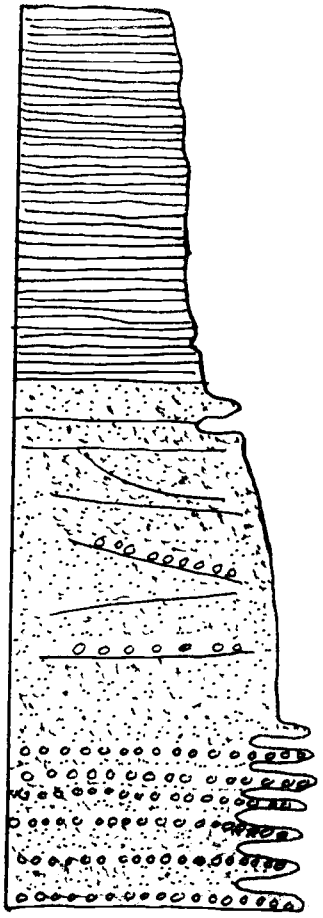

Outcrop X_5
T37N R1W
Sec. 24 SW 1/4

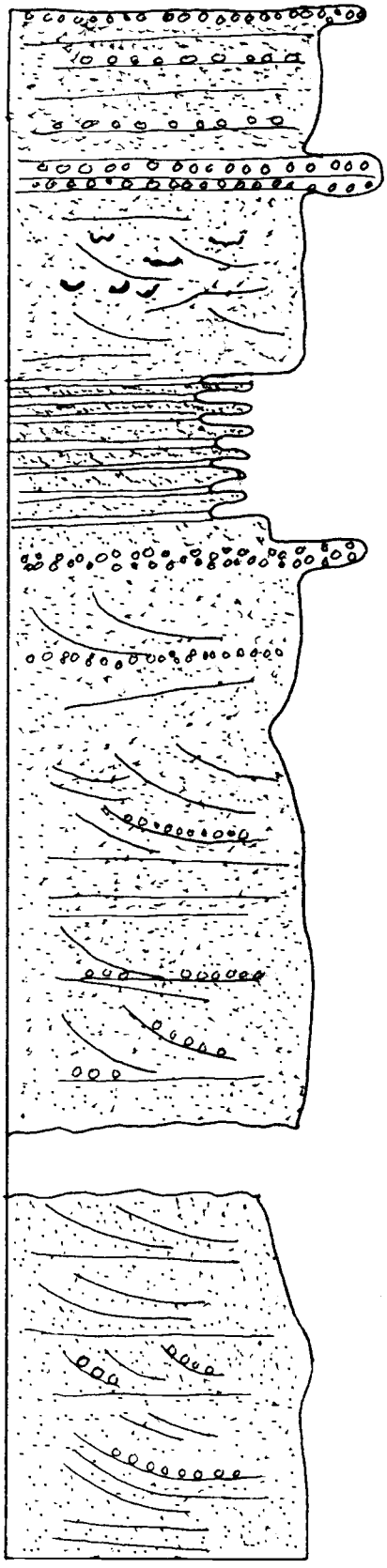

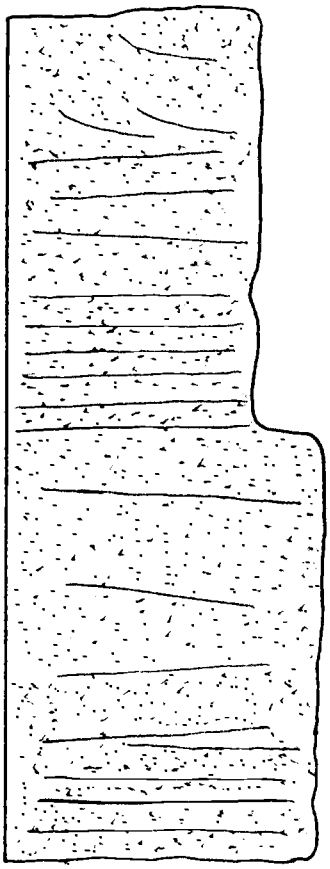

Outcrop X_4
T37N R1W
Sec. 25 NW 1/4

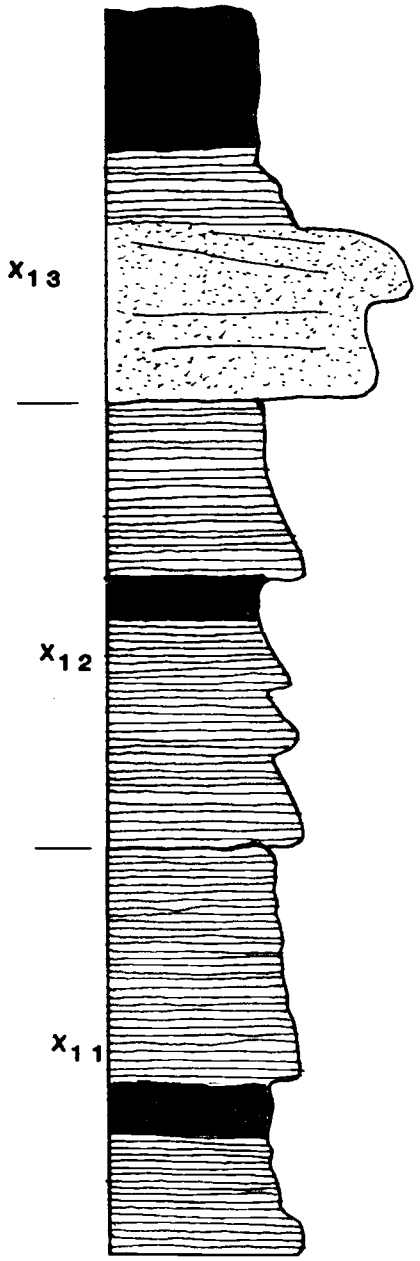

Outcrops X_{11}, X_{12} and X_{13}
T37N R1W
Sec. 24 NW 1/4

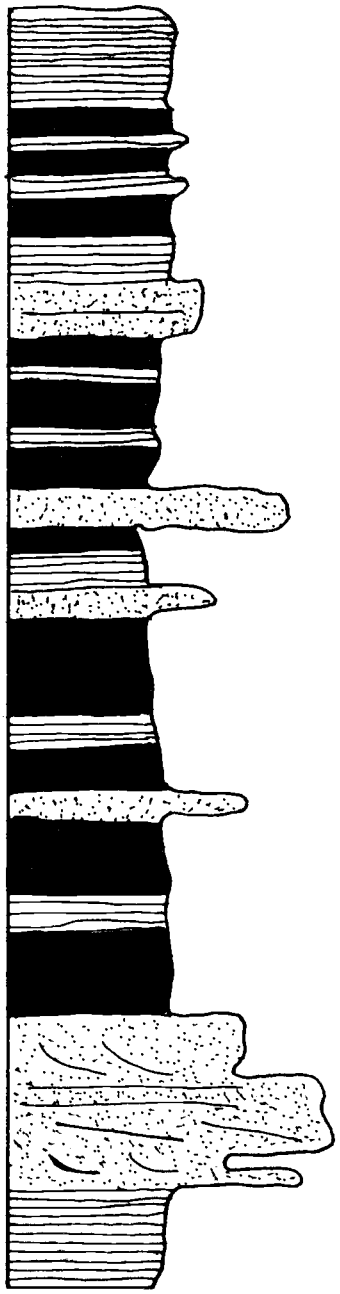

Outcrop X_{21}
T37N R1W
Sec. 36 NE 1/4

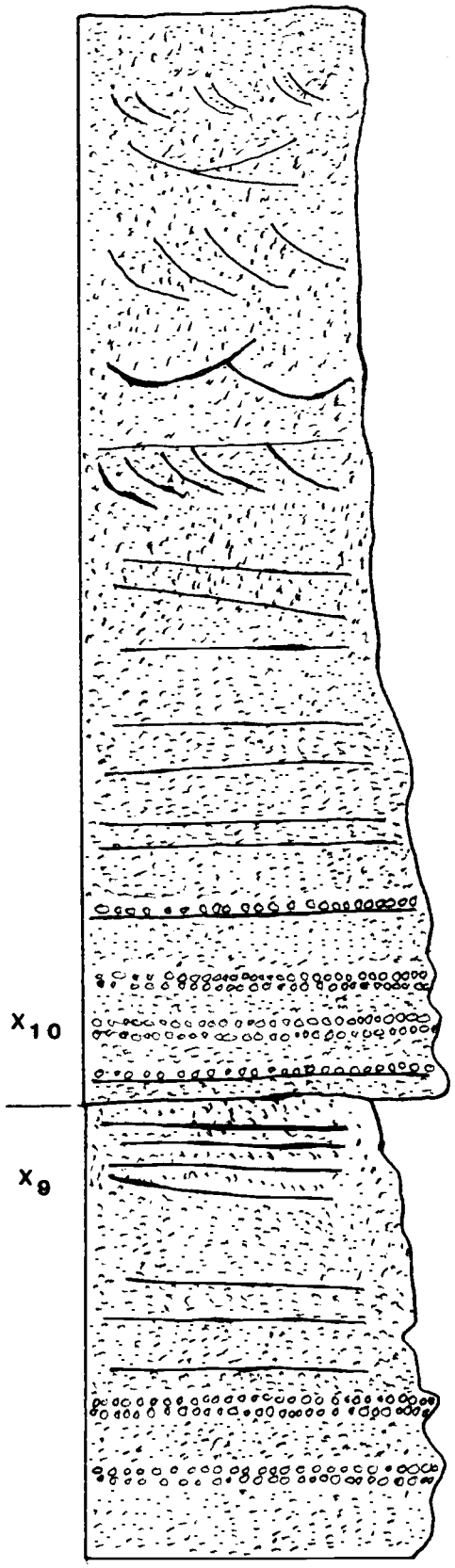

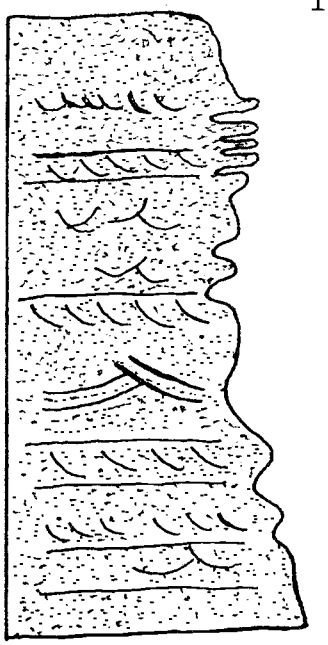

Outcrops X_9 and X_{10}
T37N R1W
Sec. 25 SE 1/4

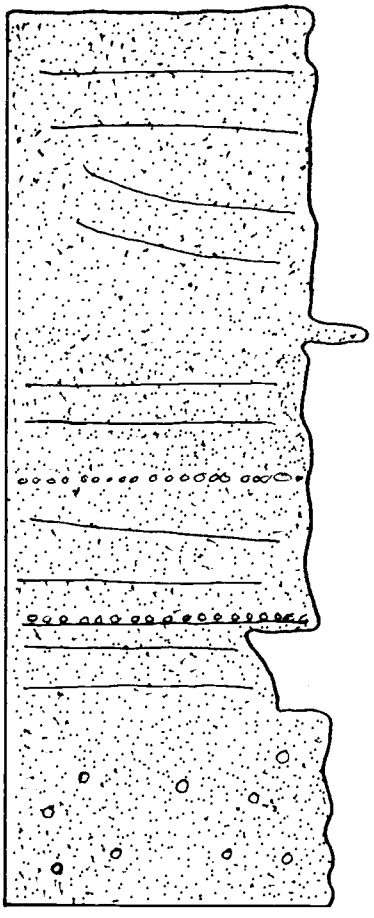

Outcrop X_{17}
T37N R1W
Sec. 25 NE 1/4

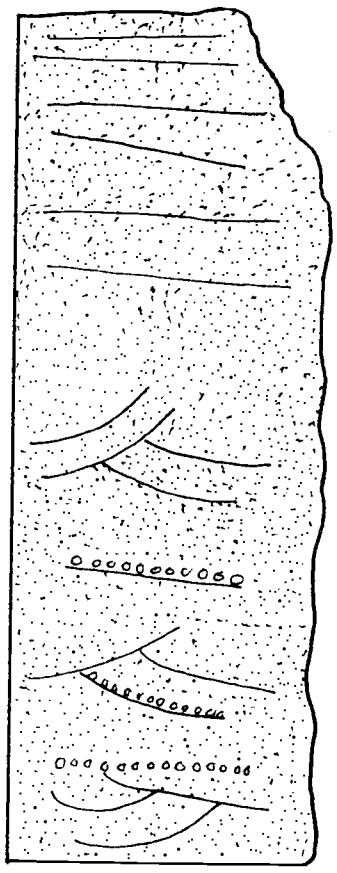

Outcrop X_{20}
T37N R1W
Sec. 36 NE1/4

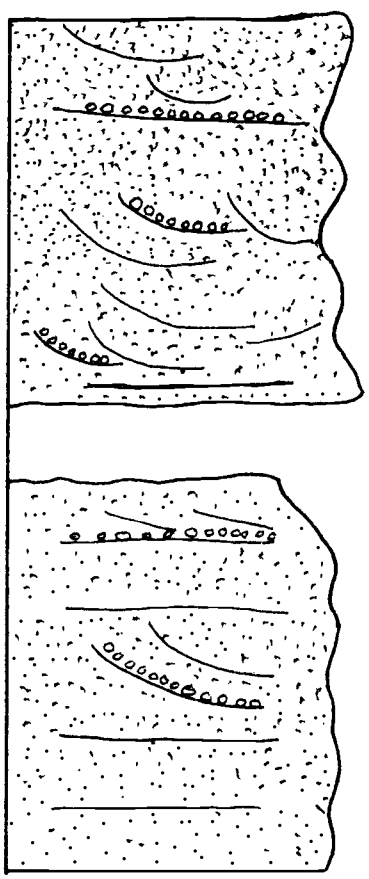

Outcrop X_6
T37N R1E
Sec. 31 NW 1/4

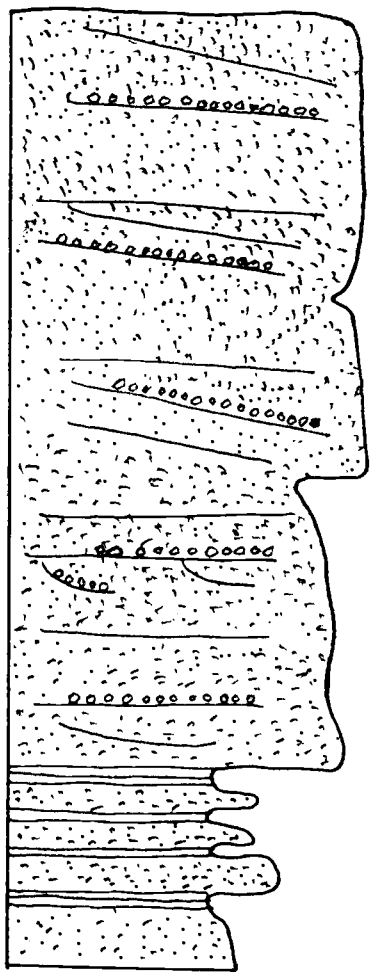

Outcrop X_8
T37N R1E
Sec. 31 SE 1/4

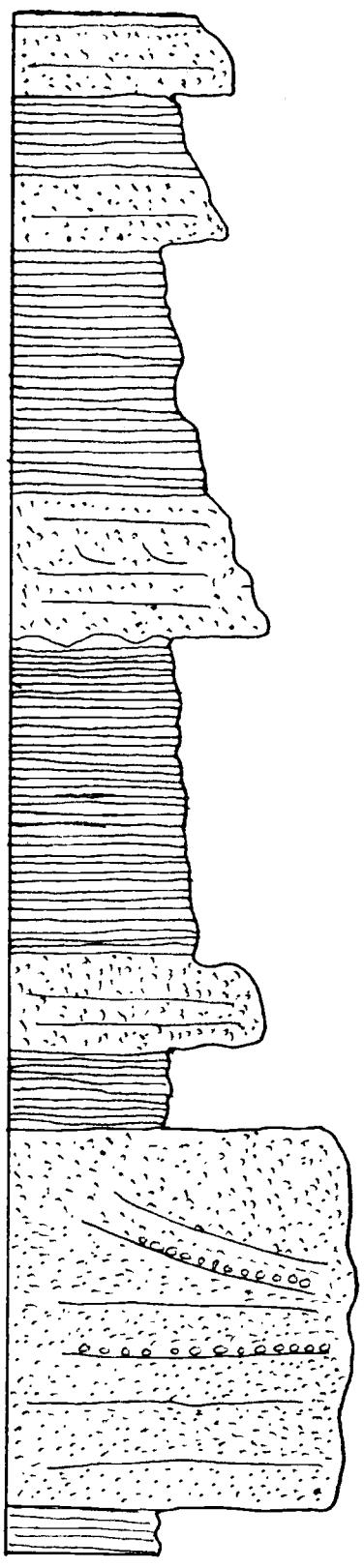

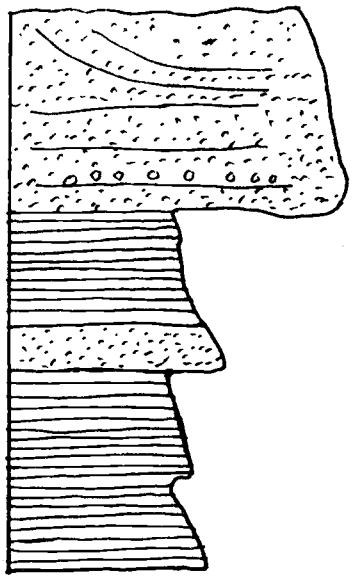

Outcrop X_7
T37N R1E
Sec. 31 SE 1/4

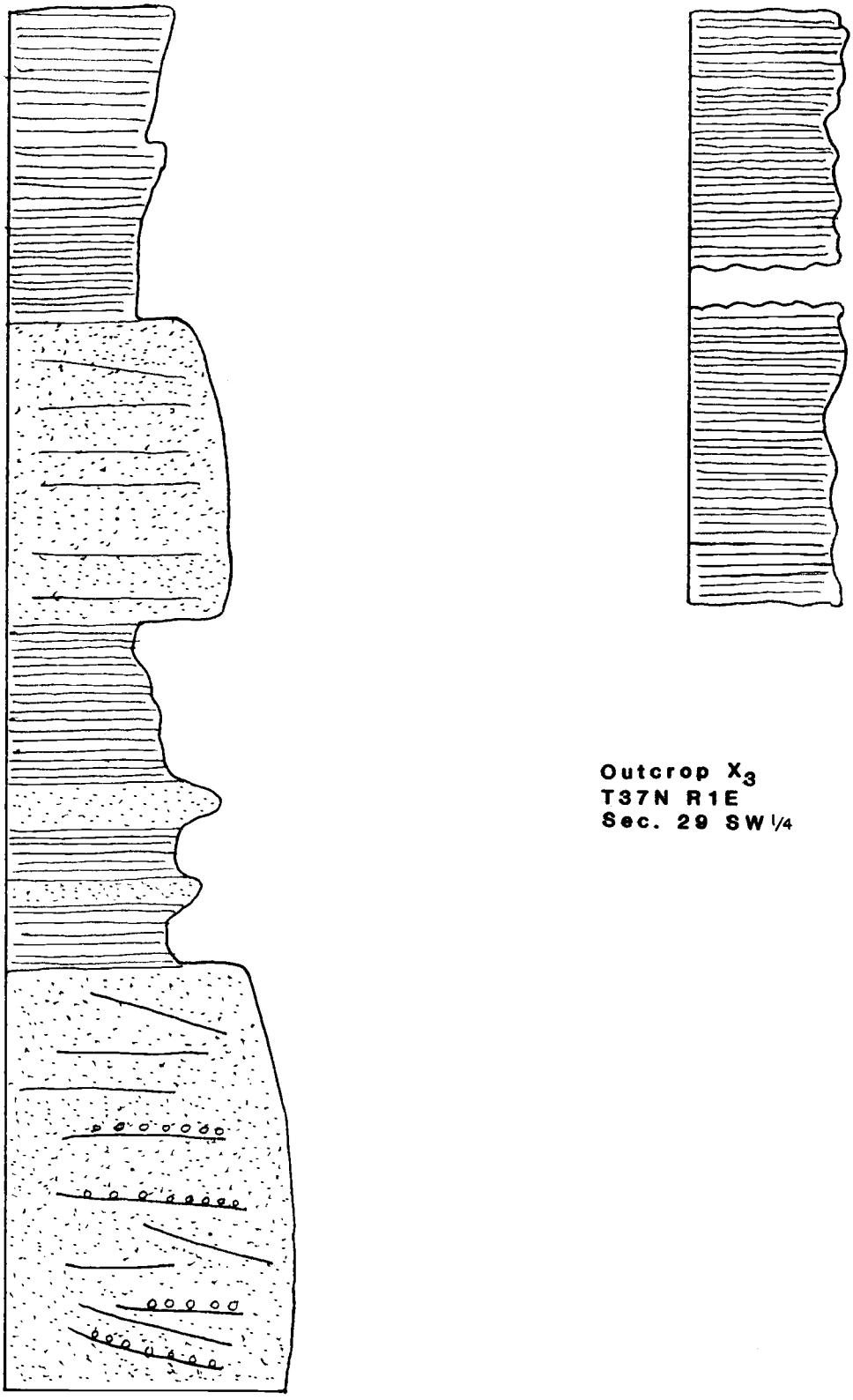

Outcrop X_3
T37N R1E
Sec. 29 SW 1/4

Southern Section Outcrops

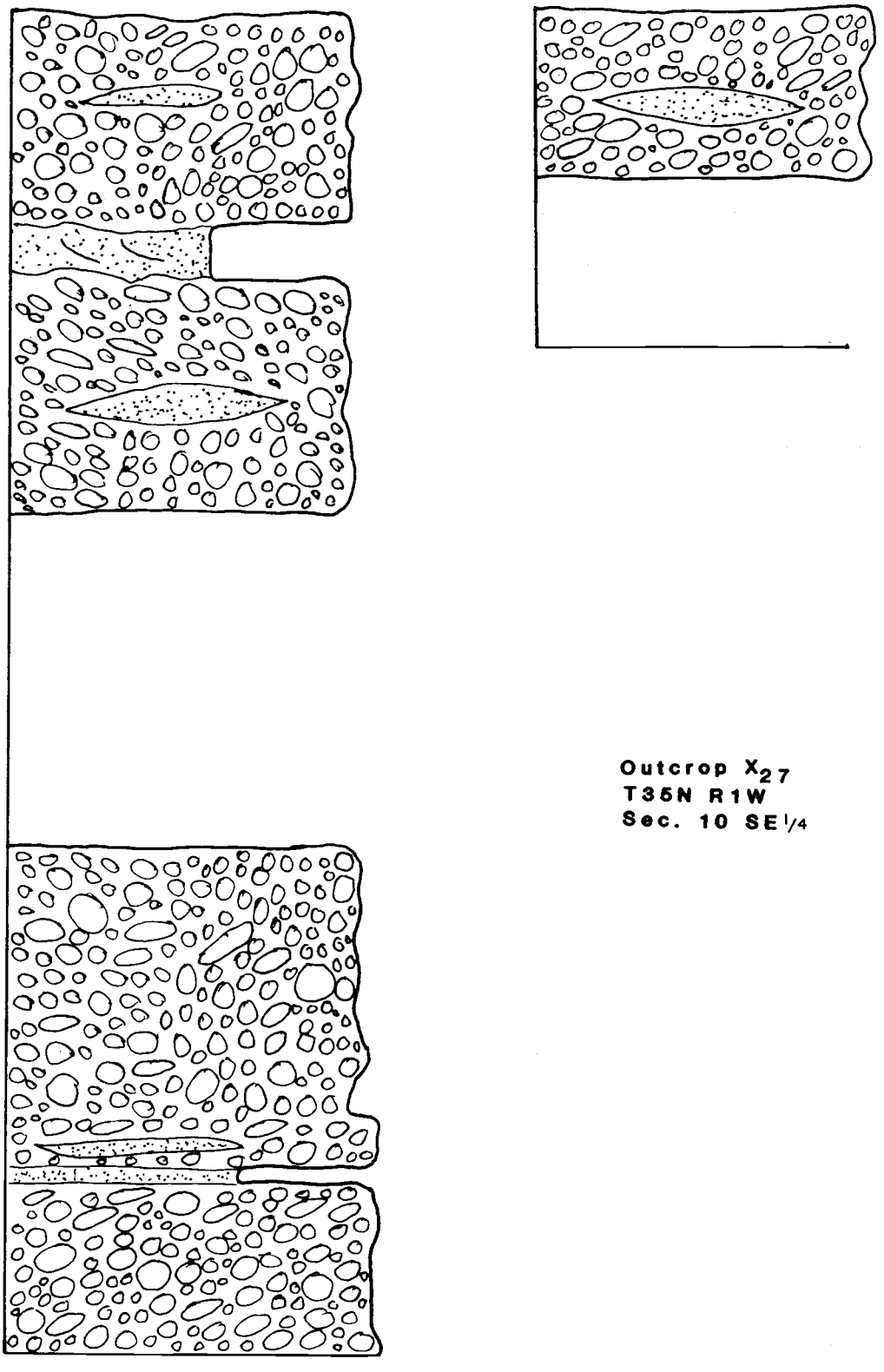

Outcrop X_{27}
T35N R1W
Sec. 10 SE 1/4

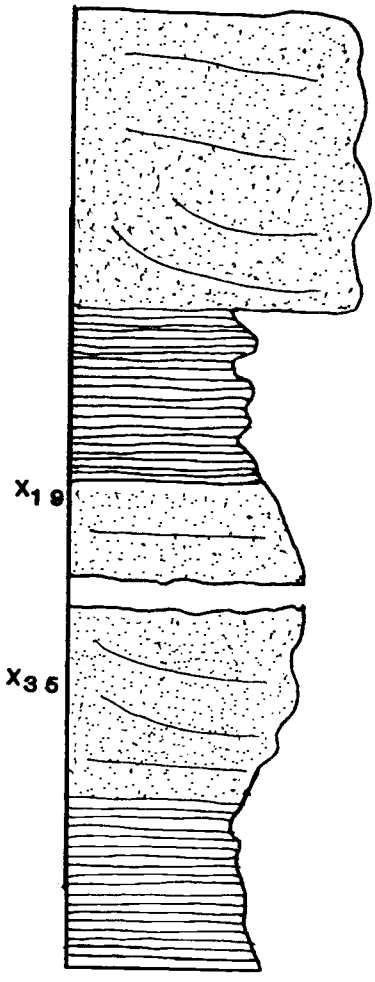

Outcrops X_{19} and X_{35}
T35N R1W
Secs. 11 and 14

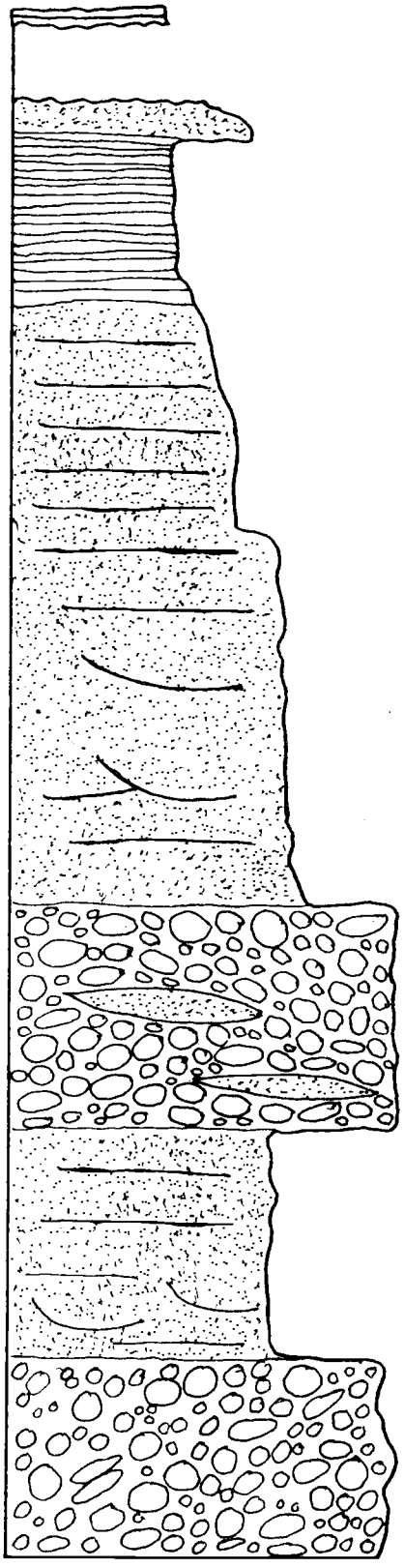

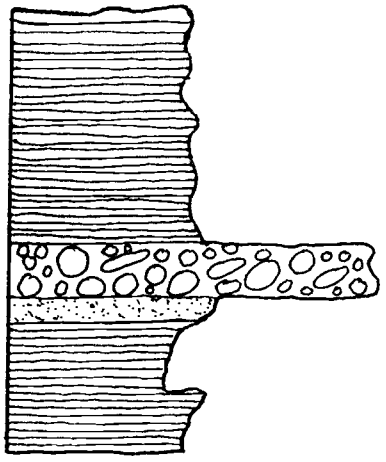

Outcrop X_{15}
T35N R1E
Sec. 31 NE 1/4

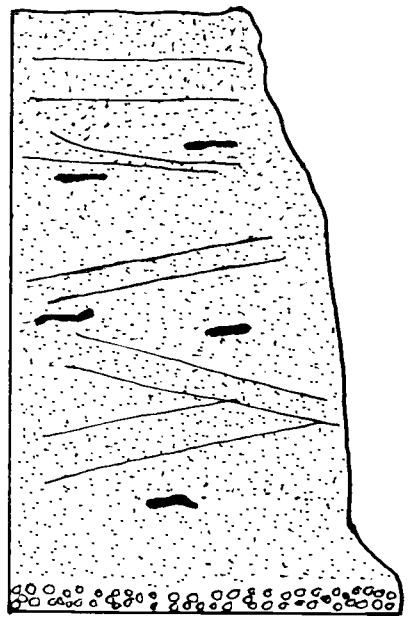

Outcrop X_{25}
T35N R1W
Sec. 36 NW 1/4

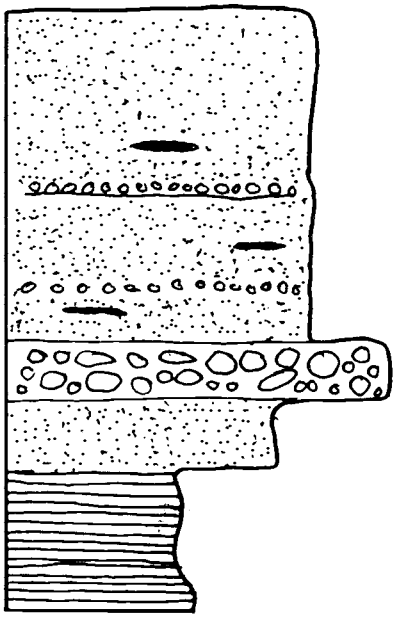

Outcrop X_{31}
T34N R1E
Sec. 6 NE 1/4

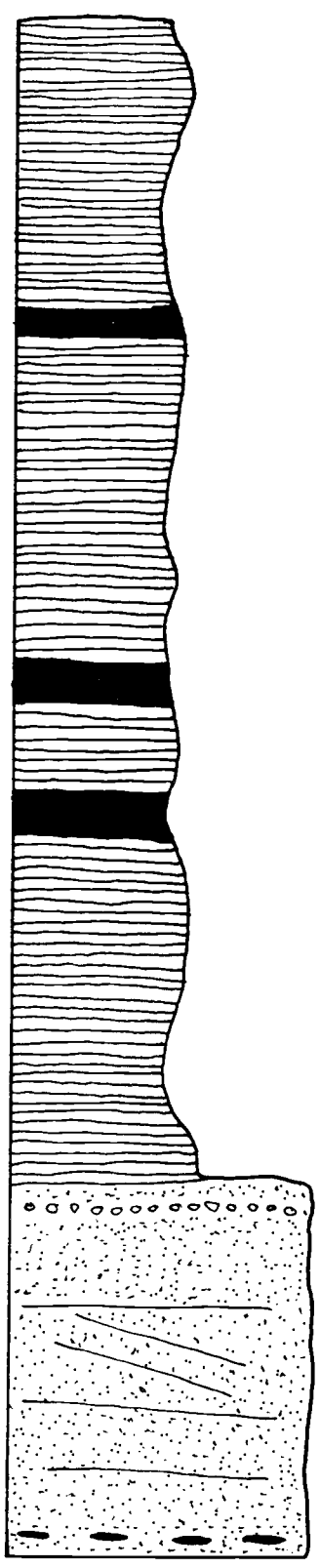

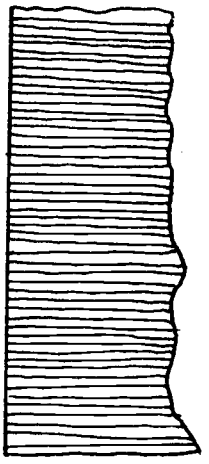

Outcrop X_{29}
T34N R1E
Sec. 5 NW 1/4

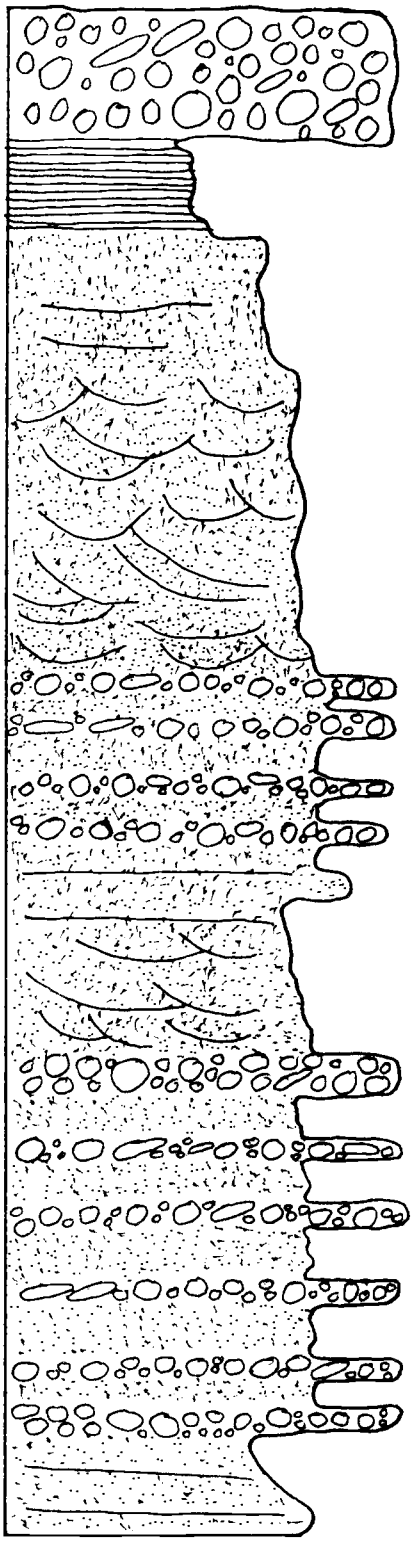

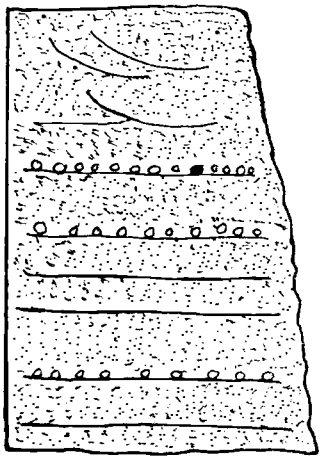

Outcrop X_{14}
T34N R1E
Sec. 5 NW 1/4

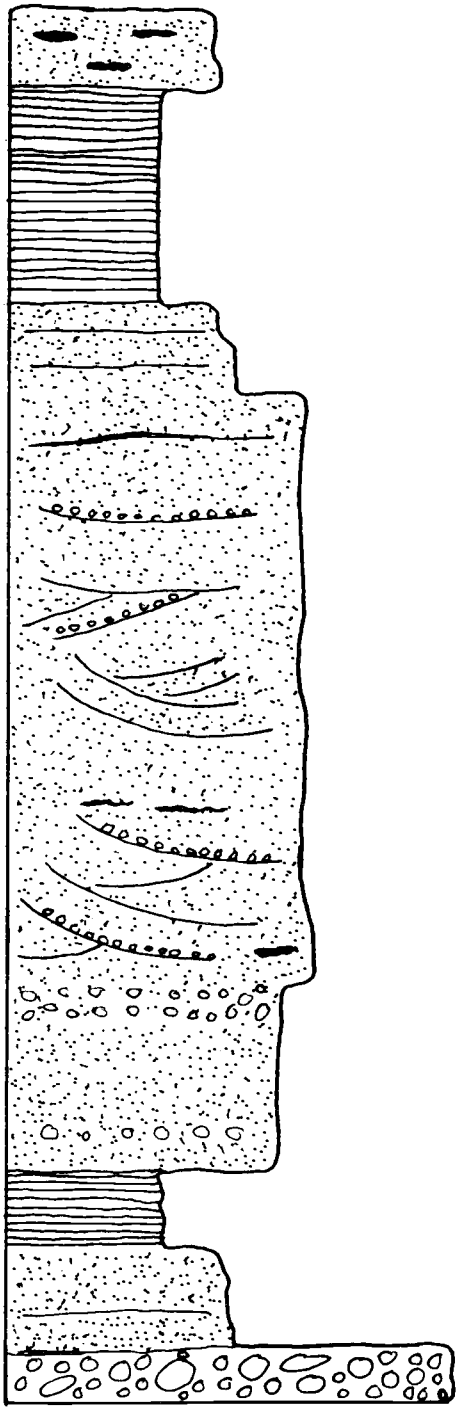

Outcrop X_{28}
T34N R1E
Sec. 5 SW 1/4

Coal Mine Area Outcrop

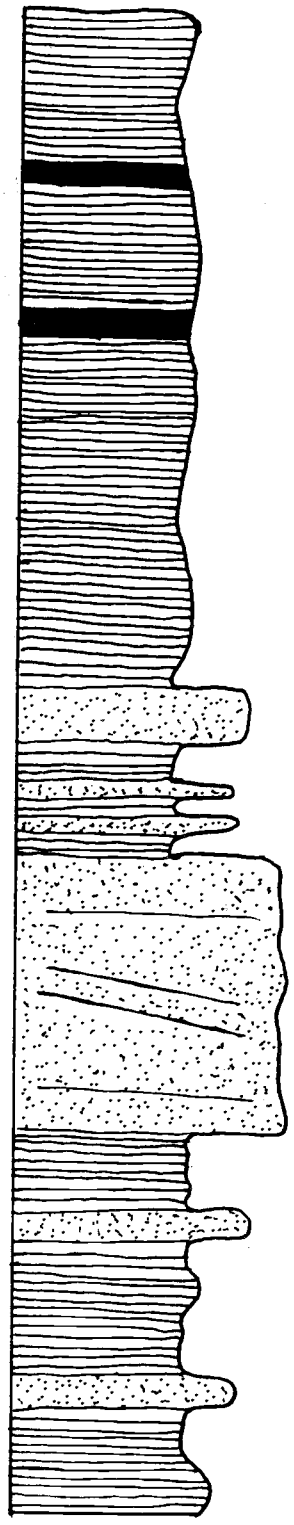

Outcrop X_{30}
T38N R1E
Sec. 22 SW 1/4

APPENDIX II

Results of Point-counts on Sandstone Samples

Sample/%	SX_2	O SX_1	** KSS	SX_{28} (a)	SX_{31}	MC_{11}	SX_{10}	SX_{19} (a)	SX_{19} (b)	SX_{21}
Monocrystalline Quartz	27.6	11.6	10.	10.4	13.6	27.2	24.4	20.4	18.4	24.4
Polycrystalline Quartz	6.8	5.6	4.	1.6	-	2.0	8.8	3.2	3.6	8.0
Plagioclase Feldspar	15.6	15.2	15.	10.4	12.0	9.6	11.6	13.6	18.0	10.0
Orthoclase	16.4	15.2	8.	4.0	3.6	13.2	13.6	10.8	10.0	14.8
Microcline	0.8	-	0.	-	0.4	0.4	-	-	0.8	1.2
Volcanic Rock Fragments	2.8	9.2	10.	18.0	16.0	-	6.0	2.8	10.0	2.0
Sedimentary Rock Frag.	6.8	18.4	14.	14.0	16.0	3.2	11.6	13.6	12.8	7.2
Metamorphic Rock *	0.4	0.8	0.	1.2	0.8	-	1.2	2.0	0.8	2.4
Granitic Rock Fragments	3.2	2.0	-	0.4	1.2	-	-	0.4	-	1.6
Chert	0.4	2.8	5.	1.6	-	0.4	0.4	0.8	0.8	1.6
Biotite	4.4	-	2.	0.8	1.2	12.0	6.0	3.6	2.0	1.2
Muscovite	-	0.4	0.	-	-	3.2	2.0	3.2	-	1.6
Hornblende	-	0.4	-	0.4	1.2	-	-	2.0	1.6	0.4
Epidote	1.2	2.8	-	0.4	-	1.2	0.8	1.6	1.2	-
Actinolite	5.0	3.6	-	-	2.4	-	-	0.4	-	-
Clinopyroxene	-	-	-	0.4	0.4	-	-	-	0.4	-
Orthopyroxene	-	-	-	-	-	-	-	-	0.4	-
Garnet	-	-	-	-	-	-	-	-	-	-
Oxyhornblende	-	-	-	-	-	-	0.4	-	-	0.4
Magnetite (or Ilmenite)	-	0.8	5.	0.4	-	1.6	0.4	0.8	0.4	3.2
Sphene	-	-	-	-	-	-	-	-	-	-
Apatite	-	-	-	-	-	-	-	-	-	-
Tourmaline	-	-	-	-	-	-	-	-	-	-
Glaucophane	-	-	-	-	-	-	-	-	-	-
Clay Matrix	11.6	11.2	21.	5.6	31.2	26.0	12.8	20.8	19.2	20.0
Calcite Cement	-	-	-	0.4	-	-	-	-	-	-

* = Eocene Montgomery Creek Formation
** = Cretaceous marine sandstones from
O = Samples from sandstone interbeds

APPENDIX III

Grain Size Distribution of the Sandstones (Histograms)

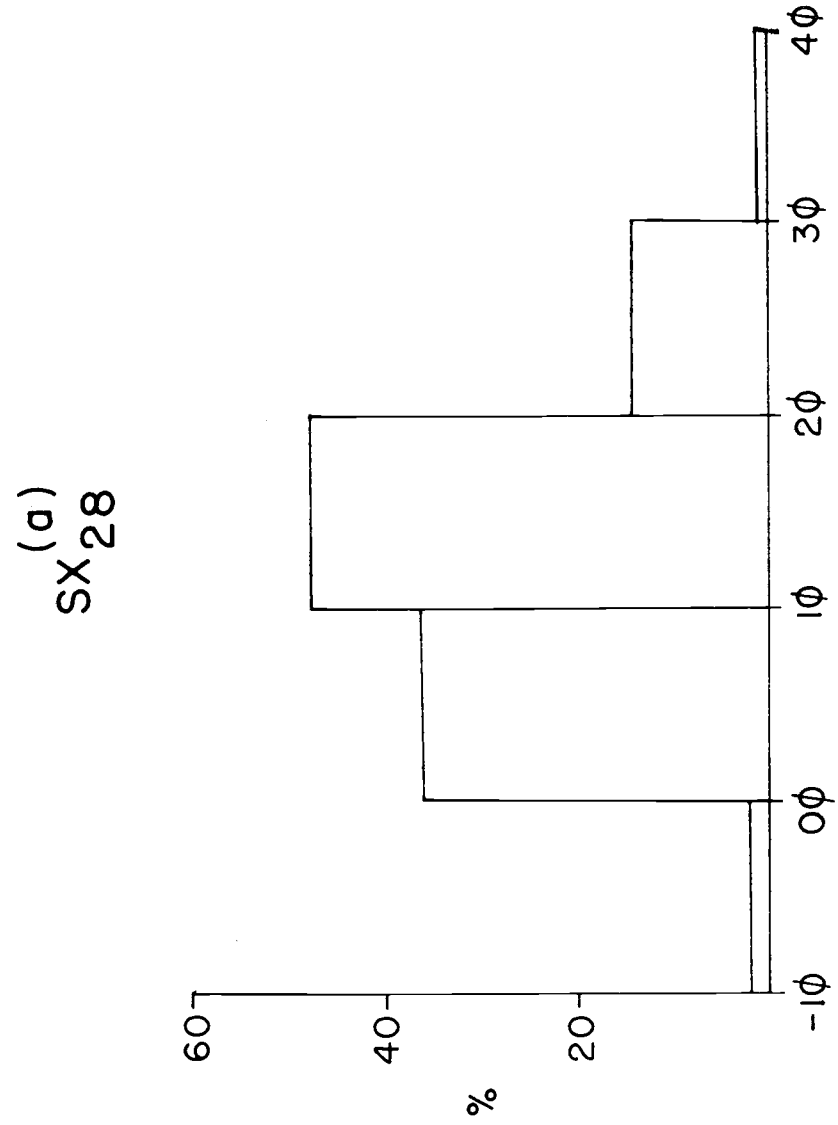
(a)
SX28
60
40
20
%
-1φ
0φ
1φ
2φ
3φ
4φ

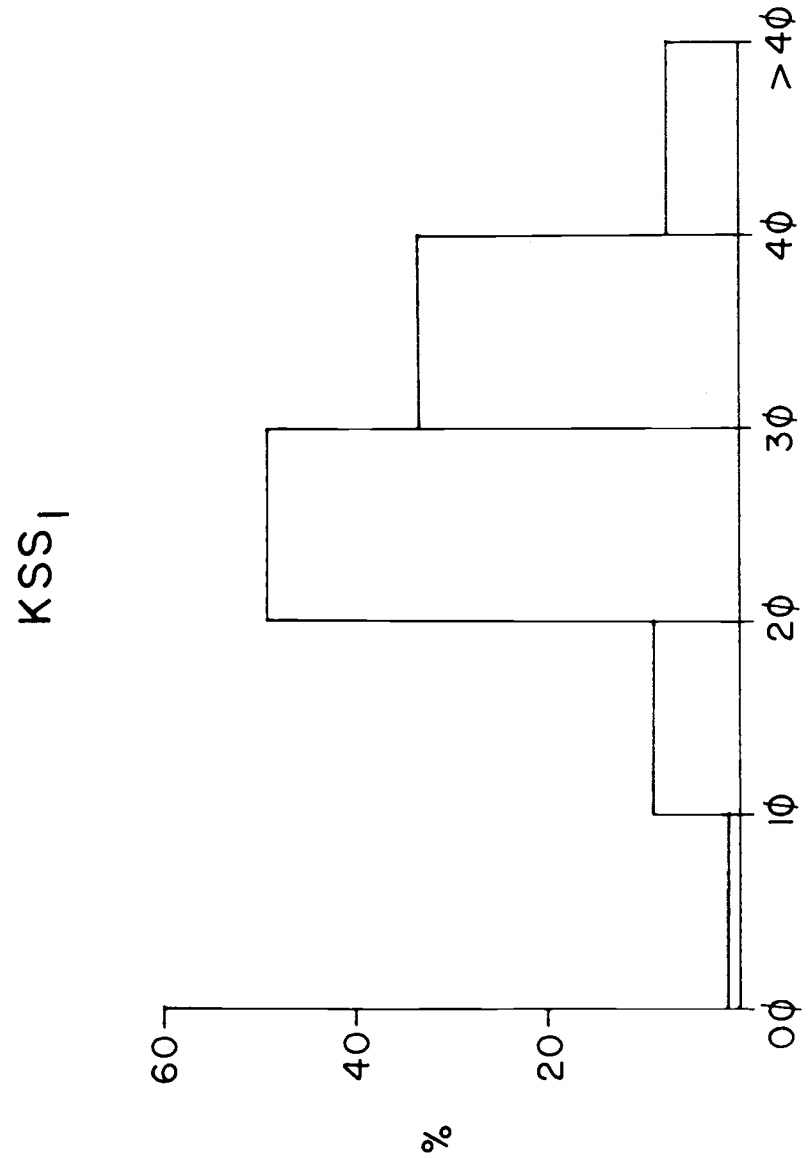
KSS I
60
40
20
%
0φ
1φ
2φ
3φ
4φ
>4φ

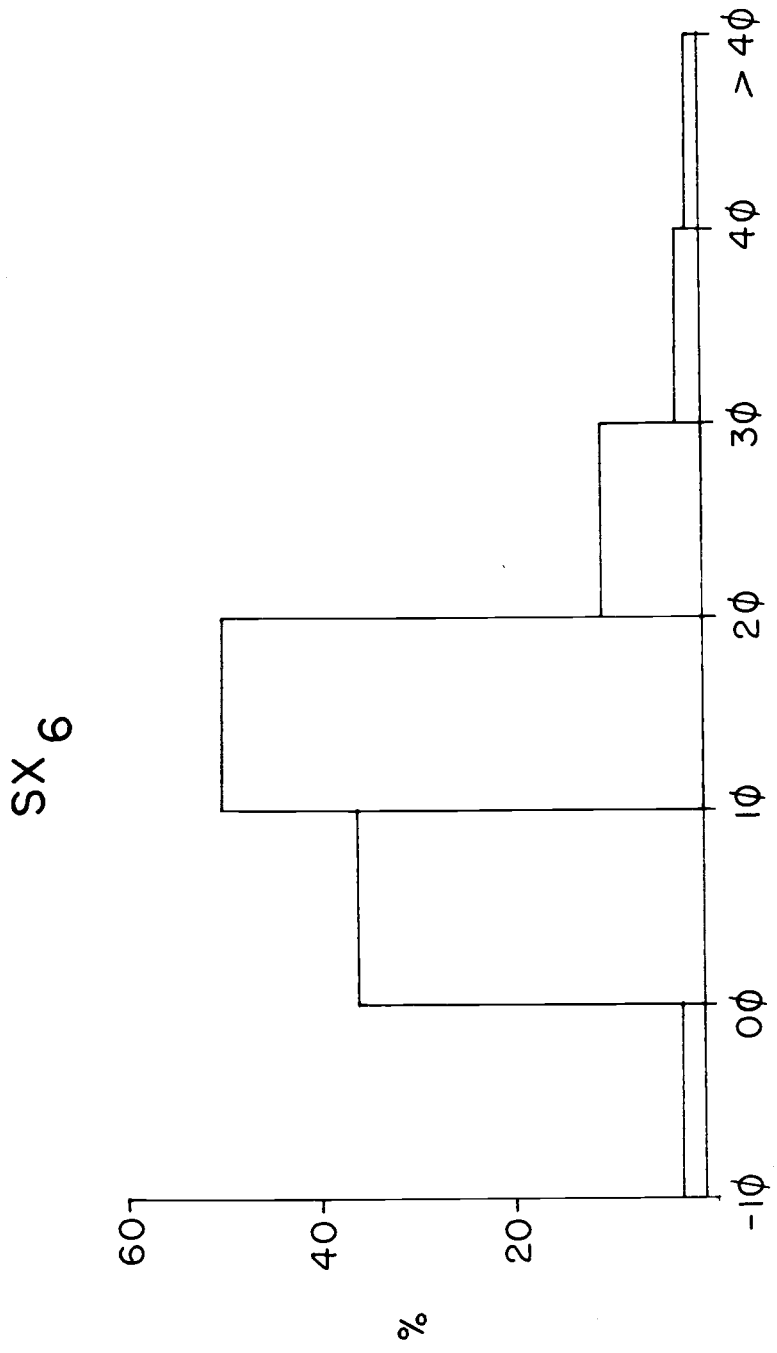
SX 6
60
40
20
%
-1φ
0φ
1φ
2φ
3φ
4φ
> 4φ

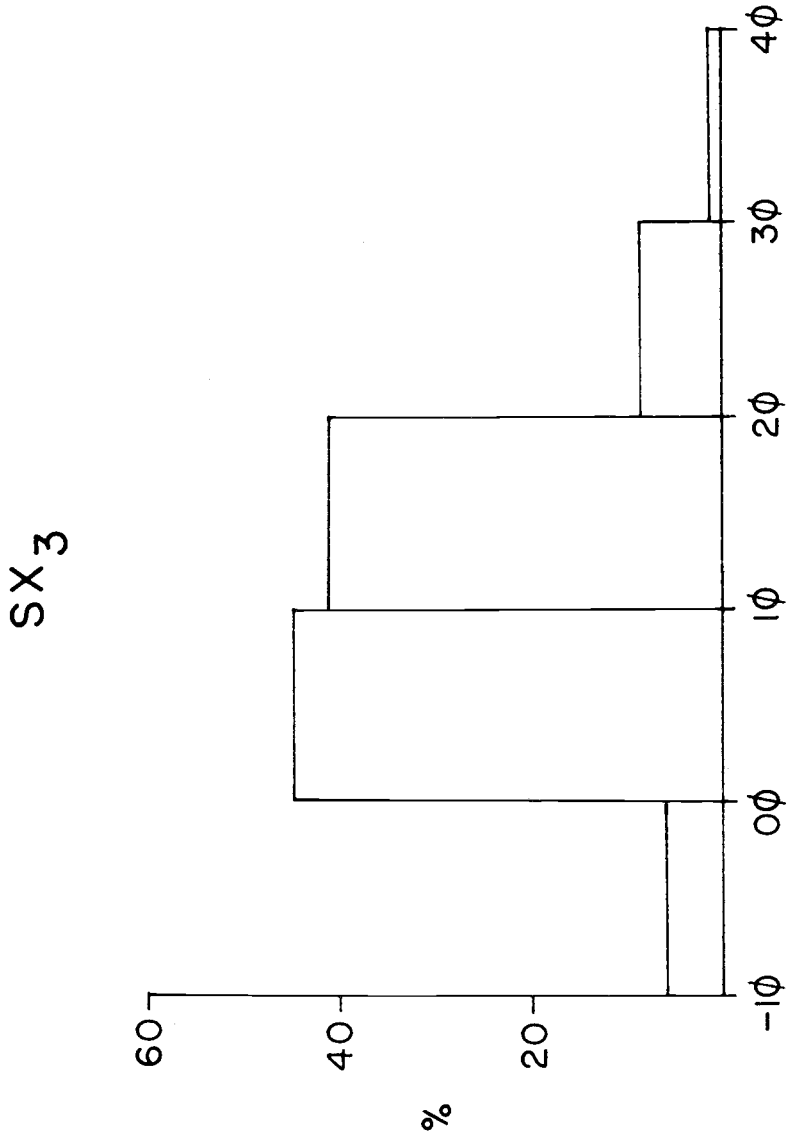
SX3
60
40
20
%
-1φ
0φ
1φ
2φ
3φ
4φ

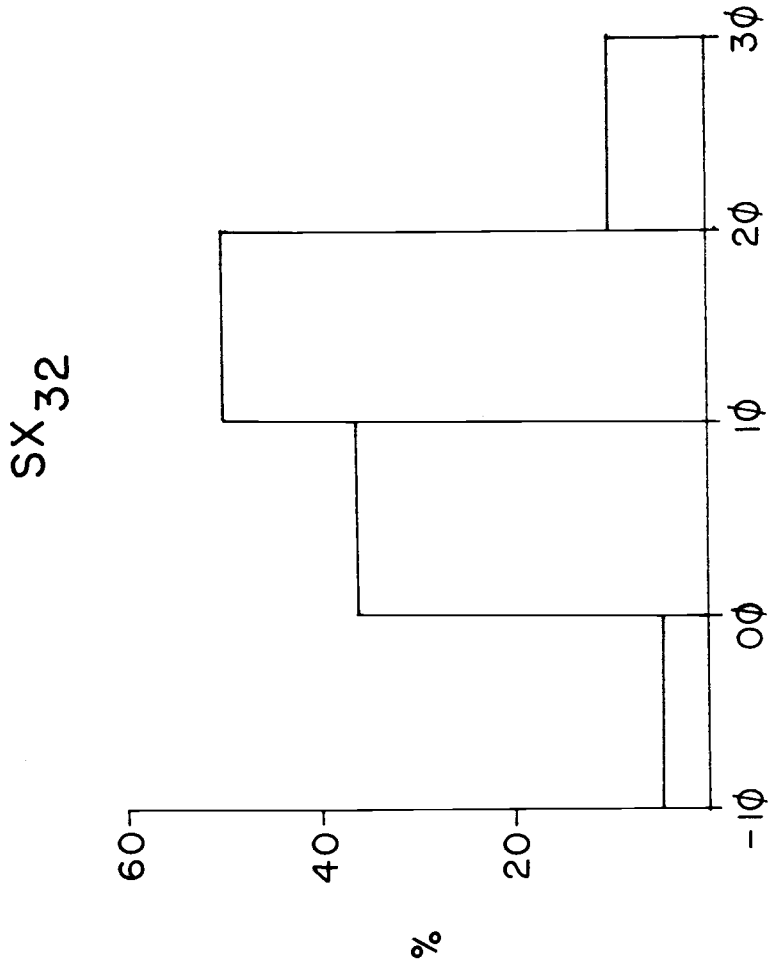
SX32
60
40
20
%
-1φ
0φ
1φ
2φ
3φ

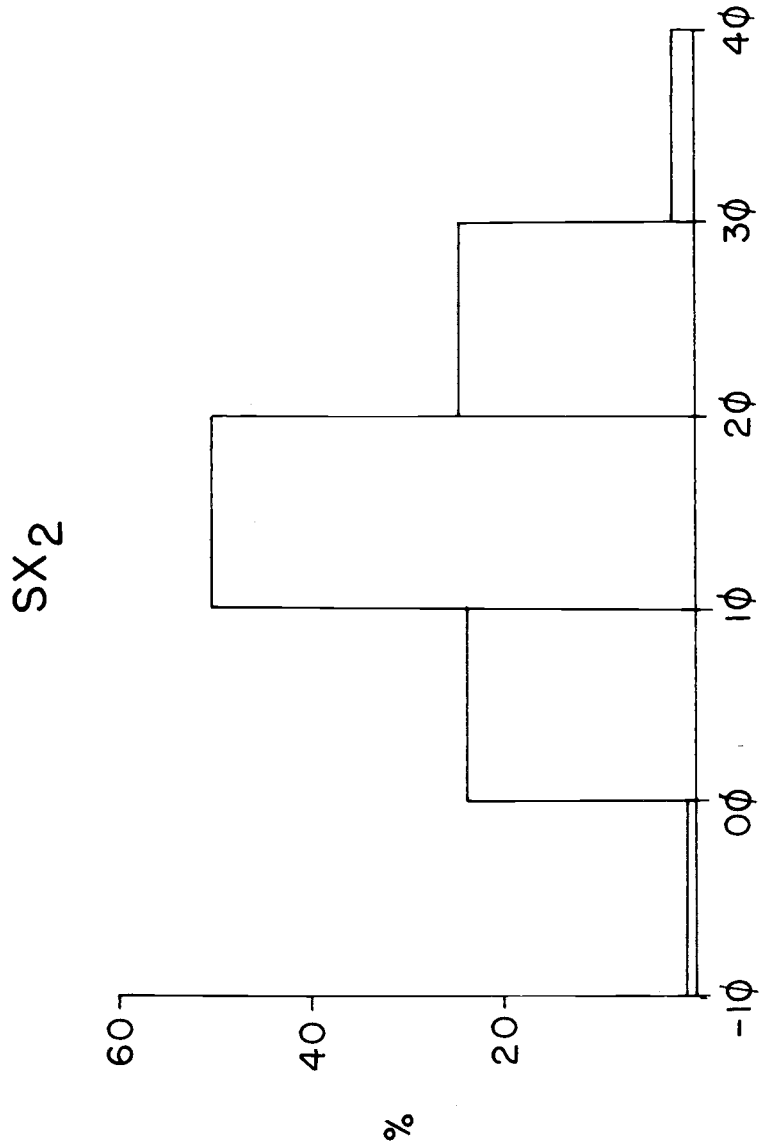
SX2
60
40
20
%
-1φ
0φ
1φ
2φ
3φ
4φ

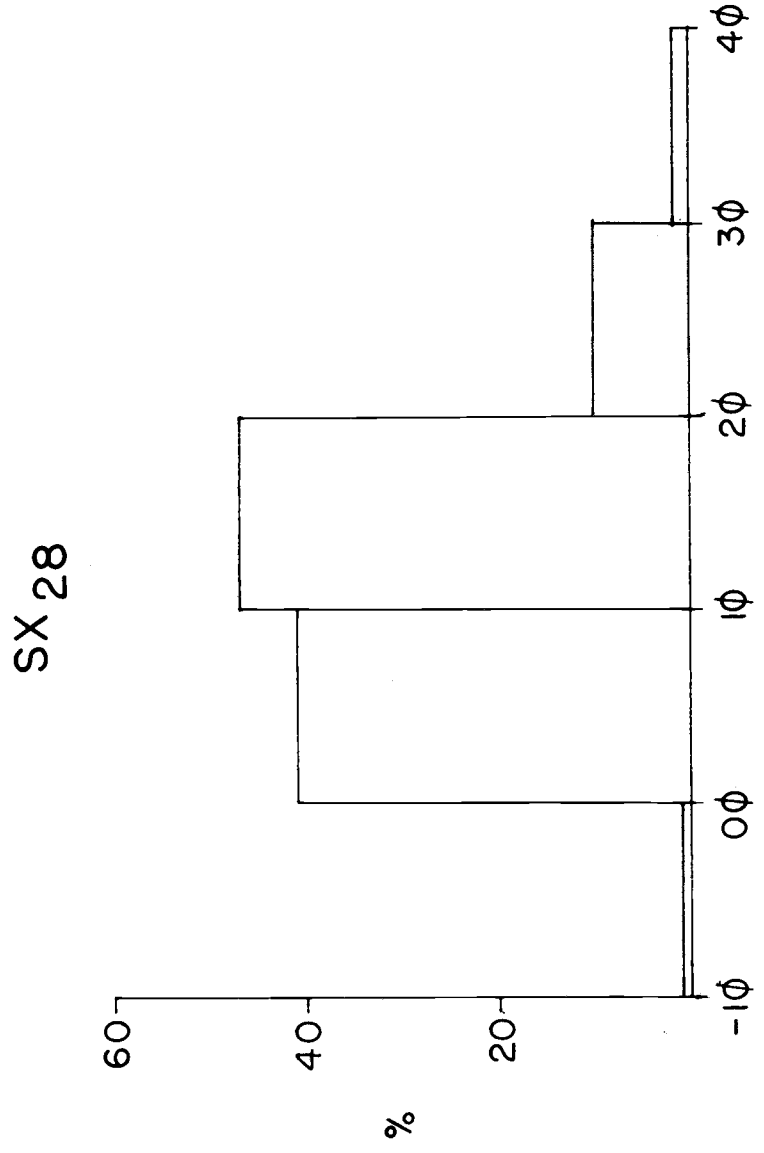
SX28
60
40
20
%
-1φ
0φ
1φ
2φ
3φ
4φ

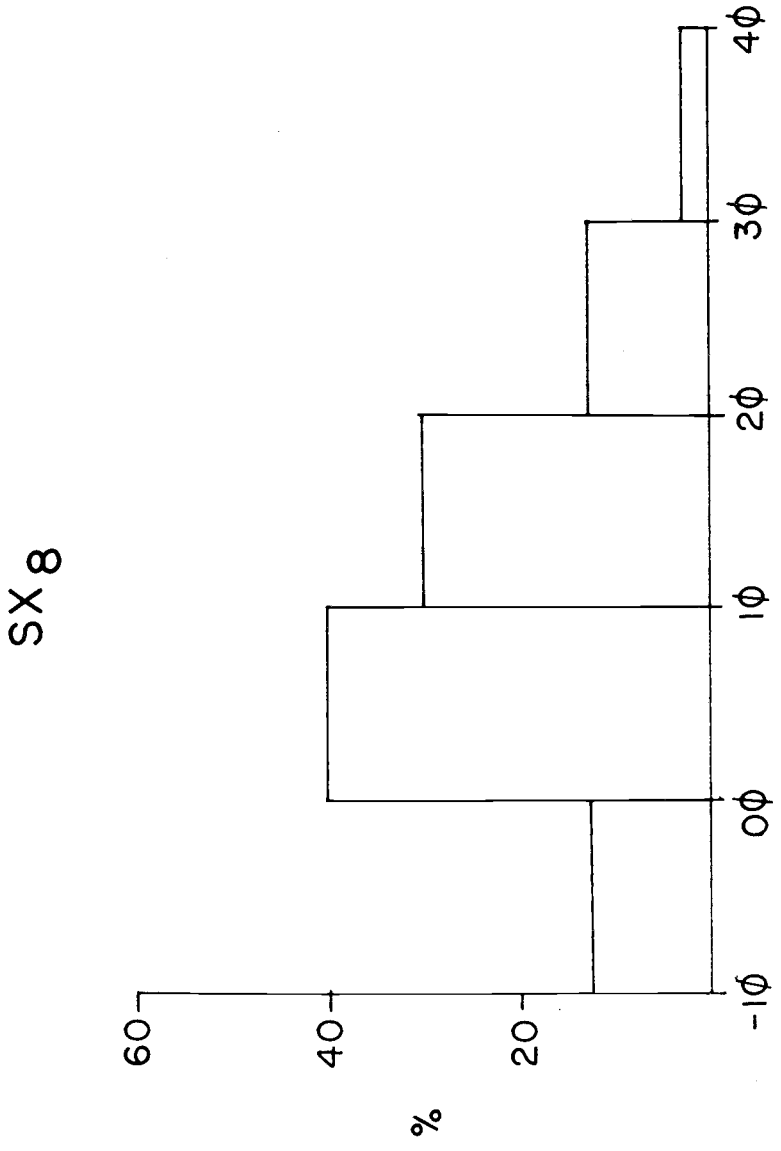
SX8
60
40
20
%
-1ϕ
0ϕ
1ϕ
2ϕ
3ϕ
4ϕ

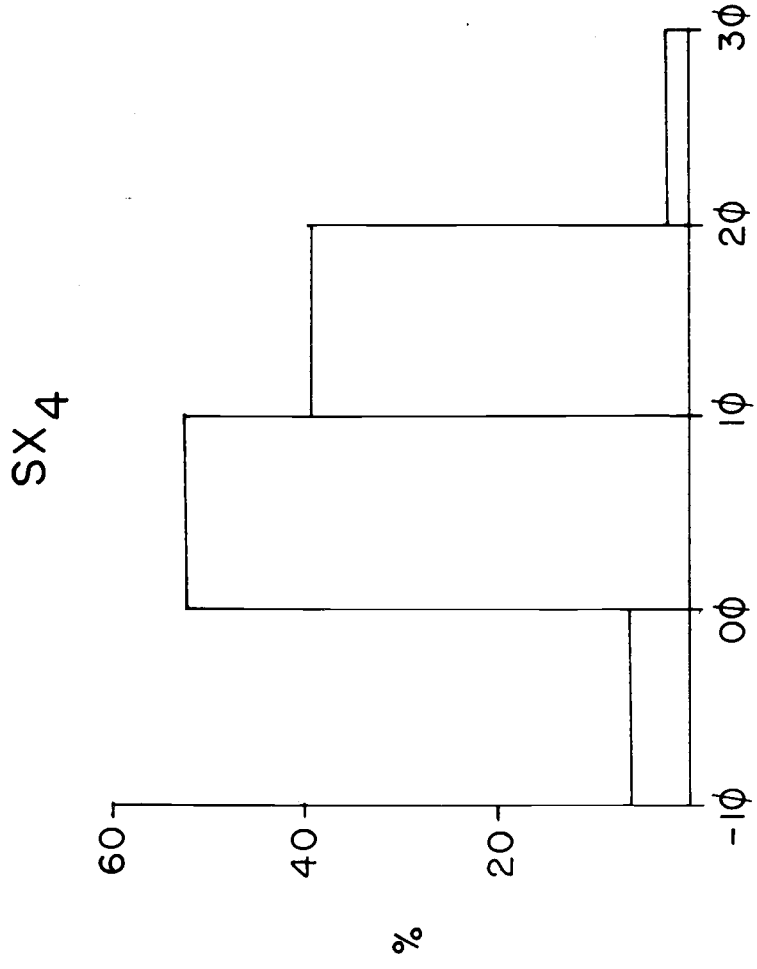
SX4
60
40
20
%
-1φ
0φ
1φ
2φ
3φ

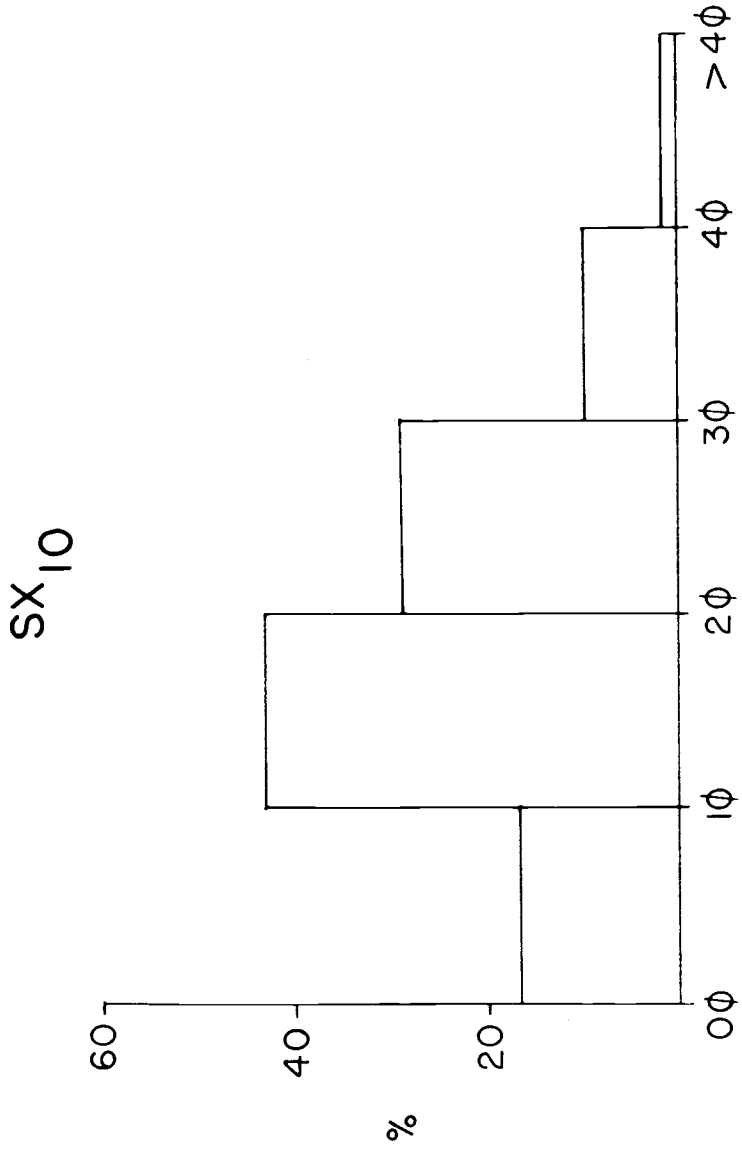
SX10
60
40
20
%
0φ
1φ
2φ
3φ
4φ
>4φ

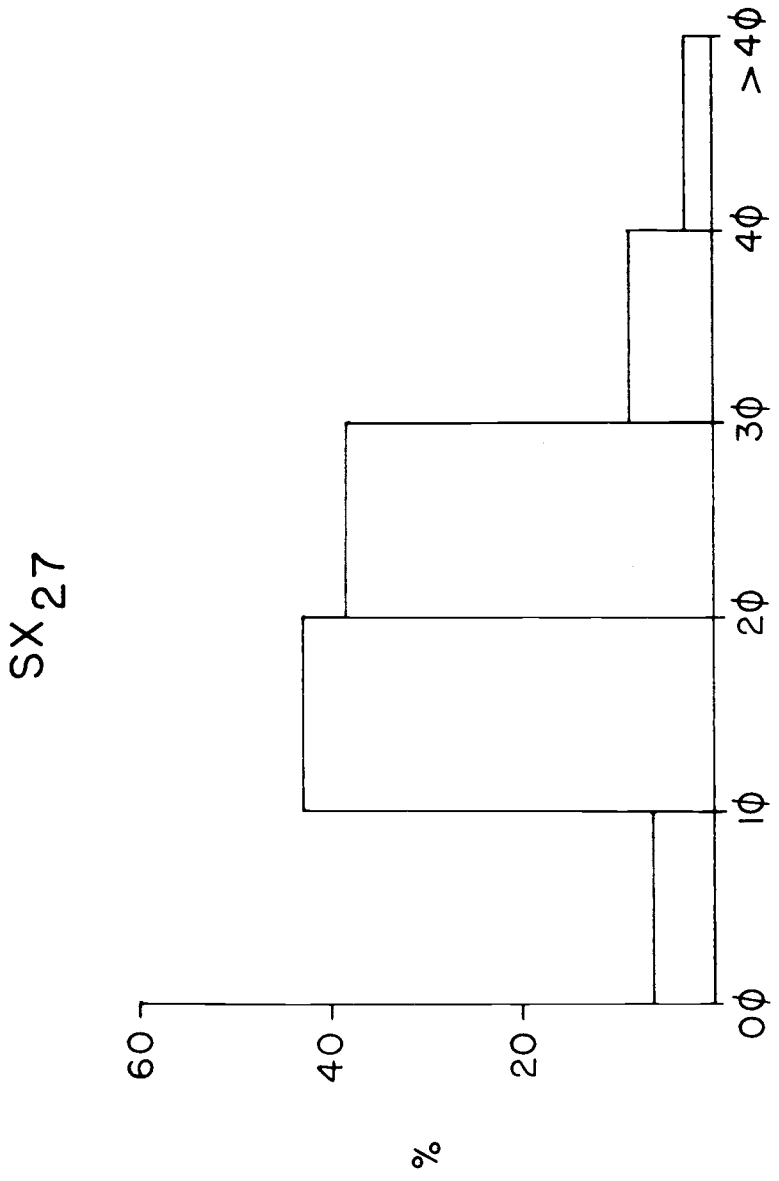
SX27
60
40
20
%
0φ
1φ
2φ
3φ
4φ
>4φ

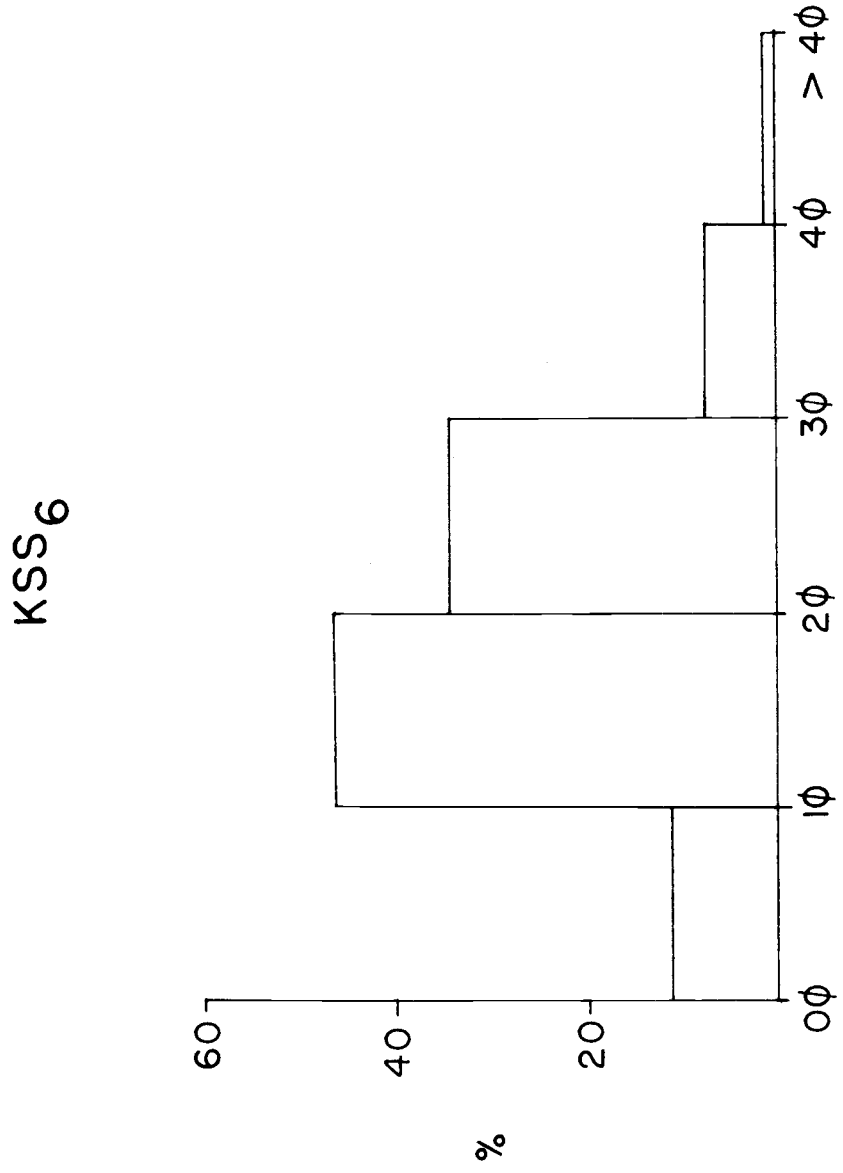
KSS6
60
40
20
%
0φ
1φ
2φ
3φ
4φ
> 4φ

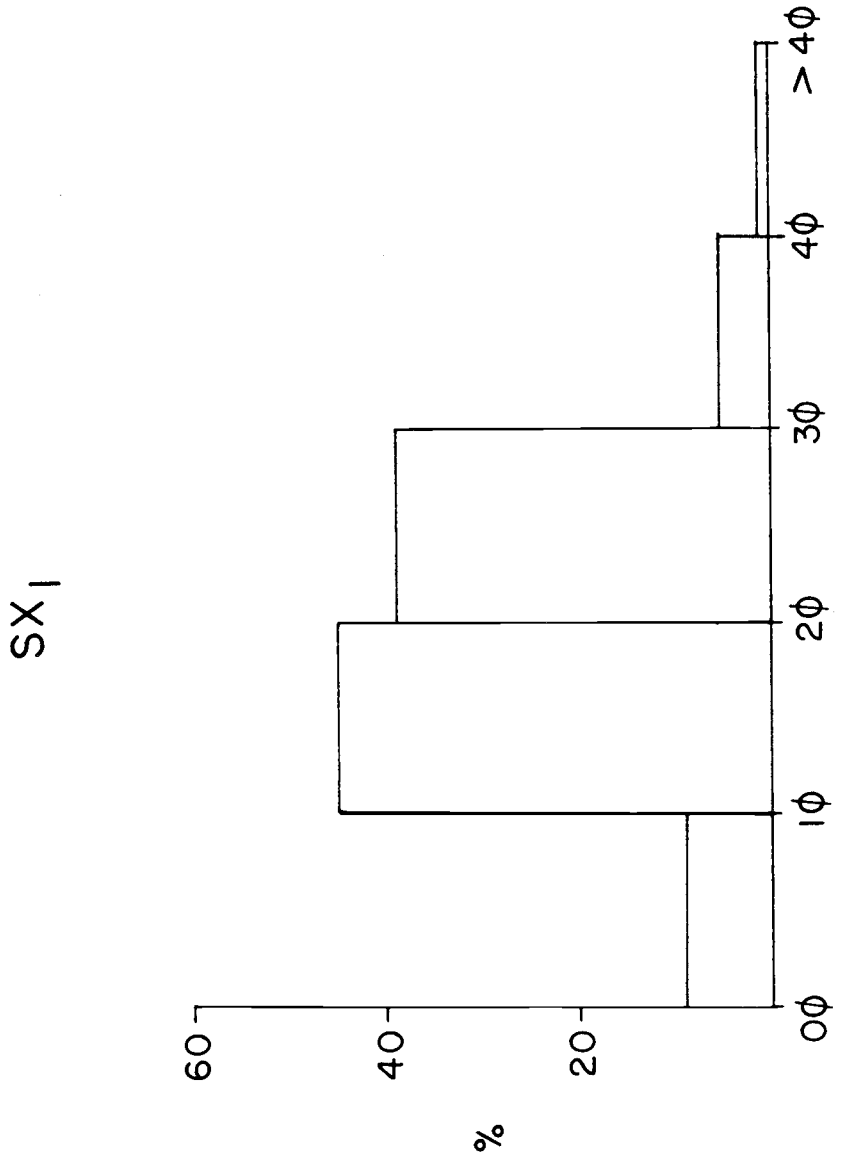
SX I
60
40
20
%
0φ
1φ
2φ
3φ
4φ
> 4φ

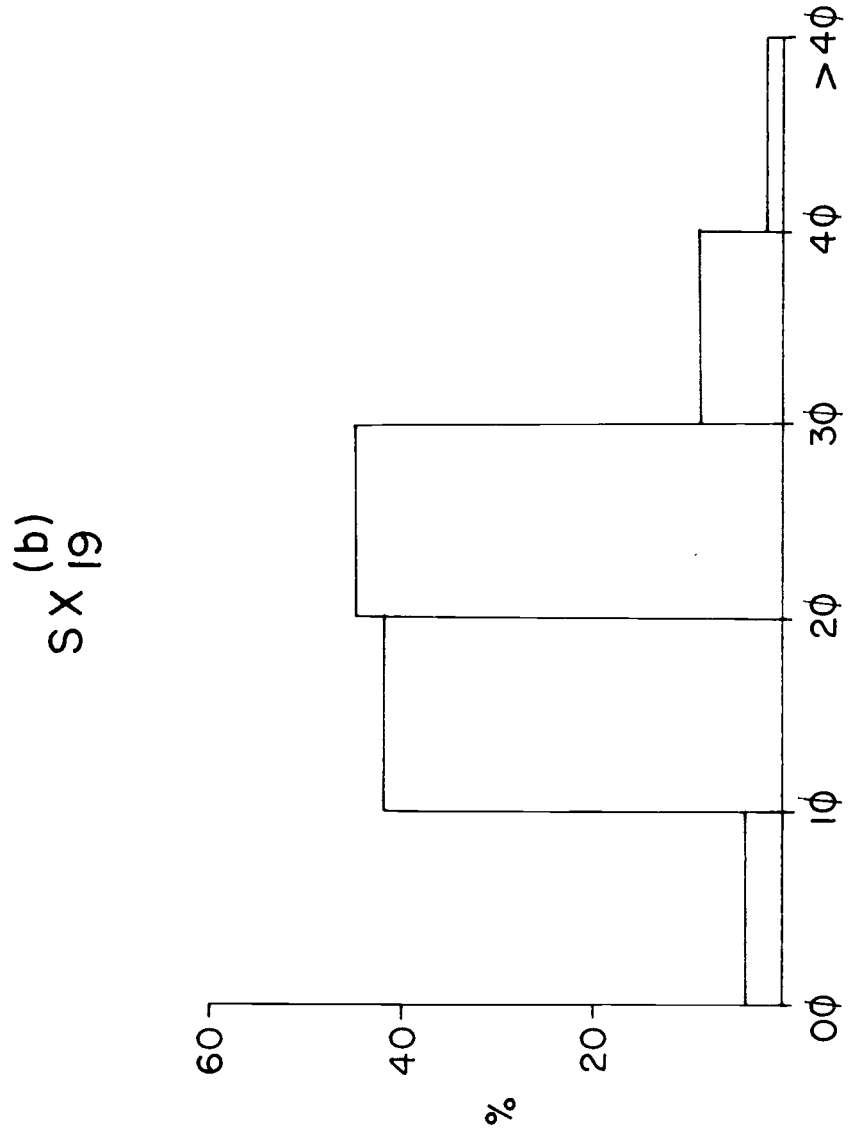
SX (b)
19
60
40
20
%
0φ
1φ
2φ
3φ
4φ
>4φ

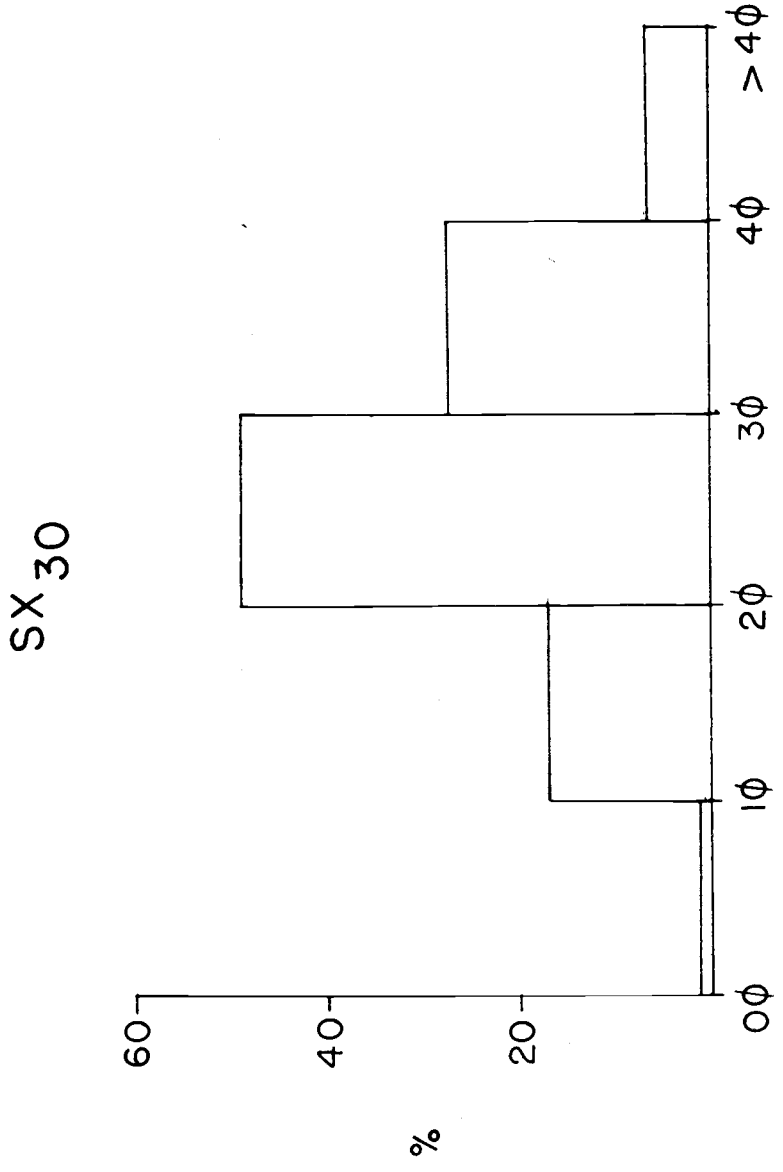
SX 30
60
40
20
%
0φ
1φ
2φ
3φ
4φ
>4φ

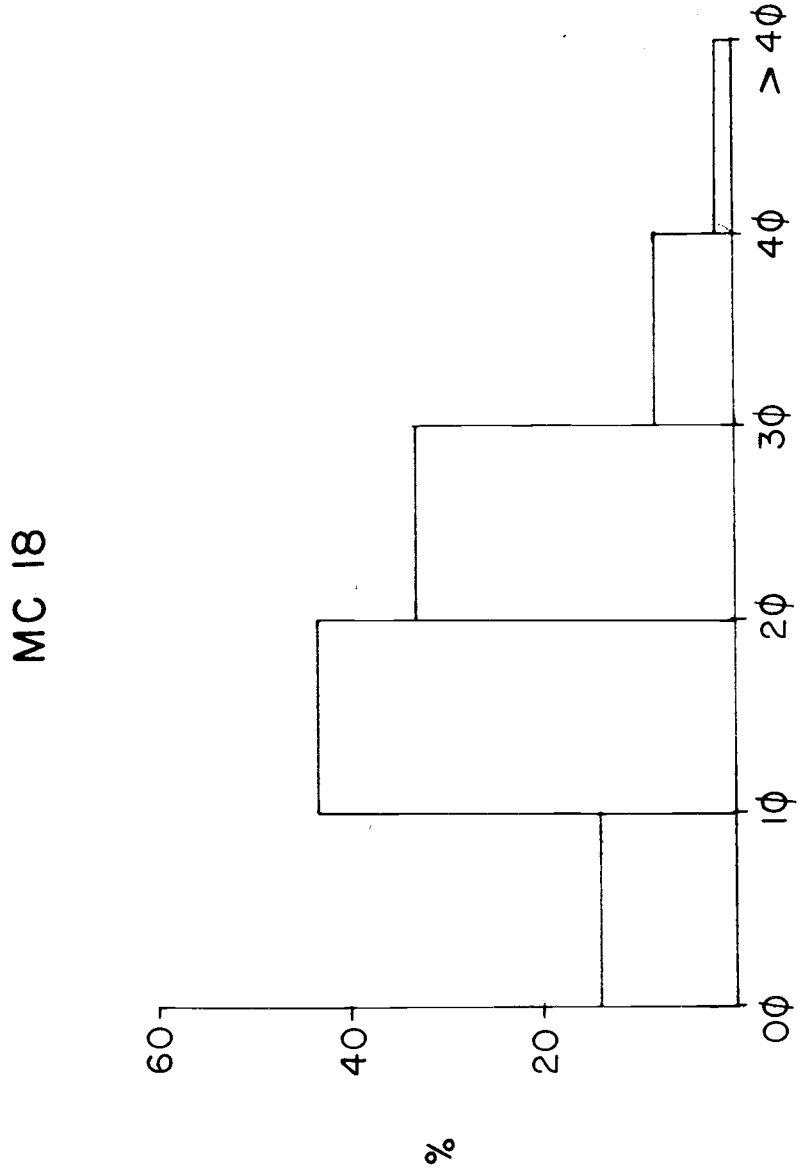
MC 18
60
40
20
%
0φ
1φ
2φ
3φ
4φ
>4φ

APPENDIX IV

Grain Size Distribution of the Sandstones (Cumulative Frequency Diagrams)

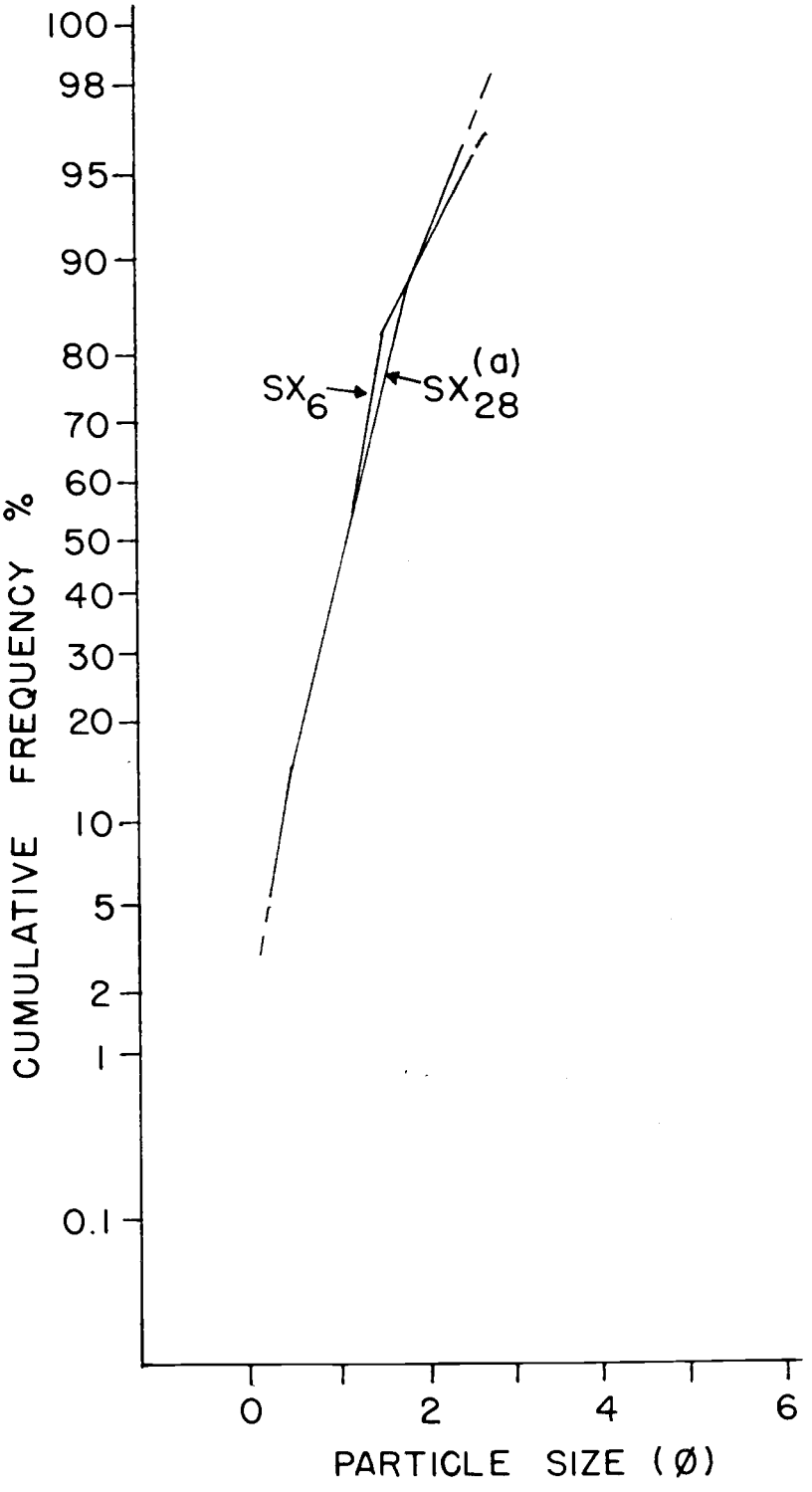
100
98
95
90
80
70
60
50
40
30
20
10
5
2
1
0.1
CUMULATIVE FREQUENCY %
SX6
SX(a)28
0
2
4
6
PARTICLE SIZE (Ø)

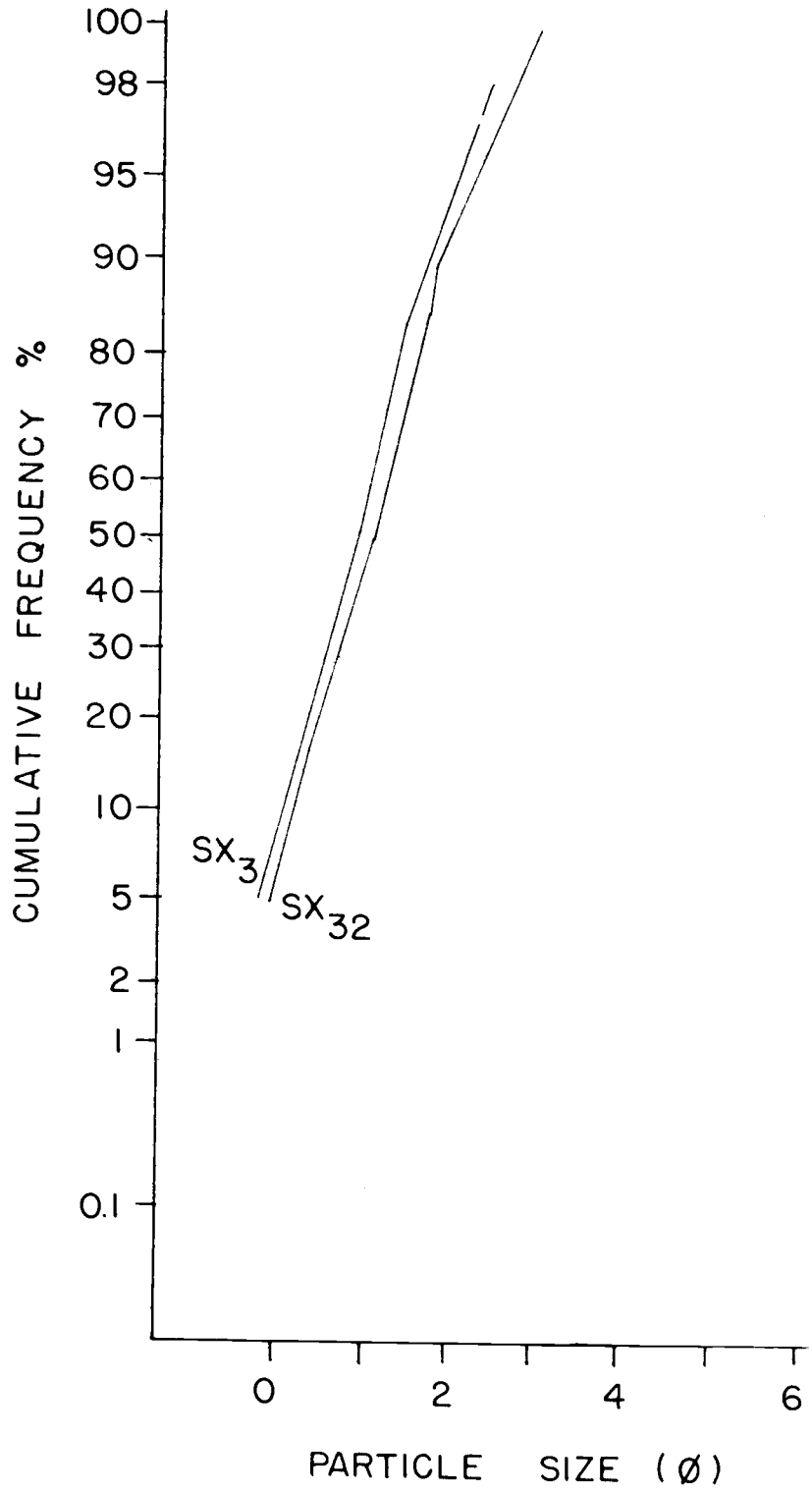
100
98
95
90
80
70
60
50
40
30
20
10
5
2
1
0.1
CUMULATIVE FREQUENCY %
SX3
SX32
0
2
4
6
PARTICLE SIZE (Ø)

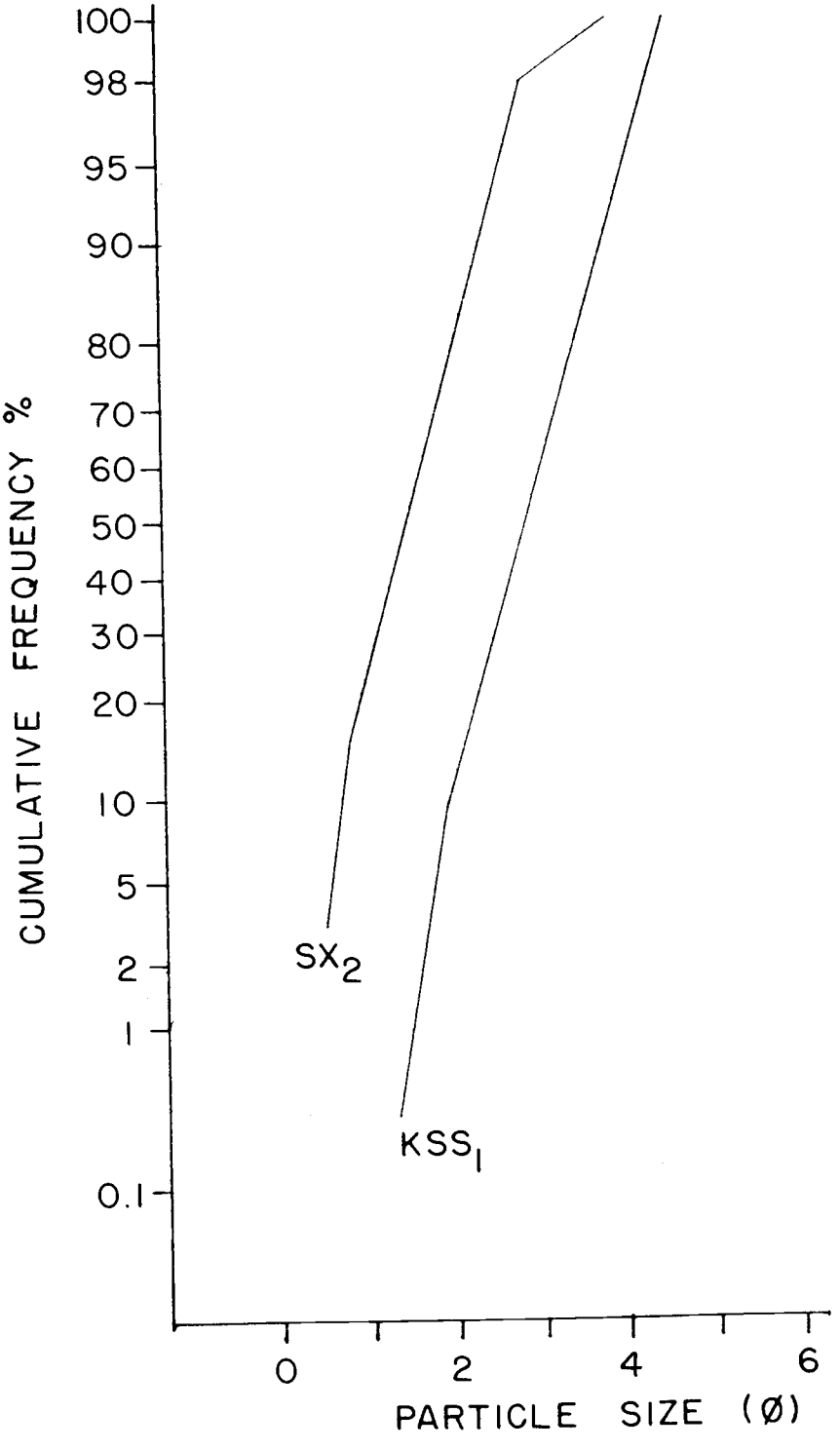
100
98
95
90
80
70
60
50
40
30
20
10
5
2
1
0.1
CUMULATIVE FREQUENCY %
SX2
KSS1
0
2
4
6
PARTICLE SIZE (Ø)

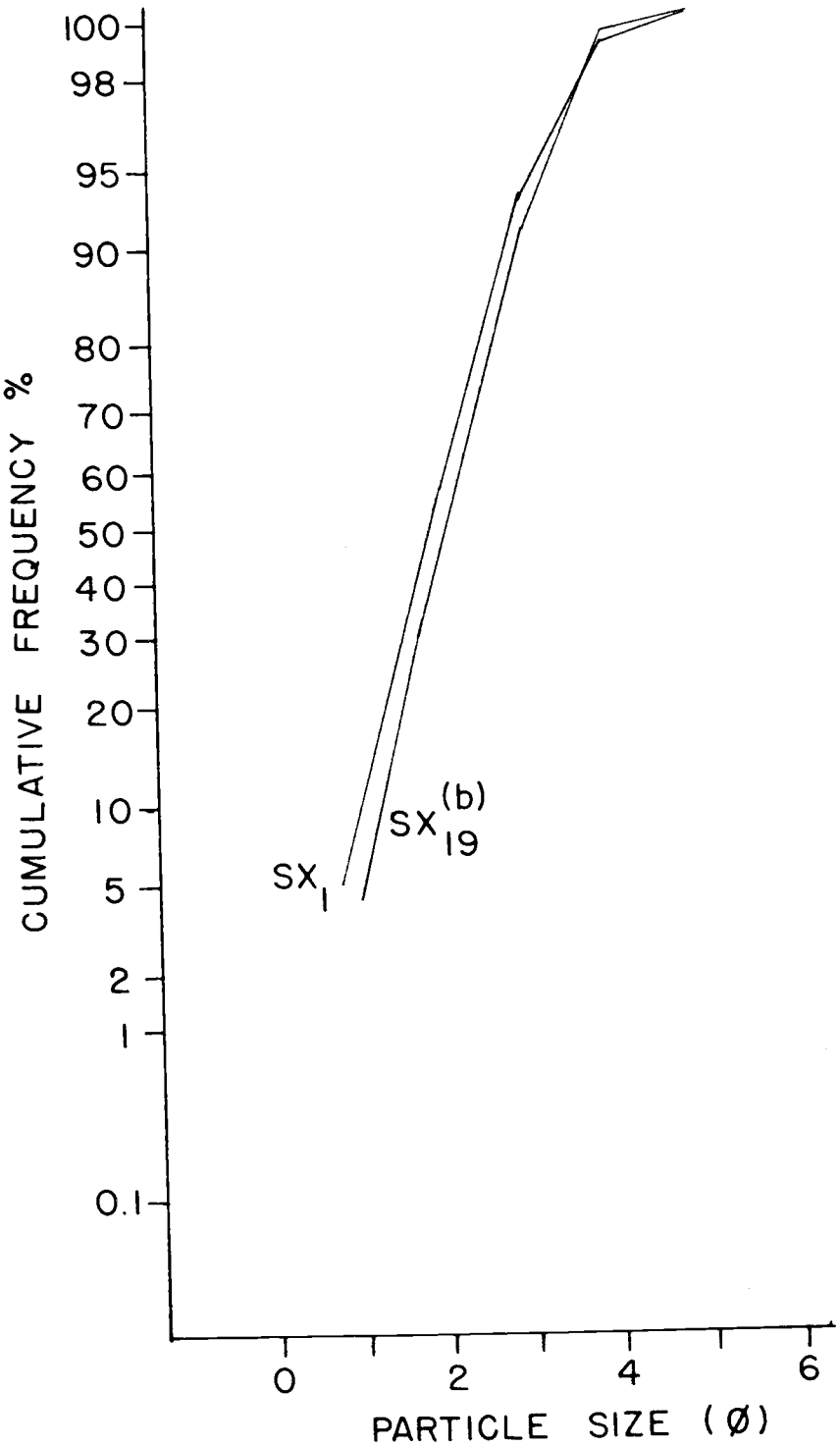
100
98
95
90
80
70
60
50
40
30
20
10
5
2
1
0.1
CUMULATIVE FREQUENCY %
SX1
SX19(b)
0
2
4
6
PARTICLE SIZE (Ø)

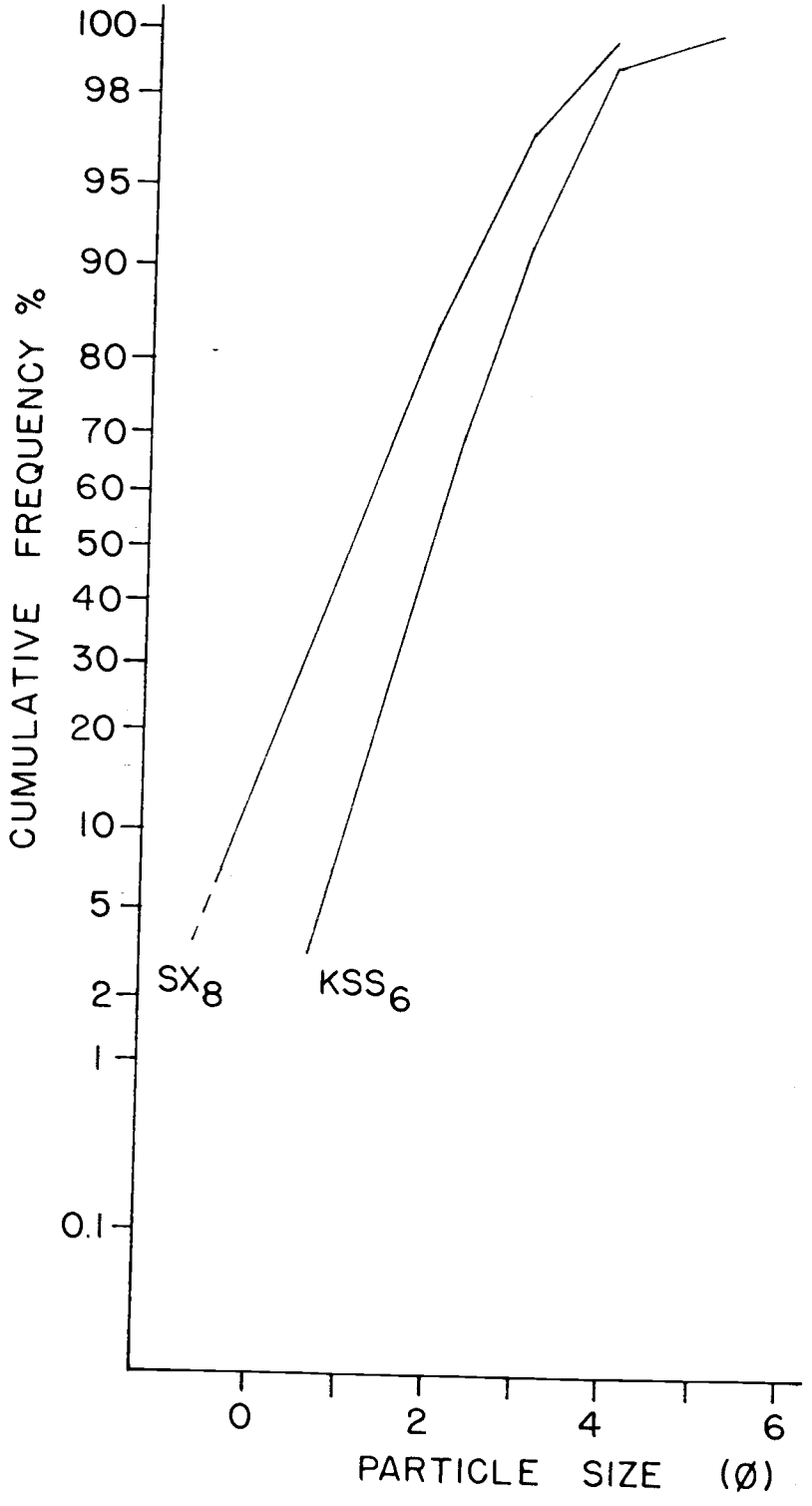
100
98
95
90
80
70
60
50
40
30
20
10
5
2
1
0.1
CUMULATIVE FREQUENCY %
SX8
KSS6
0
2
4
6
PARTICLE SIZE (Ø)

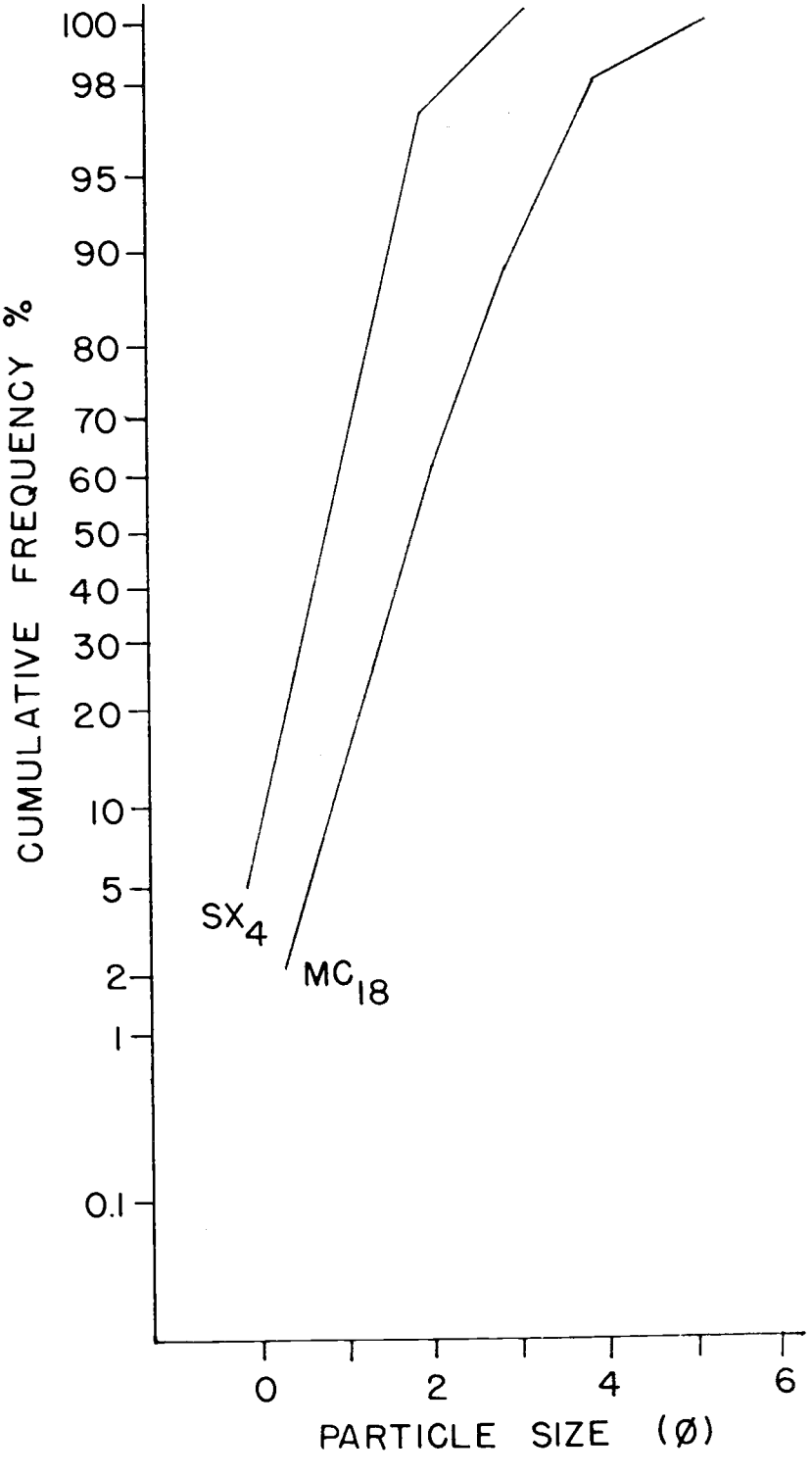
100
98
95
90
80
70
60
50
40
30
20
10
5
2
1
0.1
CUMULATIVE FREQUENCY %
SX4
MC18
0
2
4
6
PARTICLE SIZE (Ø)

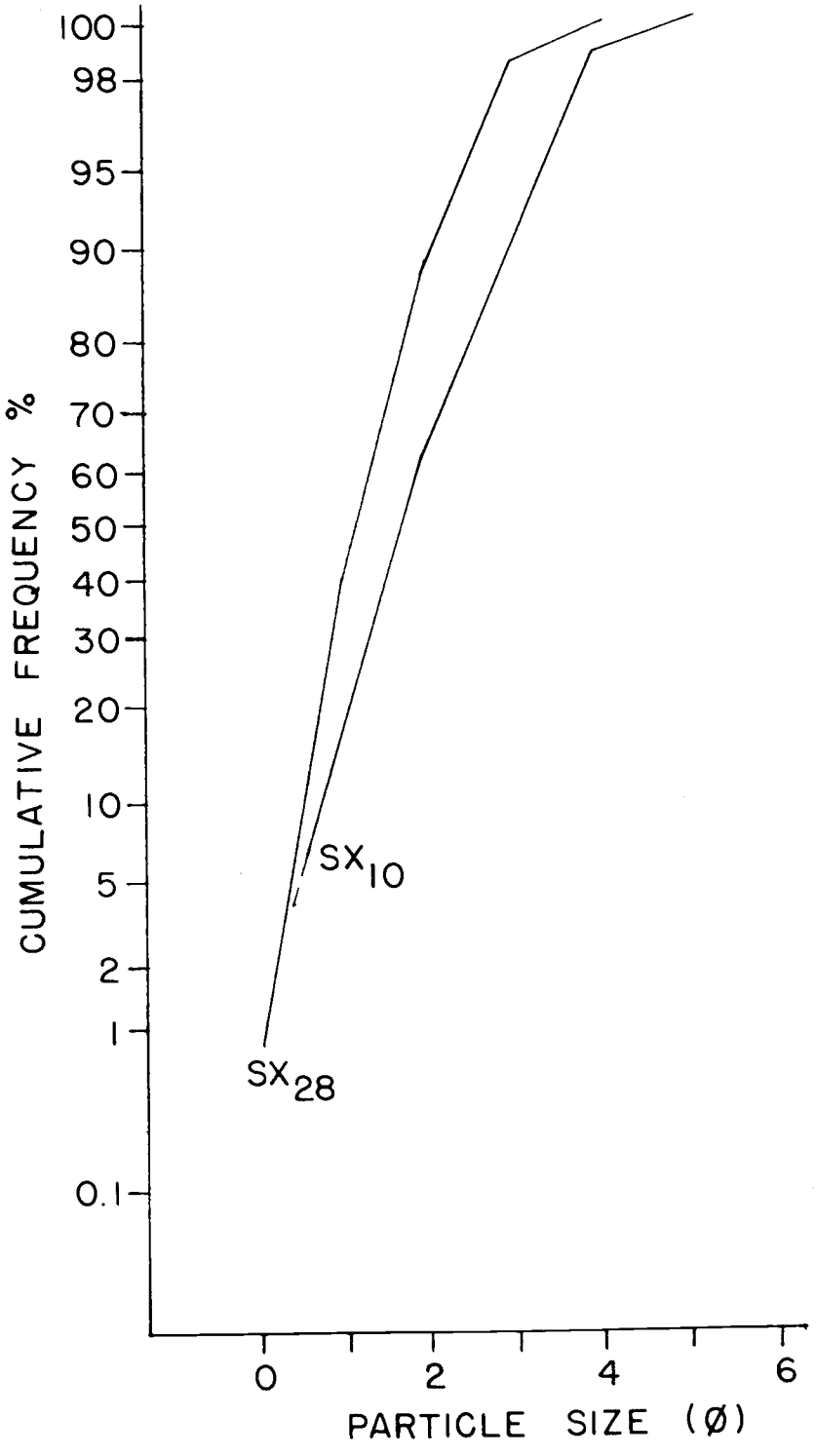
100
98
95
90
80
70
60
50
40
30
20
10
5
2
1
0.1
CUMULATIVE FREQUENCY %
SX10
SX28
0
2
4
6
PARTICLE SIZE (Ø)

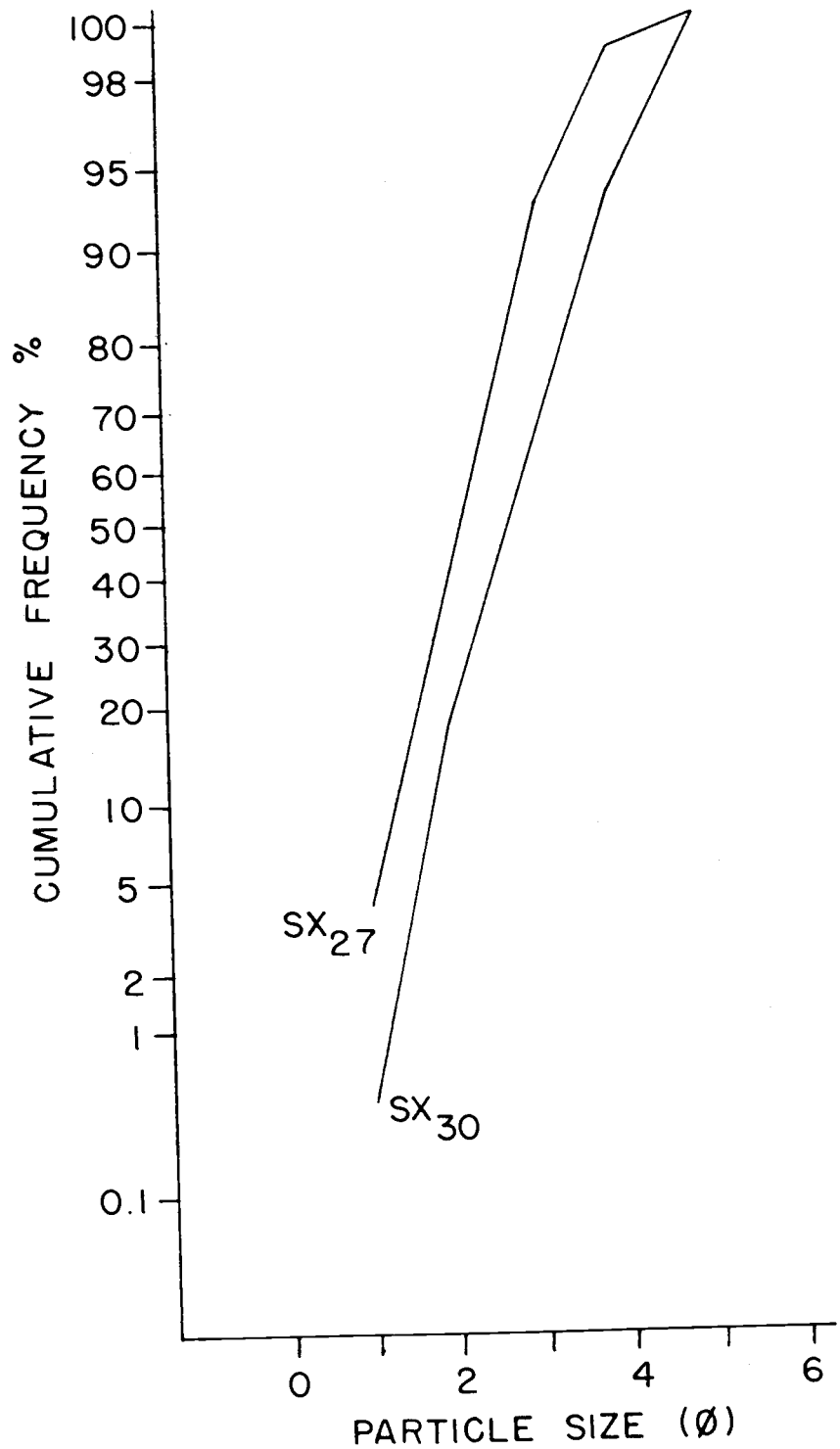
100
98
95
90
80
70
60
50
40
30
20
10
5
2
1
0.1
CUMULATIVE FREQUENCY %
SX27
SX30
0
2
4
6
PARTICLE SIZE (Ø)